ISTANBUL TECHNICAL UNIVERSITY ★ GRADUATE SCHOOL

SENSOR FAULT DETECTION, ISOLATION AND ACCOMMODATION APPLIED TO B-747 AIRCRAFT LATERAL DYNAMICS

M.Sc. THESIS

Akan GÜVEN

Department of Aeronautics & Astronautics Engineering

Aeronautics & Astronautics Engineering Programme

FEBRUARY 2021

ISTANBUL TECHNICAL UNIVERSITY ★ GRADUATE SCHOOL

SENSOR FAULT DETECTION, ISOLATION AND ACCOMMODATION APPLIED TO B-747 AIRCRAFT LATERAL DYNAMICS

M.Sc. THESIS

Akan GÜVEN
511161101

Department of Aeronautics & Astronautics Engineering

Aeronautics & Astronautics Engineering Programme

Thesis Advisor: Prof. Dr. Cengiz HACIZADE

FEBRUARY 2021

ISTANBUL TEKNİK ÜNİVERSİTESİ ★ LİSANSÜSTÜ EĞİTİM ENSTİTÜSÜ

B-747 UÇAĞI YANAL DİNAMİKLERİNDE SENSÖR HATA TEŞHİS, İZOLASYON VE DÜZELTİLMESİ

YÜKSEK LİSANS TEZİ

Akan GÜVEN
511161101

Uçak ve Uzay Mühendisliği Anabilim Dalı

Uçak ve Uzay Mühendisliği Programı

Tez Danışmanı: Prof. Dr. Cengiz HACIZADE

ŞUBAT 2021

Akan Güven, a M.Sc. student of İTU Graduate School student ID 511161101, successfully defended the thesis/dissertation entitled “SENSOR FAULT DETECTION, ISOLATION AND ACCOMMODATION APPLIED TO B-747 AIRCRAFT LATERAL DYNAMICS” which he prepared after fulfilling the requirements specified in the associated legislations, before the jury whose signatures are below.

Thesis Advisor :	**Prof. Dr. Cengiz HACIZADE** Istanbul Technical University	....
Jury Members :	**Dr. İsmail BAYEZİT** Istanbul Technical University	....
	Dr. Aykut KUTLU Esen Sistem Entegrasyon	....

Date of Submission : 26 January 2021
Date of Defense : 15 February 2021

To almighty GOD,

“Verily We have granted thee a manifest Victory”

FOREWORD

This study is mainly aided by my supervisor Prof. Dr. Cengiz Hacızade.

I anounce my sensitive and sincere appreciation to him as he supported me for a long term with advices, guidance and patiance, also directored as to establish this futuristic important thesis.

I also wish to thank to my lecturers and all the staff inside the ITU family for their help and kind behaviours.

At last, I wish to present my profound thanks to my whole family for their support, patience and everything throughout my study at İstanbul Technical University. And I am thankful for having accomplished my post graduate education as the Master's Degree with a brand of a genuine Aeronautical Engineer.

January 2021

Akan GÜVEN
Aeronautical Engineer, M.Sc.

TABLE OF CONTENTS

Page

ABBREVIATIONS

EFCS	**:** Electronic Flight Control System
EOM	**:** Equations of Motion
FCC	**:** Flight Control Computer
FCL	**:** Flight Control Laws
FDD	**:** Fault Detection and Diagnosis
FDI	**:** Fault Detection and Isolation
FTCS	**:** Fault Tolerant Control Systems
LTI	**:** Linear Time Invariant
OLKF	**:** Optimal Linear Kalman Filter
RKF	**:** Robust Kalman Filter

SYMBOLS

$\boldsymbol{b}$	: Wing span
$\boldsymbol{dt}$	: Sample time
$\boldsymbol{g}$	: Center of gravity
$\boldsymbol{h_e}$	: Altitude
$\boldsymbol{k}$	: Time index
$\boldsymbol{m}$	: mass
$\boldsymbol{p}$	: Body roll rate
$\boldsymbol{q}$	: Body pitch rate
$\boldsymbol{r}$	: Body yaw rate
$\boldsymbol{t}$	: Detection time
$\boldsymbol{t_i}$	: Instant time
$\boldsymbol{w}$	: Process noise
$\boldsymbol{x}$	: State
$\boldsymbol{y}$	: Measurement output
$\boldsymbol{z}$	: Measurement noise
$\boldsymbol{E}$	: Expected value
$\boldsymbol{K}$	: Kalman gain matrix
$\boldsymbol{P}$	: Estimated error covariance
$\boldsymbol{Q}$	: Process noise covariance
$\boldsymbol{R}$	: Measurement noise covariance
$\boldsymbol{S}$	: Wing area
$\boldsymbol{V_t}$	: True air speed
$\boldsymbol{\alpha}$	: Angle of attack
$\boldsymbol{\beta}$	: Sideslip angle
$\boldsymbol{\beta_e}$	: Estimated sideslip angle
$\boldsymbol{\delta_a}$	: Aileron deflection
$\boldsymbol{\delta_e}$	: Elevator deflection
$\boldsymbol{\delta_r}$	: Rudder deflection
$\boldsymbol{\delta_{th}}$	: Thrust setting

$\boldsymbol{\varphi}$	**:** Yaw angle
$\boldsymbol{\theta}$	**:** Pitch angle
$\emptyset$	**:** Roll angle
$\boldsymbol{\chi_e}$	**:** Distance in X_e direction
$\boldsymbol{y_e}$	**:** Distance in Y_e direction

LIST OF TABLES

Page

LIST OF FIGURES

Page

SENSOR FAULT DETECTION, ISOLATION AND ACCOMMODATION APPLIED TO B-747 AIRCRAFT LATERAL DYNAMICS

SUMMARY

The contents of the thesis illuminates and performs an amendotary fact on model-based fault detection and diagnosis method that helps to the pilot to have a safe flight in the subject of enhanced flight controls also, reduces the complexity and much simpler computational operations. The FDD techniques purposes to gather a much more sensitive fault detection success on faults that are resulted by noise, system uncertainities and disturbances.

FDD model constructed in this thesis built into Boeing-747 civil aircraft. There are two studies. The first one is B-747 aircraft is taken as a nonlinear closed-loop B-747 aircraft model from Simulink airlib library and by using Simulink linearization toolbox, the aircraft lateral states are linearized and converted into state-space model and used in Matlab to calculate the detection, isolation and accomodation of sensor faults till occurred. The other study is, there is an established fault detection system includes a nonlinear closed-loop B-747 aircraft model to verify the effectiveness of sensor fault detection method, an estimator that observes the lateral states at the same time the aircraft is having a level-flight, a fault indicator subsystem that indicates the faults on the system by applying faulty responses and once for all a reconfiguration subsytem that discriminate by contrasting the states those are gathered from sensors just as instantly and by this way, it determines whether the condition of the flight is faulty or fault-free. Kalman filter is utilized to diagnose the fault and detect as a linear estimator design.

From the sight of Kalman filter innovation sequence statistics, the sensor measurement channel faults are detected, isolated and accommodated with adaptive and reconfigurated Kalman filter algorithms. Also, the simulink study reduces the adverse affect resulted by model uncertainity, forms a residual with high sensitivity to sensor faults and sustains a safe fault detection method colloborated with the deny of false alarms with is vital for system safety. State estimation illustration makes it possible to guess and observe while a unwanted system behaviour is erupted and succed detection of faults. The designed system is vital for sensor stuck detection on earlier stage to have much lesser threshold values for sensitivity to alarms in case of multi-simulation cases are tested in MATLAB Simulink.

Keywords: electronic flight control systems, sensor fault detection, state estimation, Kalmanfilter,state-spacemodels

B-747 UÇAĞI YANAL DİNAMİKLERİNDE SENSOR HATA TEŞHİS, İZOLASYON VE DÜZELTİLMESİ

ÖZET

Bu tezin ilgilendiği konu içeriği, uçuş kontrol sistemlerinin kabiliyetlerini iyileştirerek, daha az kompleks sayısal hesaplamalar gerektiren durum-uzay modeli ve simulink model tabanlı yaklaşımla hata teşhis ve tanımlama kavramlarına düzeltici bir çözüm sunmaktadır. Bu model tabanlı hata algılama ve tanılama teknikleri, gürültü, sistem belirsizlikleri veya bozulmalara göre hata algılama kavramının hassaslığını arttırmayı amaçlar.

Bu tezde oluşturulmuş hata algılama modeli bir sivil uçak modeli olan Boeing-747 yolcu uçağına uyarlanmıştır. Burada iki ayrı çalışma yapılmıştır. İlk olarak Boeing-747 yolcu uçağının lineer olmayan Simulink modeli, airlib yardımıyla alındıktan sonra yine Simulink linearizasyon programı yardımıyla lineerizasyonu gerçekleştirilmiş ve yanal durum-uzay modeli elde edilip Matlab programında kodlanarak sensor hatası durumunda teşhis, izolasyon ve düzeltilmesi sağlanmıltır. İkinci çalışma ise Simulink' de lineer olmayan B-747 yolcu uçağı modeli kullanılmıştır ve sensor hata tespiti ve düzeltilmesi sağlanmıştır.Bu kısımdaki hata algılama sistemi dört adet alt sistemden oluşur. Bunlardan ilki, lineer olmayan kapalı döngü uçak modeli, ikincisi uçağın sabit yükseklik ve hızda ilerlerken durum-uzay halindeki koşullarını tahmin eden bir gözlemci, üçüncü olarak sisteme hatalı cevap girdisi için hata gösterici alt sistemden ve son olarak sistemin hatalarını, uçağın durumunu sensörden elde ederek, gerçek zamanlı karşılaştırarak uçuş durumunun hatalı ya da hatasız olduğuna karar veren yeniden düzenleyici alt sistemden oluşmaktadır. Lineer gözlemleyici olarak Kalman filtre tasarımı ile hata teşhisinde başarılı olunmuştur.

Kalman filtresi inovasyon istatistik metodu kullanılarak, sensor ölçme kanalındaki hataları tespit eder, hangi sensörün hatalı olduğunun teşhisi ve düzeltilmesi sağlanır. Simulink çalışmasında ise, modelde mevcut olan belirsizlik yayılmalarını azaltmakta ve ani hatalara karşı hassas kalan(rezidüel) elde etmekte ve sistemin emniyeti için mühim olan hata reddini değerlendirerek hata algılaması işlemini doğru olarak gerçekleştirir. Uçağın durum-uzay model durumlarının tahminini görüntüler ve hatalı durumlar gösteren sistem cevaplarının gözlemlenip, hatanın algılanmasını gerçekleştirier. Burada kullanılan tasarım, MATLAB Simulink' te uygulanan çoklu senaryo testleri doğrultusunda eşik değerini daha azaltarak uçağın sensör hatasını daha erken algılanmasını sağlar.

Anahtar Kelimeler: elektronik uçuş kontrol sistemleri, sensör hata tespiti, durum tahmin, Kalman filtresi, durum uzay modeli

1. INTRODUCTION

The cutting-edge technology which is used by the aviation industry maintains reliable solutions to make aircraft more and more safe and sound both recent event future years. The weight load that aircraft exposed to is significant because it has an affect on flight sustainability. Electronic flight control systems are developed for the purpose of enhance the aircraft stability and decrease the structural loads during flight. To maximize the fault detection and restrict the flight control system failures, aircraft design optimization has been developed. Discovering such faults on an earlier stage has many advantages to prevent the error before it becomes non-tolerable and limit the unstable situation. By the invention of the EFCS, many methods are developed to make solutions for reducing the overall weight problem which has the role of the old fashioned mechanical interfaces from the pilot input to the related control surfaces. The important facts such as noise, fuel consumption, aircraft range etc. are enhanced as a result of reducing the redundant weight loads in the aircraft. Industrial practices are used with redundancy-based methods to gather more reliable consequences. Recent model-based approaches are considered to be an interesting research field [1].

What is EFCS system? It is an electronical system that supports the pilot and diminishes the pilot workload by making the aircraft more controllable while facing unwanted situations and make the flight safe also improve flight performance. The sensors on the aircraft which are measuring the altitude, speed, attitude etc. can be imposed during flight as a result of the weather conditions or the material wearing, so the signals coming from those are either influenced, therefore the airplane flying properties can be affected. Even if those faulty conditions faced, EFCS is responsible to maintain its regular process.

Kalman filter is considered to be the most efficient observer method to estimate states of a civil aircraft when there are noise occurrence coming from the sensor and

model are Gaussian and it also presents an adaptive approach in relation to the estimation theory.
In the scope of longitudinal stability of several types of aircrafts, there are alike research and studies revealed in literature. However, lateral stability has less part on research field and that is why one purpose of this study is having a contribution to few sources.

1.1 Aim of Thesis

This thesis work aims to accomplish and manage in conditions of sensor fault detection, isolation and accomodation is done on the B-747 aircraft flight control system. To detect and isolate the fault, through statistics that are related to innovation sequence of the Kalman filter is investigated. Further, for fault accomodation aim, Reconfigured Kalman filter and Robust Kalman filter methods are investigated.
Convenient data is used for the state-estimation problems because the physical event and the measurements are maintaining a prior knowledge which helps to generate estimation of state of the dynamical variables. The purpose is accomplished by a method that reduces the error statistically. To handle the model estimation and the measurements, the state estimation problems provide more reliable estimates of the system variables [2].

Bayesian filters are used to estimate the states and by this sight of view it is decided to use the whole convenient data to reduce the uncertainties when a decision making or a condition faced. As incoming is data acquired, it is incorporated with the former data to generate the principal for the statistical processes [3].

In linear systems with Gaussian noises, Kalman filter is a popular filtering process. Linearization methods are applied to Kalman filter and it is adapted to have less restricting conditions. Among the whole application techniques to come up with for complex systems, Kalman filters might be a constructive solution [4].

In this study, to estimate the lateral states of the model of Boeing 747 in several steady state flight conditions also has error cases in sensor measurements, Kalman filter is applied. Kalman filter in the model is responsible to filter the noise on the sensors and estimate the outputs of exact lateral state values during several flight conditions simulation and this is accomplished by integrating the complex civil aircraft model with Kalman algorithms. Gaussian white noise with zero mean and covariance matrix is used in the estimation of linear state performances. After performing several flight simulation cases, the performance effectiveness of varying Kalman filter is analysed.

1.2 Contribution of the Thesis

The fundamental contribution of the paper is using Kalman filter innovation sequence statistics to detect and isolate the sensor fault and also to make an observer-based approach for sensor fault detection of a Boeing 747 aircraft. For providing a safe flight, this study emphasizes that a reliable model based approach to an aircraft can show the performance of the FCC that is critical for pilot to take action in any faulty condition to sustain the safety of flight. Amplitude response related to a decided threshold level and elimination of false alarms are seen in several simulation cases in the study.

For estimating the states of a Boeing 747 during in a steady-state flight condition, Kalman filter as a linear observer is indicated in operating many flight simulation conditions.

1.3 Organization of the Thesis

In Chapter 2, the literature review took place to outline the aircraft control systems, FDD theoretical background, the fact of fault classification and types of observers.

In Chapter 3, Fault detection, isolation and accomodation methods are introduced. The measurement noise-increment fault and adaptive Kalman filter is examined from performance sight.

In Chapter 4, Fault detection, isolation and accomodation methods are implemented and graphical results gained. Further, with root mean suare error method, the other sensor measurements with no fault case, OLKF, RKF are Reconfigured Kalman filter algorithm gathered values are discussed.

In Chapter 5, The other study methodology is given with the data analysis, mathematical model of the aircraft B 747, fault detection bu using Kalman filter algorithm and designed Kalman filter implemented into Boeing 747 model as an observer to estimate the states and information represented about the simulation cases and based on the observer-based methods, results are given.

In Chapter 6, Discussion of the suggested fault detection method, and contribution of the study to future research aspects.

2. LITERATURE REVIEW

2.1 Development of Aircraft Flight Control System

Sensor fault detection and isolation based on Kalman filtering technique is referenced in various studies. Kalman filter innovation sequence mean is based as an approach to detect and isolate aircraft sensor and control surface faults [5].

A faster converging Kalman filter for sensor fault detection and isolation is brought. The faults are detected and isolated in a shorter time with initialization of the covariance matrix, and using an EKF compared to classical Kalman filter method [6].

Bias and noise increment fault cases are examined for the aim of detection and isolation of sensor faults for wind turbine systems. And the result was successful either bias and multiplicative fault detection and isolation achieving suggested method [7].

A modified adaptive fading extended Kalman filter (AFEKF) is suggested for satellite fault detection and isolation process which include three stages and it differs fault detection and isolation, also type of fault recognition [8].

Moreover, information of sensed variables kinematic relations is utilized for analytical redundancy further to the present hardware redundancy on modern airplanes. To accomplish this, an EKF is benefited [9].

Furthermore, based on a hybrid Kalman filter, the subjact about non-linear railway vehicle suspension gained well conclusions during the struggle for sensor fault detection [10].

Another study shows the issue of isolating actuator and sensor faults in nonlinear systems. The given way of solution exploits the analytical redundancy in the system via state observers design. If the correlated residual (calculated by suggested method) excess its threshold, fault detection is managed. Process of isolation is operated by practicing a residual banks also a logic law [11].

Based on Kalman filtering technique, fault accomodation is variously analysed in the literature. One of the study is the attitude control system sensor fault detection, isolation and accomodation of a three-axis satellite are examined. To assess residuals and detect the sensor faults, adaptive thresholds are set up. Further, an accomodation system is build in sight of reconfiguring the accessible actuators. Conclusions show that the attitude control error is preserved bounded [12].

Further, a model based approach for sensor fault detection in civil aircraft control surface investigated [13].

The EFCS was firstly introduced by Wright brothers in 1902 which the initial design let to occur innovations of the modern EFCS. Between 1950' s, fundamental pilot autopilot stabilization functions and aircraft handling properties are artificially enabled by the release of analog FCC. Furthermore, in 1972 the analog FCC was replaced by digital fly-by-wire control system technology. In 1987, it was the first commercial aircraft, Airbus A320, which is performed the fly-by-wire control systems on the common control surfaces on transportation airplanes field [14].

The EFCS is established to overcome severe necessarities based on safety and availability, ruled by the aviation industry. Mechanical flight control system, are less safe, has high mass properties, hard to provide devices, control is lesser, and hard to engage with technical improvements. On the contrary, the more EFCS improved, the more complexity of the system became unevitable. As a result, ramification on malfunction conditions are seen based on aircraft design aspect, therefore it preserves its raising seriousness. Target of EFCS is to detect faults and have a safe flight at the entire flying stage with replacing redundant hardware and contrast for assesing firmness tests and cross-checks [14].

Conventional mechanical systems are developed and became mechanical hydraulic systems which propagate actuators to enable large forces on the control surfaces but, it ads an extra complexity to control system. The fly-by-wire EFCS sustained an enhanced solution. FCC make it easier control system by receiving and sending signals which made gathering more improved handling quality. By this new fly-by-wire technology, it became possible to have better aircraft maneuverability, handling quality, fuel efficiency and safer flight operation .

Runaway (aka hardover) and jamming(stuck at a fixed position) are the two fields of EFCS failure conditions which are related to aircraft control surfaces. Runaway is considered as an undesired position movement of the control surface and if it is not detected, it will continue to move till the moving surface stops. This failure could be due to the FCC not working properly or an electrical equipment failure or a mechanical breakage and could mislead the aircraft from its pitch route or expose the aircraft to excess structural loads according to runaway dynamics. The solution for that problem would require a structural reinforcement which means a heavier aircraft and as a consequence, the fuel consumption will rise. Therefore the detection must be maintained even if a small change in the elevator trim position is observed, so the fault rate plays a role in determining the detection time. Civil aircrafts are generally configured with two elevators independently and whenever an error occurred, there are double pair of actuators which one is active and one is in ready mode on each elevators to sustain a safe flight. System reconfiguration is performed after the runaway is detected. In reconfiguration process, there is a turn on assignment on the actuators. The actuator which is in the passive mode is changed to active mode and the active actuator changed to passive mode. Jamming case is considered as a mechanical problem has occurred sourced by a system failure that the control surface stuck at its current position which results a raise in the fuel consumption related to drag take place due to stuck control surface. In case of a cross-wind landing, assumed that the rudder is jammed, additional drag will affect the aircraft.[1]
Because of the weight property has a vital place on the fact of an airplane, if there are redundant hardware implementation, it will increase the total weight of the airplane adversely. To overcome this issue, mathematical models and algorithms are formulated and embedded into the FCC System. The conventional flight control computer operates the main flight control surfaces to run the aircraft along its flight

path but also sustains finer control for stable specifications. Flight control computer (FCC) has the data that is performed for calculation a command to servo control each mobile surface. Inertial acquisition system which is consisted of many redundant parts, makes is possible to have the required data. FCC has two main issues, delivering command signals and monitoring signals and if there is a variation that exceeds the signal threshold, detection verified. As a fault detected, FDD makes sure that pilot is aware of the failure and begin to follow error instructions and. By this way, FDD easies the pilot workload and sustain the aircraft safe flight envelope.
One of the essential mission that FCC responsibilities is assuring the Flight Control Laws (FCL) computation that originate a command to servo-control of each of the control surfaces. For FCL data processing, the piloting objectives and the state of the aircraft is analyzed by making a comparison. A set of sensors using anemometric and inertial measurements, aircraft states such as attitude, speed and altitude is gathered. The output is gained by performing an attainment system which includes generally three redundant units. The FCC takes those three units of flight data to calculate a valid and solely specific value needed by FCL. This process called “consolidation” and has to validate two steps: eliminating other parameters from sources and taking just the right value and then to show one by one of each non-related source to ignore the faulty one [15].

During flight, the faults can be occur by a sudden change in the measurement channel, noise raises, continuous bias..etc. and that would lead to a significant value change in the Kalman filter innovation sequence statistiscs [16]. The main thing that is important is to remark the fault occurrence, detect it not after too late for pilot. Therefore, the time of occurrence must be recognized and as soon as possible so the detection scope would be minimized which makes it possible to prevent the fault become more vital, aircraft become more vulnerable. On the contrary, the fault detection system must be robust and gauge the superfluous system. With the help of a potent fault detection, via a small reconfiguration in the position deviation of the control surface, the aircraft could overcome a critical fault before it eventuates.

2.2 Fault Detection Methodology History

The initial studies on Fault Detection and Isolation has begun since 1970's and has a wide range of part in the literature by keeping on improving solutions. Simulation environments and real flight tests have validated the FDI methods are valid. Recent control methods are more efficient compared to the old-fashioned ones as long as there are critical problems occurs on altering flight cases, yet, there are still many flight missions that require high level of robustness use classical methods. The succeed studies in the reference part, guided this study to establish its framework, which almost all have a common subject as FDI but they are distinguished on the way of their path. As regarded from the historical sequence, those studies can be summarized as below that are used to make this study possible:

Residual generator for FDI which affects states of the sensor of a civil aircraft, come up with a design set of residuals. To diagnose the incident, a multinomial method is used to design residual generator [17].

2.3 Approach of Fault Detection and Diagnosis

Civil aircraft consist of many FCC and hydrolic and electronic power supplies that enables control surfaces. Cross checks, consistancy checks and built-in tests are some of many ways to diagnose the error. Monitoring and command channels are put on control surfaces or actuator positionswith correlated sensors so by this way, fault detection is succeded with viable coherent checks between two redundant signal values are calculated in two FCC channels. Because of calculating the same signal among separate channels, it is logical to differentiate the incompatibility of result of a channel, sensor or FCC input value etc. In failure cases of an aircraft, to maintain the safe flight there are two actuators on each of the control surfaces, that are main actuator and second as a backup. The moment there is a brake on main actuator, it is automatcally switched to passive mode and the backup actuator is switched to active. An assignment among two actuators is utilizied at the time there is a false alarm rate that is said to be the convenient actuator is disabled and rather than the faulty actuator and control surfaces and outcomes a decreased flight control. The methods can be used for the sensors instead the faults are not as vital as in actuators. If a misdetection occurred in a sensor it may result as a inconvenient position, speed and altitude, attitude data. Fault detection and isolation (FDI) techniques are mainly divided into two segments as the management of hardware and analytical redundancy [1].

The decesion system targets to clarify the divergence of the residuals from zero and non-zero residuals to know probable fault. The alarm starts when the signal appears off the given threshold in a given time period and they diverse belong to fault type. A comparison between detection performance and false alarm rate must be done because there is a risk of false alarm rate if the threshold value is decided as a low value and on the other hand the lighter faults are going to be misdetected if the threshold value is chosen as high value [1].

2.3.1 Hardware redundant system

More than one sensor is used in cross monitoring as a fact in hardware redundant systems. The weight of the aircraft rises also the expenditure because of having too many hardware buildup. A place to put the hardware is needed and difficult to have because of the limited convenient area of the instruments. Therefore, it is not feasible to have hardware redundancy and for the future it conserves its problems as weight and cost in the field of FDI [18].

2.3.2 Analytical redundant system

Analytical redundant systems targets to analyze the main model behaviour and to the normal nominal reaction by the way of matemathical model monitoring and for FDI it is indicated to model based approach. A common model-based FDI system consist of a residual caulculator, evaluator and a threshold calculation ends by decision making process. The FDI structure makes sure data value related to starting, position and severity of the error. The process of residual generation is met by reconfiguration of sensor or actuator set to achieve fault isolation and manages the control action to correlate the defective reactions caused by system input and output values together with afterwards failure decesion data of FDI. The purpose to make the right decision on the subject of fault detection, if there is a fault occurs or not, the residual evaluation makes it possible.

The airplane sensor signals generally show commonly has three speciality: randomness, dynamic and dynamic dependent. And the randomness comes mainly from the noise property, athmospheric weather conditions, pilot inputs and unknown uncertainity and those properties can be embeeded to the model to examine the results. In uncertainity occurance, the right decision makingis needed for randomness approach. Alterations in perform of flight results changes on aerodynamic coefficients, that makes the flight dynamics diversely profound. Techniques in redundant systems includes esimation of the states, adaptive filter, statics, Kalman filters in randomness method.

Because of the occurrence of uncertainities in system model, the actual system and model is not equal from view of control theory.The uncertainity is remarked in a robust controller as forming the controller. A feasible solution is searching on performance and simplifying the model.In reality, faults are exposured to system in stochastic way and they are not related to uncertainities of the system. However, a robust controller can overcome particular errors such fractional damage and it is convenient to supress them in specific rate. Therefore, the system dynamics change rapidly because of the stochastic situations and for the controller, no advance knowledge stands. Whatever the case is for the aircraft, it is required to perform as usual during an error confronted.

Following the faults which led to changes in plant dynamics caused by essential structural changes, control reconfiguration is strictly needed. To compare the fault detection between sensor and actuator faults, the observation of sensor fault are simple than the latter because there is connection lost among plant and controller instead in actuator errors, there is loss of control of plant. On behalf of nominal status, the measurements track the estimative norms within a given tolerance value stated by amplitude of uncertainities occurred by measurement noise from the sensor and random system irregularities. The FDI system evaluates the process by inspecting the errorenous sensor output during it deviates from its estimated norm.

The purpose of the FDI system is to detect faults in early stage, targeting where the fault takes place and figure out the reasons, managing fault correction to prevent more damage to the system or loss of service emerges. Glitches might appear in just one unit of the sensors, actuators or other regions and have an adverse affect in system behaviour. The FDI system commonly prefers simple specifications as:

- Minimum detection delay.
- Compact remark of the fault type among various faults.
- Excellent robustness to many noise and uncertainity origin and their effects from the system.
- Fine detection rate and low false alarm rate [15].

Since 1988, Aerospace systems were designed to meet system safety, reliability, maintainability and survivability requirements in the light of fault detection and diagnosis system and as a more modern approach replaced it as fault tolerant-control systems (FTCS). During flight operation performed, a desired flight performance has to be cultivated with the help of fault settlements, which is called fault-tolerant control system. A lot research and studies have been put to form a FTCS for safety in the field of aircraft safety, space vehicles, power plants and also the industrial plants. Redundancy and auxiliary systems are important in a FTCS because it affects the efficiency of the system.

The active fault tolerant control works on faults and failures in a theoretical way and there is a complex system attached with subsystems that has reconfiguration, fault detection and diagnose, it is pricey. When there is a fault occurred there happens a time delay throughout the whole process starts with fault occurrence and FDI method and after the reconfiguration of the controller, that is the first string about constraint of the active FTCS method. During this operation, because of there are inconsistency of controller and the complex system dynamics, there could be a jeopardy of control loss on the system. Also, the control-mismatch could crush the FDD process and break down to collect the required data to establish the faulty system model whether there is a problem. That means, all along the time delay, an arrangement of controller must to be maintained to stabilize the whole system [19].

The passive fault tolerant control deals with some foreknown set of faults that can be categorized as a robust control. It can only enhance the control when there is partial loss fault such as sliding mode control in FTC. The ambiguities, unknowns in the system dynamics are responded by a robust control with less performance of ordinary control and SMC plays a feasible role in this process [20].

2.4 Diagnostic Algorithm

Fault tolerant control diagnostic steps are separated as shown:

- Fault detection step: In this step, determination of if there is a fault appearance or not is done. Also at the time diagnosed just as the system exposure to a fault.
- Fault isolation step: As we can imply from the name of the step, the fault location is informed by isolation of the fault on scope of when a component fault occur.
- Fault identification and fault estimation: The process of identification of the fault and estimation of its severity evaluated.

Generally diagnostic algorithm specifications can be interpreted as below:

- Input is not the merely fact that has affects on the dynamical system, the initial state is also vital. If the there is a problem with unmeasurable initial states, state observation problem would occur.
- The disturbance mostly unmeasurable which affect the aircraft plant. Taking into account that unmeasurable disturbance has an influence on response of the plant, consistency check must be performed [21].

Several criteria are used in the purpose for evaluating FDI algorithm performance are on below:

- Fault localization rapidity
- Precision to slow growing faults
- Incorrect alarm estimation
- Unsuccess error detection
- Wrong fault segregation [22].

2.5 Classification of Faults

Faults can appear in sensors, actuators and at the whole systems. As their arise of place, they are segregated and classified.

2.5.1 Sensor faults

Sensor faults inside a system, there are cases of erroneous measurement of signal $y(t)$. Several redundant sensors backed up for straight or variously checking and validating the whole system state variables in modern aircraft systems. As a result of a disruption in the sensor unit, verifying sharpness and loose mounting of the sensors, there will occur a sensor fault. In a sensor fault, it could lead to a flight control break and add non needed behavior of the aircraft [23].

Bias means, there is already an offset or error along the true signals and measured signals and can be formulated as:

$$y_i(t) = x_i(t) + d_i \ here\ the\ disturbance \rightarrow\ \dot{d}(t) = 0, d_i(t_F) \neq 0 \tag{2.1}$$

Drift is related to when there is an inaccuracy or sensor sensitivity is lost, the measurement error will grow as the time pass by.

$$y_i(t) = x_i(t) + d_i \ here \rightarrow d_i = \lambda_i t, \qquad (0 < \lambda_i < 1\ , \forall t\ \geq t_F) \tag{2.2}$$

Loss of Accuracy is a situation that true values are not matched with the measurement values.

$$y_i(t) = x_i(t) + d_i \ where\ |d_i(t)| \leq d_i, \qquad \dot{d_\iota} \rightarrow 0\ \ \forall t\ \geq t_F \tag{2.3}$$

Freezing, instead of true value, sensor signals will show a constant value.

$$y_i(t) = x_i(t_F)\ \forall t\ \geq t_F \tag{2.4}$$

2.5.2 Actuator faults

At the last stage of control-action process, actuators have essential mission to bring the required power which moves the control surface. In modern aircraft systems, actuators have hydraulic or pneumatic powered systems. To maintain the required energy power, actuators are designed obligatorily to be heavy that brings with a high weight of each actuator. So the weight is important for an aircraft, therefore, number of actuator that a plane can have is limited. And this led to focus on study in the field of actuator faults in aircraft systems. In aircraft systems, variety of actuator faults is present and mathematical formulations of actuator faults.

One of the control surface to steer the aircraft is the rudder and it is generally attached at the rear of the fin or vertical stabilizer that makes the pilot possible to control the rotation of the plane on its vertical axis, yaw movement that plane is available to rotate right and left direction [24].

In civil aircraft, the control surface rudder, includes generally three hydraulic independent actuator parts, which are performed by backed up distinct connections as for redundancy in case of an emergency condition the plane examines. Civil aircrafts have mostly three redundancy systems, as to say for a control surface, not only there is a primary control surface as itself, but also there are secondary control surfaces which are ready to use in case of a vital failure as an unusual way to accomplish the mission of the primary control surface [25].

Rudder, aileron aircraft control surfaces are given input by pilot and by this aircraft rotates. The rudder plays a role of yaw movement and ailerons has a duty of roll movement. Commonly, there is a slight contribution of ailerons during a coordinated turn of the civil aircraft turning by rudder. By this way, the pilot is available to hold the plane in the arc of the rotation. Also pilot can prevent the plane from slipping or skidding which are the two facts that has an adverse effect by means of the flight performance.

However, utilizing rudder and ailerons at the same time but in inverse directions is scarcely used by pilots. They use rudder and ailerons in contra way while they have to decrease altitude by exposing the plane to more drag or they encounter a situation like there are severe conditions on the runway, to overcome crosswinds and keeping up the plane on the line of glideslope.

One of the main incurrence of loss of control of an aircraft is the failure of the perform in the control surfaces, actuators, such as rudders, ailerons and elevators. The rudders confronts enormous forces, moments and it has a limit to endure. If those external forces on the rudder, exceed the limit of rudder to resist, there could be loss of rudder control mechanism or partial damage, structural loss of the rudder could be examined.

Abrupt Faults: Those faults are considered as severe faults and directly affects the condition of the control action. Abrupt faults commonly arise from an instant damage on a control surface related to surrounding environment has happened or electric short circuits. As a result of their rapid alterations, these faults can be identified quickly such as a jerking actuator struck. A sudden actuator struck can be described as:

$$u_F(t) = u(t) - \varepsilon u(t_F) \quad where \ \ \varepsilon \epsilon \, [-1,1], \qquad \forall t \ \geq t_F \tag{2.5}$$

$$When \ \varepsilon \epsilon \, [-1,0]$$
$$\rightarrow an \ additional \ unwanted \ faulty \ control \ effort \ is \ fed \ into \ the \ control \ loop$$

Incipient Faults: Compared to abrupt faults, incipient faults are regarded as moderate faults and have a significant influence on the control action' s time duration. Incipient faults could be seen in the event of hydraulic system or pneumatic system leakage. As leakage proceeds gradually, these faults are difficult to observe. Mathematical formula of an incipient fault can be described as:

$$u_F(t) = u(t) + su(t_F) \quad where \ \ slope \ s = \frac{u(t_F)}{t_F}, \qquad \forall t \ \geq t_F \tag{2.6}$$

2.5.3 System constituent faults

This type of faults, properties of the system matrices and aerodynamic coefficients are generally altered. Aircraft systems consist of many various subsystems which are complex and related to each other, and if a fault appears between those systems, it is tough to identify them. However, it is vital to detect those kind of fault on behalf of a fighter aircrafts which require high flight performance comes with inevitable continual structural damage.

2.6 Observers and General Applicability

Observers are usually utilized to effectuate a residual signal. Gathering system outputs by estimation through the measurement followed by gaining the residuals from weighted output estimation errors is the essential mission of the observer-based FDD. In an aircraft, the occurrence of the faults can be seen in the main perform element or the auxiliary system elements such as bias, drift in sensors, output of the controllers and the control surface actuators. If there is a case that a fault arises from the actuators, this means, the capability of system control is unable due to one of the actuators. On the other hand, the accuracy of the measurements is diminished due sensor fault which will result on the system become fewer observable. Else the whole plant nature will alter if there is a fault in the process component.

High-rate systems are categorized as related to their inclusion of system complexities such noise, uncertainties, inputs that are not known, parameters, states and disturbances which alter as the time passes by. According to great magnitude of events, noise is described in various methods. Unknown inputs are developed from environmental place which have an impulse on the system and might refer to several dynamic response, multitudes of crush, and magnitudes for an individual system. As ordinarily, high-rate systems include a few time-varying element which has resulted from a destruction or alteration in mechanical composition from fracture of parts. Furthermore, the unsteady behave of the system may cause disturbances, that lead to trigger resonances at the system or on sensors. Instant state estimation for complex systems are utilized inside a feedback loop to overcome destructive cases and the state estimation whenever there is a situation encountered that there is unknown of the desired states which cannot precisely calculated. Wiener was first introduced the research zone of state estimation, caused Kalman's endeavor. Besides, improvements and enhances in estimation and control theory with cooperate with computers, made it possible to form observers attached with instant convergence specifics. Alike observers can sustain safe and agile systems on the point of real-time incident view [26].

More specifically, the moment when encountered a high-rate dynamic region, the estimator competence to sense, analyze and anticipate the soundness of the system, might be precious for several varying parts. Nonetheless, this recognition and adjustment process solely handled when there is a time continuous estimation while the high-rate dynamic situation happen and high-rate at this juncture described as in microseconds.

Complex high-rate situation problem ingredients can be encapsulated by high amount of uncertainties comes with the extraneous forces, huge grade of unsteadiness and bulky disruptions, and originated from alterations in system adjustment sourced unknown dynamics.

Those three essential facts must be taken care of by a high-rate estimator that discriminates the system whether the system is high-rate or not. As a matter of fact that, easy enabling estimator contrast to intricate estimator, the easy one corresponds to having a better convergence rate achieved compared to the complicated estimator about computation, properties and application. On the other hand, applications and indicators are exposed to various type of incidents, they affect the act of observers [26].

In practices, there can be noise occurrence in measurements by the sensor, execution of algorithm and vitiation of estimation values, etc. By embedding a noise function truely inside a filter, noise can be removed but it brings out computational cost. The observer gain might be elevated to diminish time of convergence, but, it can arise an adverse impulse the accuracy of the estimation as the noise will gain a higher value. Another prevailing issue for numerous operable applications is uncertainty. All manner of approaches have been done to cope with system uncertainties. In a situation that there is a system with complex properties that results absence of a precisely comprehension of the physical depiction of the model, mostly data driven observers have dominance. Statistical methods work better in account of having the previous data information is current to provide totally comprehension of the statistical specification of the system's actions. Model-driven observers have the ability of rapid convergence and precise, exact estimations associated with well described system models. Nonetheless, in real time world environments, it is hard and severe process to model the systems exactly similar as in real world due to uncertainties [26].

Kalman filter (KF) is utilized to differentiate alongside a healthy and failure condition. Any of filter or observer has varying susceptibility to failure modes like system, actuator, control surface and sensor failures. The competence to distinguish between noise, gust and control input failures of a filter is important. Kalman Filter is an ideal prediction fact that has a sensitivity to individual and entire failure, such like a component (system or control surface), actuator and sensor failures, failure insensitive observer merely deals with sensor faults, Robust Kalman filter precise to system, actuator, sensor and nonconstant control surface and the last, Failure Mode Sensitive observers are solely cope with particular original failure modes. According to above-named filters and observers could be executed in the meantime inside the codes of failure detection and isolation [27].

3. METHODOLOGY

3.1 Overview

The paper is studied for linearized lateral dynamics of B-747 aircraft and sensor faults are integrated to the measurement channels of all the lateral states as sideslip as continuous bias fault on both sideslip angle and yaw rate sensors yet the remaining sensors which are roll rate and roll angle sensors have a measurement noise-increment sensor faults. For the last case, double sensor faults are performed at the same time on roll rate and roll angle sensor measurement channels. The linearization process is accomplished by using Matlab Simulink Linearization toolbox and the state-space model gathered.

Further the study took place in Matlab software and Kalman filter algorithm is used for estimation of the aircraft’ s lateral states and carry out the healthy system’ s actual values and estimated values are close to each other. The requirements for optimal linear Kalman filter algorithm such as process noise and measurement noise are presumed correctly and satifying results are succeded along the noise reduced and estimation values are converged.

Lateral measurement channels are malfunctioned through continuous bias and measurement noise-increment faults for a time period and measurement states are observed that errors are obviously implied. Varying Kalman filters are investigated to reach better estimation results and enhance estimation in more powerful way despite sensor fault occurs. Robust Kalman filter algorithm is embeeded with two types of scale factors in case of measurement noise increment fault, the single measurement noise scale factor and multi measurement nosie scale factor for fault isolation.Those two methods are compared to each other and the results are emphasized. The Robust Kalman filter algorithms are embeeded to the codes and estimation results are compared and assessed wisely.

Fault isolation is examined via threshold fact with chi-square test and the threshold value is determined to assess Kalman filter innovation sequence statistics.

After fault isolation is done, the robust kalman filter estimation values are seen entirely.

In searching of possible solution for the sensor fault conditions, the Reconfigured Kalman filter algorithm is used and for broken sensor channels, the input from measurement channels dimension is reduced therefore, the algorithm has more calculation load.

And for the last section, the nomimal case results and state estimation results of OLKF, RKF and Reconfigured KF are compared to each other in all fault cases based on the sight of root mean square error and the most efficient Kalman filter algotrithm that has superior resuts is pointed out carefully.

Also, civil aircraft model plant is studied for FDD related to enhance and indicate the feasibility of fault detection and diagnosis. A different mathematical solution is aimed to improve the fault detection operation for better flight performance. When sensor fault exist on civil aircraft' s lateral measurement channels, sensor value errors are recognized via measurements exceeded a minor threshold value. Thereafter, to prevent the aircraft expose to additional structural loads, which is a bad situation for all types of aircrafts, augmentation of the fault detection feedback is focused. For many flight simulation cases, the simulation terrain, circumstances are set up and the inspection of the system' s responses are evaluated. By this path, the aricraft preserve its constant flight form and submit a fast and accurate reply to displeasing sensor faults. Sensor fault occurrence is highly vital which could lead aircraft to lost its control system because it aims to gauge the system states and they have a huge affect on the process straightly whether they are merely used as inputs for feedback control. The measured outputs are generally more adequate to feed back the airplane for control ambition. In sight of the application of modern control theory, in the moment the measured outputs needs to have acceptable data related to system dynamics, it is convenient to use data to estimate and observe whole system state values. Following that, estimated values are exerted for feed back purpose.

A non-linear fixed-wing aircraft model which is tuned accurately in MATLAB Simulink program, is capable to calculate non linear dynamics, also has a control system to use for simulations. An ideal way of EFCS belong to a fixed airplane

EFCS consist of the elevator, rudder, ailerons, spoilers, flaps, etc. , moving surfaces, any of them are controlled by pilot from the cockpit, mechanical joint couplings and the required functions to sustain the control of the aircraft plant.

The mathematical model for actions of an airplane is mixture with complex subsystems and includes six set of nonlinear coupled differential equations, which is also named as six degree of freedom (6 DOF) rigid body formulations that come out from the result of carried out forces and moments resulted from aerodynamics, gravitation and thrust. To make it possible to reach easier calculations, those equations are separated to two types as lateral dynamics and longitudinal dynamic equations by taking particular suppositions. Comprehended to the true airspeed, altitude and flight path, a set of local approximates for the forces is planned. The main flight controls of an aircraft are roll, pitch and yaw control and managed by perturbation of ailerons, elevators and rudder and in addition to that, they have an effect on each other as a coupling effect. Lateral control system takes lateral stick inputs generated from pilot and provides anti-symmetric control demands throughout both interior and exterior control surfaces. For the required yaw angle, the pilot gives an input as sideways to the rudder. In our second study, the control system designed for yaw control. Inertial position changes, control inputs, airspeed and altitude are some of the states of the full nonlinear dynamics of aircraft model.

The sensor fault detection model is constructed and precise routes are defined with the nonlinear aircraft model. While the flight condition, the rudder is essentially regarded as the strongest element that plays part in lateral dynamics. Lateral oriented equations of motion (EOM) is integrated with side force, yaw moment, roll moment of aircraft displacement. The residual is spawned out from subtracting the estimated channel signal and monitored channel signal instantaneously. Fault appearance is determined by investigating the residual value. The evaluation is exerted whether its value exceeds a predefined threshold value or not and carries out the sensor that is broken. If the threshold value is higher than the residual value, this means the sensor remain healthy, however, if the value is surpassing the limit, there is a fault presence seen in sensor. Threshold limit is related to the residual error amount due to measurement errors, model approximates and disturbance signals because they are not precisely decoupled. The state measurement values are observed and analyzed in faulty and non-faulty conditions.

FDI scheme executes when solely one fault at instant time period is occurred in one sensor and basically this approach is valid. The judgment law could be handled to detect faults which has an impact on the whole renewal sequence.

When there is a sensor fault or an actuator fault, for the FDI, the flight control computer is responsible to find which sensor/actuator is faulty and estimate the sensor states or actuator's stuck position. Diagnosing the failed control surface or sensor and estimating their values are utilized for control implementation.
In the filter, the process of the sensor stuck fault and the rate of decrease in the control effectiveness is analysed. The measured value of the states and the values of the states which gained by estimation is going to be similar to each other in case of there is no fault seen. However, in case of a fault, the data gathered by the estimation filter and measured outputs will diverge. Whenever there is a stuck fault on a control surface of an airplane, it is difficult to warrant an FDI scheme related to bias influence that affects the control stuck surface and the contribution of any control surfaces can led to this control surface stuck fault. To give an example, if it is assumed to be there is a stuck fault at $5°$ on the left horizontal stabilizer of the airplane, the influence due to the stuck control surface is approximately similar to the right horizontal stabilizer that will have a stuck fault at $-5°$ [28].

EFCS has an integrated coupling elements also the divided subsystems have profoundly coupled and this results an absence of measured states. Analytical redundancy is performed in the view of isolation process in those systems. Into the high-fidelity model, sensor fault detection subsystem is embed which has coupling effects. This fault detection subsystem can detect bias, drift an enhanced sensor noise which has no backup as hardware, therefore analytically backed up. In EFCS, feedback loop utilize the measured sensor values of the states, so sensors play significant role. Analytical sensor redundancies such like fault detection systems, computes and detects the fault mathematically and alerts autopilot and control system instead of using hardware that are heavy, costly and vulnerable to physical effects. If the analytical sensor redundant system precisely measure and accurate for the system model, it gives an advantage for the civil or military aircraft by means of flight performance. Our focus is on the field of lateral dynamics model of civil aircraft and how to implement a sensor analytical redundancy. The sensor is stuck at determined range of values and gives incorrect output values and instantly identified by the fault detector and indicated at the subsystem which is named fault indicator. After detection complete, a reconfiguration system activated as to gain estimated signal value from the mathematical model instead of the erroneously sensor signal from the feedback loop.

Full description model of the civil aircraft is established by management process which includes simulation of the ambiance, gust and wind and disturbances, implementing the algorithms, and construction of many subsystems. The detection and reconfiguration to sustain a safe flight is illustrated by those subsystems and adjusted, well organized in the simulation model. Each of the subsystem has specific responsibility and they maintain each other as input and output data to accomplish the detection of fault on sensor and followed by taking the necessary action to overcome the faulty condition and enhance the situation that the pilot encounters. All necessary adjustments can be arranged by changing the properties of subsystems and the full high fidelity model status can be observed entirely yet, the more complexity system is, the more subsystem it includes.

In MATLAB Simulink, a cruise flight at a constant altitude and airspeed is treated with maintaining flight safety. In every situation during flight such as a change in yaw and roll angle do not alter airspeed of the aircraft and altitude is steady because there is an equilibrium in forces that the thrust force is in equilibrium with the drag force and weight force is equivalent with the lift force. Simulation process is performed with properly adjusted parameters which consist of altitude, angular rates, positions and time. Those parameters will match the requirements of a constant flight path during flying straight and level and it is essential to adjust parameters because by this way, the aircraft will precisely answer about the level of noise and model faults.

Single fault is utilized and steady state flight is appointed to point out input and output adjustment separately.

The navigation sensors gauge the acceleration and rotation value of the aircraft and use them to calculate the position and also use them to integrate with the speed and direction values, and followed by indication of the data to the pilot when the flight is performing. The errors showed up on the position may flourish as a result of minor uncertainties in the measurements by time. Sensor faults are considered as the main resource of the faults compared to the other fault references such like turbulence, wind, gusts and instant temperature changes and the sensor noise which is occurred by bias or white noise, may have a huge influence on the FDI process. For the reason that they have similar properties, it is hard to distinguish between sensor faults and sensor noise.

3.2 Analyze of Boeing-747 Data

In this study, the aircraft model is a civil aircraft type of Boeing-747 that has four turbofan engines, wide body inter-continental aircraft. This model serves as a suitable multi-purpose test bed for model and design approach. The Boeing-747 aircrafts specifications are; a flight range of 11,000 kilometers, a cruise speed of 910 km/h and an altitude of 10,500 m.

The main focus in this study is the lateral orientation of the civil aircraft. The equations of motion are exactly present lateral and linear motions. Lateral dynamics are separated from the longitudinal dynamics yet, they have a contribution with lateral dynamics as directional. Transfer functions that cover longitudinal input parameters to lateral output parameters are not described because the numerical model of airplane has decoupled minor disturbances [29].

Contrariwise to the longitudinal dynamics, clarification of lateral directional dynamics is hard on behalf of stability procedure do not differ. Emphasizing that commonly it originates a remarkable value of coupling fact [30].

Nonlinear model of Boeing 747 proposes whole nonlinear dynamics. Altering the lift on the rudder, yaw control is achieved and also deflexion of a control surface both changes the angular rate and moment of center gravity (g).

We can see aircraft reference frame relate to body-fixed frame F_E in Figure 3.1. F_O means origin at g, F_W means wind axis reference frame, F_S means stability axis reference frame and F_B means body fixed reference frame. If the angular rate is changed, it has an impulse at sideslip and roll angle instantly. Furthermore, on control surfaces on the airplane, there are coupling effects on each other during the action. For example, reaction to the deflection of a specific control surface or the whole control surfaces, yaw rate (r) could be changed.

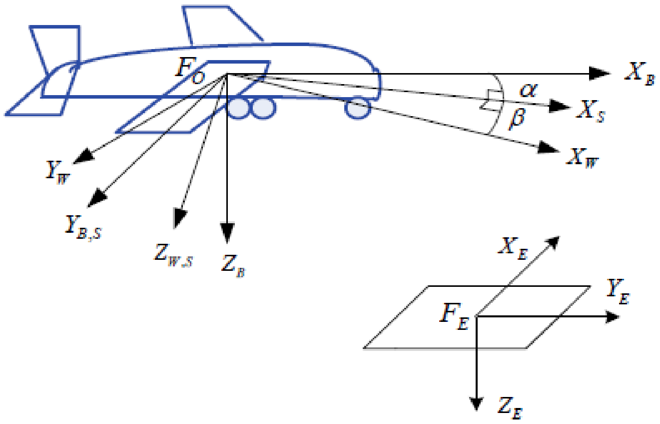

Figure 3.1 : Framework of aircraft references [14]

To maintain linear estimation method, linear time invariant (LTI) system is used in Boeing 747 because LTI models guarantee a reliable accurate linear model for closed loop feedback system. Linearization is done on trim region of aircraft which are a true air speed of 0.85 Mach and an altitude of 35,000 ft and those parameter values result fewer faults because of being at trim points.

The trim fact is vital for investigating aircraft attitude behavior. By this way, the non linear equation of motion of the aircraft can be solved to gather state and control vectors that satisfy the states time derivatives are equal to zero or have a steady value. Some necessities, restraints are assumed to accomplish a balance of the plant.

The perturbation inputs and remaining states of the aircraft are replaced by trim calculations related to condition of action that the time derivate of whole angular velocities are zero. There are many situations that trim fact can be utilized such as steady state flight, level turn, push-over/pullover, specific power turn, thruststabilized turn and beta trim and every condition has its specific requirements and challenge and segregated parameters, i.e. flight controls, airplane states and engine states [14].

Adjustment of parameters of Boeing 747 Model is done via using MATLAB Simulink. The altitude of the airplane which performs a cruise flight is 10,500 m and a true airspeed (TAS) of 910 km/h. Trim and linearization process is applied at this flight condition and the specifications are demonstrated such like trim data, lateral direction inertia and aerodynamic coefficients in Table 3.1 [29]. The nominal data value of mass and inertia are constant and if an airplane flies into a non-trimmable scope, a fault is considered as non atonable.

Table 3.1 : Boeing 747 trim conditions and aerodynamic coefficients.

Initial Flight Condition of Boeing 747	Value
V_T	826.772 ft/s
α	0.0582 rad
β	0 rad
φ	0 rad
$\emptyset$	0 rad
p	0 rad/s
q	0 rad/s
r	0 rad/s
θ	0.0436 rad
x_e	0 ft
y_e	0 ft
h_e	35,000 ft
δ_{th}	0.49 rad
δ_a	0 rad
δ_e	0 rad
δ_r	0 rad
$Geometry\ and\ Inertias$	$Value$
S	5500 ft^2
b	196 ft

Table 3.1(continued) : Boeing 747 trim conditions and aerodynamic coefficients.

Initial Flight Condition of Boeing 747	Values
m	$636{,}636\ lbs$
I_{xx}	$18.2\ x\ 10^6\ slug-ft^2$
I_{zz}	$43.1\ x\ 10^6\ slug-ft^2$
I_{xz}	$0.97\ x\ 10^6\ slug-ft^2$
Lateral aerodynamic stability coefficients	Value
c_{l_β} : roll moment caused from sideslip angle derivate	-0.160
c_{l_p} : roll moment caused from roll rate derivate	-0.340
c_{l_r} : roll moment caused from yaw rate derivate	0.130
$c_{l\delta_a}$: roll moment caused from aileron deflection	-0.013
$c_{l\delta_r}$: rol moment caused from rudder deflection	0.008
c_{n_β}: yaw moment caused from sideslip angle derivate	0.160
c_{n_p} : yaw moment caused from roll rate derivate	-0.026
c_{n_r} : yaw moment caused from yaw rate derivate	-0.280
$c_{n\delta_a}$: yaw moment caused from aileron deflection	-0.001
$c_{n\delta_r}$: yaw moment caused from rudder deflection	-0.100
c_{y_β} : side force caused from the side slip derivate	-0.900
c_{y_p} : side force caused from roll rate derivate	0
c_{y_r} : side force caused from yaw rate derivate	0
$c_{y_{\delta_a}}$: side force caused from aileron deflection	0
$c_{y_{\delta_r}}$: side force caused from rudder deflection	0.120

Solving EOM to describe lateral movement of the aircraft, the derivative values of L, N and Y related to the non dependent variables v, p and r, are gathered by estimating whole coefficients.

c_{l_β} is named as dihedral effect. This effect is resulted from β disturbance seen and makes the airplane gain a tendency to roll therefore, it plays a crucial role in planning the lateral static stability. By the way, it has a relation with wing dihedral, wing sweep that belong to the shape of wing, fuselage and fin.

c_{l_p} is named as roll damping. It is a result of mostly wings and tail. When pilot rolls the airplane, one of the wing pressure raises and that led to a boost on lift force while other wing looses lift force. This character response can be seen as the action of yaw made by pilot, yet c_{l_r} has fewer quantity compared to c_{l_p}. The flight control system becomes unsteady if c_{l_p} has positive values.

c_{l_r} is called cross-couplink effect and this is a result, as the aircraft yaws, wing and vertical tail causes an α value change and so, the lift expanded.

$c_{l\delta_r}$ is called roll resulted from rudder. On behalf of an aircraft with conventional vertical tail, as the vertical tail' s center of pressure (cp) is above the center of gravity, this effect seen.

$c_{l\delta_a}$ is called lateral control power. Ailerons make it possible for pilot to give roll action to the airplane and they play essential role. Besides ailerons roll control, rudder deflection can contribute to roll action by resulting lift forces on the wings and roll moment appears. However, it has minor addition on roll control action with regard to ailerons.

c_{n_β} is static directional stability or another name called as weathercock stability. The airplane has a prior tendency to return to its former equilibrium sideslip angle point and generally it has a value of zero. The main mission is to sustain aircraft directional dynamic stability. The c_{n_β} amount is given with regard of vertical tail, fuselage and wing for any β.

c_{n_p} is a moment appeared by the drag occurrence on the wing surface during the aircraft' s roll movement.

c_{n_r} is if there is a pitch movement of the aircraft, it maintains weathercock damping comparable to c_{m_q}.

$c_{n\delta_r}$ is called rudder power, has a significant effect on deflection on the rudder therefore, it is the control mechanism of the aircraft' s yaw action. Also, aileron deflection contributes airplane to roll resulted from the drag which occurred on both ailerons during their movement.

3.3 Mathematical Model of Aircraft

3.3.1 Rigid body equations of motion

Equations of motion (EOM) is derived on the following assumptions:

- The aircraft is rigid
- The earth is flat and non-rotating
- Constant aircraft mass during flight
- Symmetry in the X_bZ_b plan which means the moment of inertia I_{xy} and I_{yz} are equal to zero. This assumption is eligible for an undamaged aircraft. In the case of the aircraft is influenced from asymmetric damage, the assumption does not work anymore.

According Newton' s Second Law Aircraft EoM:

Outer forces are thrust, gravity, aerodynamic forces and engine moments, aerodynamic moments are the external moments. Equations of external forces are shown as Eq.(3.1), Eq.(3.2), Eq(3.3) and the equations of outer moments are shown as Eq.(3.4), Eq.(3.5), Eq(3.6) with respect to [14] based on aerodynamic coefficients.

$$F_x = \frac{1}{2}\rho V_t^2(-c_D\cos\alpha + c_L sin\alpha) + F_{T_x} - mgsin\theta \quad (3.1)$$

$$F_y = \frac{1}{2}\rho V_t^2 Sc_Y + F_{T_y} - mgcos\theta sin\emptyset \quad (3.2)$$

$$F_z = \frac{1}{2}\rho V_t^2 S(-c_D\sin\alpha - c_L cos\alpha) + F_{T_z} - mgcos\theta cos\emptyset \quad (3.3)$$

$$M_x = \frac{1}{2}\rho V_t^2 Sbc_{lb} + M_{engx} \quad (3.4)$$

$$M_y = \frac{1}{2}\rho V_t^2 Sb\bar{c}c_{mb} + M_{engy} \quad (3.5)$$

$$M_z = \frac{1}{2}\rho V_t^2 Sbc_{nb} + M_{engz} \quad (3.6)$$

3.3.2 Nonlinearity and linearity conversion

The linearization is succeded by converting a non linear model to a typically complete or nearly to linear model, which makes it possible to linearize a complex system and move with a feasible non linear flight control system issue. The representation of partial matrix derivatives of the lateral states that relates small iterations from input and the related outputand it can be used to non linear systems such input state linearization or to the systems which needsall state measure with minimum phase models [31].

An airplane is a complex nonlinear system as it's EOM includes 12 first order non linear differential equations and 6 of them represents dynamic and remaining 6 are kinematic. Also, in dynamic equations, they includes 3 force and 3 moment equations, meanwhile in kinematics, 3 equations relates navigation and the rest 3 are describing equations of Euler angles.

Lateral dynamics equations with aerodynamic coefficients are considered through nine nonlinear equations linearized in steady state trim point. After linearization, they are utilized in the simulation' s Kalman filter section to perform sensor fault detection process. In some flight conditions whenever there is ability of aircraft to function in the equilibrium region, for example a steady state cruise flight, pull up, pull down, climb, coordinated turn and power approach, linearization can be done. In every flight conditions as pointed, for faulty case the flight parameters are adjusted at FDI scheme as suggested. If there is a parameter that is not in the identified region, FDI scheme indicate an error.

A way of converting non linear equations to linear equations is called "small-disturbance theory". What is accomplished by this theory is every variable data in non linear equation is altered by an initial foreknown value and a disturbance value or a perturbation. As robust systems deal with stabilizing systems which encounter perturbations, they result disturbances and measurement noises. To facilitate robustness, symmetrical flight condition and exterior forces are claimed to be consistent. Sensor faults affect the whole airplane structure. Differential non linear equations of B 747 is obtained from [14] and shown in Eq. (3.7), Eq. (3.8), Eq. (3.9), Eq. (3.10).

$$\dot{\beta} = \frac{1}{mV_t}\Big(-F_x cos\alpha sin\beta + F_y cos\beta - F_z sin\alpha sin\beta - mV_t(-psin\alpha + rcos\alpha)\Big) \tag{3.7}$$

$$\dot{r} = \left(\frac{\big(I_{xx} - I_{yy}\big)I_{xx} + {I_{xz}}^2}{I_{xx}I_{zz} - {I_{xz}}^2}p - \frac{\big(I_{xx} - I_{yy} + I_{zz}\big)I_{xz}}{I_{xx}I_{zz} - {I_{xz}}^2}r\right)q + \frac{I_{xz}}{I_{xx}I_{zz} - {I_{xz}}^2}M_x + \frac{I_{xx}}{I_{xx}I_{zz} - {I_{xz}}^2}M_z \tag{3.8}$$

$$\dot{p} = \left(\frac{\left(I_{yy} - I_{zz}\right)I_{zz} + {I_{zz}}^2}{I_{xx}I_{zz} - {I_{xz}}^2} r - \frac{\left(I_{xx} - I_{yy} + I_{zz}\right)I_{xz}}{I_{xx}I_{zz} - {I_{xz}}^2} p\right) q + \frac{I_{zz}}{I_{xx}I_{zz} - {I_{xz}}^2} M_x + \frac{I_{xz}}{I_{xx}I_{zz} - {I_{xz}}^2} M_z \tag{3.9}$$

$$\dot{\emptyset} = p + tan\theta(qsin\emptyset + rcos\emptyset) \tag{3.10}$$

In accordance to small-disturbance theory, the equations are established in the way to achieve non linear equations to become partially linear systems. This approach utilize minor changes of the aircraft motion from steady flight case. System state matrices computed from equations Eq. (3.11), Eq. (3.12), Eq. (3.13), Eq. (3.14) and Eq. (3.15) [32]. Based on the linearity fact, a system is linear if there is a magnitude between the input and output and it is fixed else, it can be said that the system is nonlinear. The aircraft plant system is modeled as a varying complex system so contents nonlinear equations in force, moment and motion. In equation Eq. (11) the partial derivatives of the lateral states are shown in matrix form. The input which is a small alteration is linearized and output is gathered.

$$\begin{bmatrix} D\beta \\ D\hat{p} \\ D\hat{r} \\ D\emptyset \end{bmatrix} = \begin{bmatrix} \dfrac{c_{y_\beta}}{2\mu} & \dfrac{c_{y_p}}{2\mu} & \dfrac{c_{y_r} - \frac{2\mu}{A}}{2\mu} & \dfrac{c_{w_e} cos\gamma_e}{2\mu} \\ \dfrac{c_{l_\beta}}{I'_x} + I'_{zx} c_{n_\beta} & \dfrac{c_{l_\beta}}{I'_x} + I'_{zx} c_{n_p} & \dfrac{c_{l_r}}{I'_x} + I'_{zx} c_{n_r} & 0 \\ \dfrac{c_{n_\beta}}{I'_z} + I'_{zx} c_{l_\beta} & \dfrac{c_{n_p}}{I'_z} + I'_{zx} c_{l_p} & \dfrac{c_{n_r}}{I'_z} + I'_{zx} c_{l_r} & 0 \\ 0 & \dfrac{1}{A} & \dfrac{1}{A} tan\gamma_e & 0 \end{bmatrix} \begin{bmatrix} \beta \\ \hat{p} \\ \hat{r} \\ \widehat{\emptyset} \end{bmatrix} + \begin{bmatrix} \dfrac{\Delta C_{y_c}}{2\mu} \\ \dfrac{\Delta C_{l_c}}{I'_x} + I'_{zx} \Delta c_{n_c} \\ \dfrac{\Delta C_{n_c}}{I'_z} + I'_{zx} \Delta c_{l_c} \\ 0 \end{bmatrix} \tag{3.11}$$

$$I'_x = A(\hat{I}_x \hat{I}_z - \hat{I}_{zx}{}^2)/\hat{I}_z \tag{3.12}$$

$$I'_z = A(\hat{I}_x \hat{I}_z - \hat{I}_{zx}{}^2)/\hat{I}_x \tag{3.13}$$

$$I'_{zx} = \hat{I}_{zx} \;/\; A(\hat{I}_x \hat{I}_z - \hat{I}_{zx}{}^2) \tag{3.14}$$

$$\begin{bmatrix} \Delta c_{y_c} \\ \Delta c_{l_c} \\ \Delta c_{n_c} \end{bmatrix} = \begin{bmatrix} c_{y_{\delta r}} & 0 \\ c_{l_{\delta r}} & c_{l_{\delta a}} \\ c_{n_{\delta r}} & c_{n_{\delta a}} \end{bmatrix} \begin{bmatrix} \delta_r \\ \delta_a \end{bmatrix} \tag{3.15}$$

3.4 Fault Detection Method

In the trimmed model of LTI Boeing 747 in steady state flight the lateral axis is simplified which is performed in the simulation that has four main states (x) that are consist of sideslip angle (β), yaw rate (r), roll rate (p) and roll angle $(\emptyset)$ as given Eq.(16) and two inputs (u) that includes the rudder deflection (δr) and aileron deflection (δa) given in Eq.(3.17) [33]. Aircraft main states are the true airspeed, angle of attack, sideslip angle, angular rates, Euler angles, earth-fixed referenced frame positions and altitude. In this study, a fault is assumed to be in Beta state sensor and the others are well processing. Due to that, the sideslip angle sensor is broken so all the lateral states are affected laterally.

Both pilot commands and controller command signals are routed through the actuator feeding mechanism. To design an optimal observer, it is aimed to suppose that the sensors are optimally working and to make it possible, the inputs are fed through the observer. On another aspect of view, the sensors are disturbed by white noise in the simulation which are related with the autopilot control. The sideslip force attributes a parasite drag and make the aircraft more lift because of the blanking reaction of the fuselage and by detecting the situation, it is vital to decrease this parasite drag.

Sideslip angle related errors can be seen in two different ways which are calibration error and additional white noise modelling the sensor defectiveness.

$$x = [\beta, r, p, \emptyset]^T \tag{3.16}$$

$$u = [\delta a, \delta r]^T \tag{3.17}$$

The steady state case is established and investigated with different simulation conditions. The flight specifications are, cruise flight at the 35000 ft altitude and a speed of 0.85 Mach. To design a model-based flight detection and diagnosis FDD observer, the lateral dynamic approach is utilized. The linear state-space equations are given in Eq. (3.18) and Eq. (3.19). For the success of the linearization, state-space equation shows the system model is static, does not change over time, so A and B system matrices are steady. From another point of view, the nonlinear B-747 aircraft model is not afflicted by the conversion. During there are faults on the lateral states, the lateral attitude of the aircraft is analyzed.

$$\dot{x} = Ax + Bu \tag{3.18}$$

$$y = Cx + Du \tag{3.19}$$

3.4.1 Method for linearization

In this study, the state transition matrix (A), input matrix (B), output matrix (C) and the feed forward matrix (D) are found by using linear analysis tool of MATLAB and given in equations Eq. (3.20), Eq. (3.21), Eq. (3.22) and Eq. (3.23) are convenient for trim values of the plant at steady state cruise flight at 35,000 ft altitude and 0.85 Mach true airspeed. The linearization proces is carried out by the help of Linear analysis tool in MATLAB Simulink. Firstly, lateral inputs selected and small disturbances to deflections on the input are given, then lateral states are selected as open loop output of the aircraft model and the last action is to run the simulation of the whole model, the system matrices below are accurately gained as below:

$$A = \begin{bmatrix} -0.08895 & 0.06282 & -0.9795 & 0.04362 \\ -2.419 & -0.6024 & 0.3438 & 0.01244 \\ 1.491 & -0.2827 & -1.19 & -0.2719 \\ 0 & 1 & 0.05824 & 0 \end{bmatrix} \tag{3.20}$$

$$B = \begin{bmatrix} 0 & 0.01024 \\ -0.1967 & 0.09127 \\ -0.0138 & -0.5503 \\ 0 & 0 \end{bmatrix} \tag{3.21}$$

$$C = \begin{bmatrix} 1000 \\ 0100 \\ 0010 \\ 0001 \end{bmatrix} \tag{3.22}$$

$$D = \begin{bmatrix} 00 \\ 00 \\ 00 \\ 00 \end{bmatrix} \tag{3.23}$$

By comparing the actual non linear system' s lateral state output and the related system model which is established by the linearized system state space matrices, it can be concluded that our linearized lateral state model is convenient. The system states of the lateral outputs are shown in the following figures from Figure 3.2 to Figure 3.5.

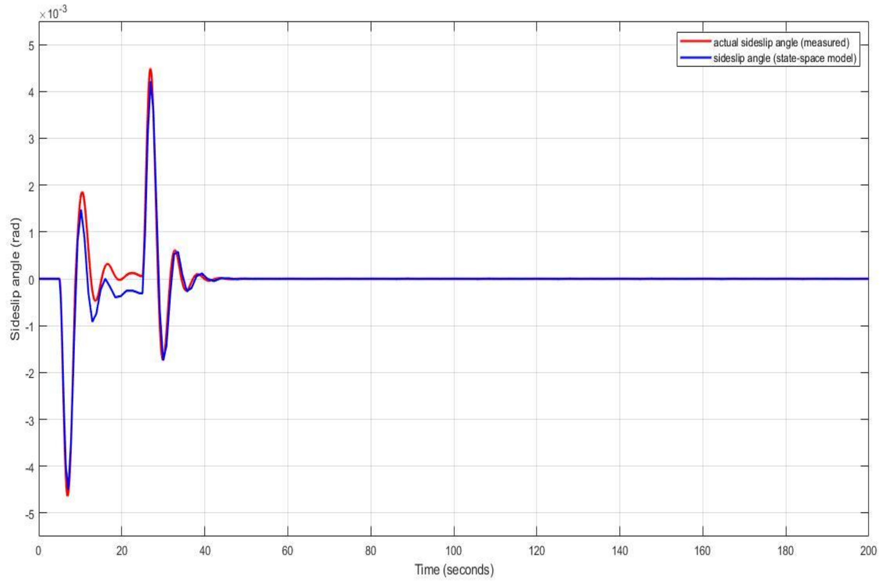

Figure 3.2 : Sideslip angle vs. time.

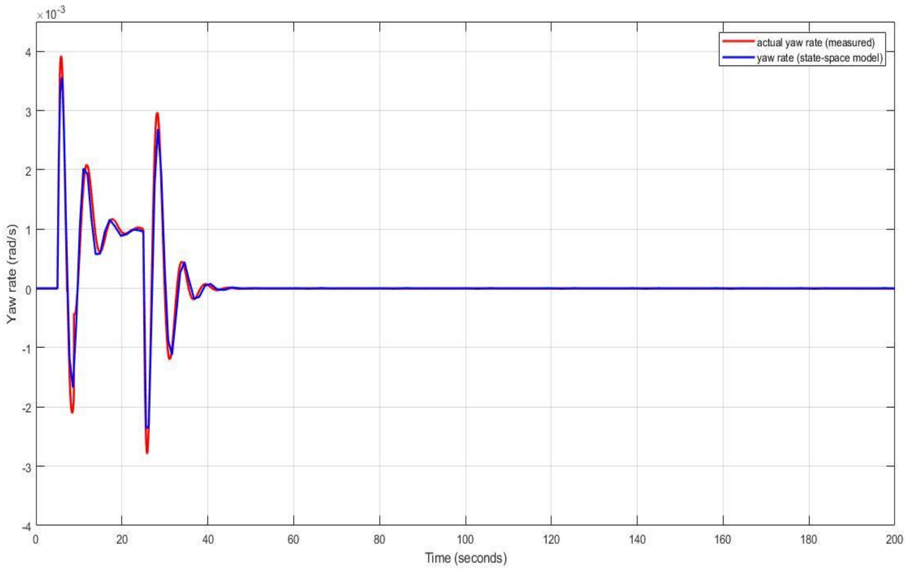

Figure 3.3 : Yaw rate vs. time.

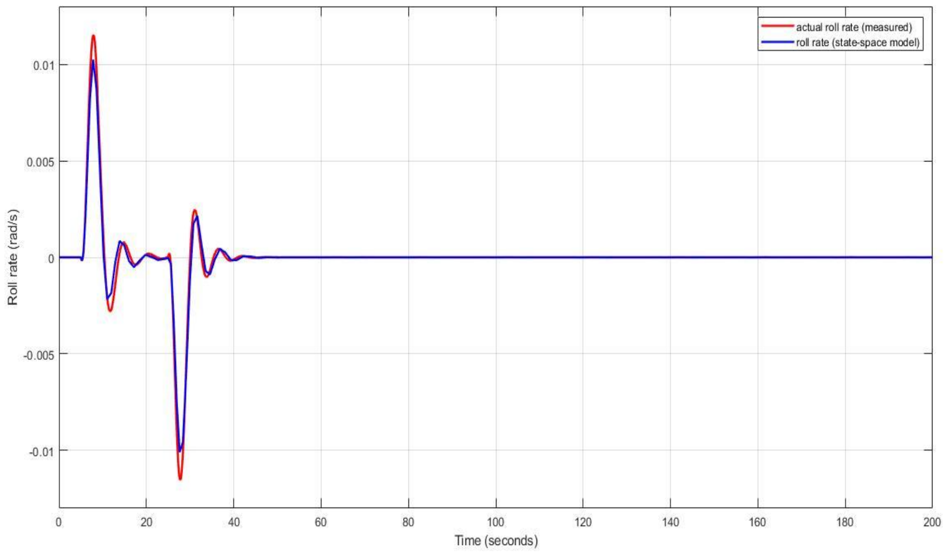

Figure 3.4 : Roll rate vs. time.

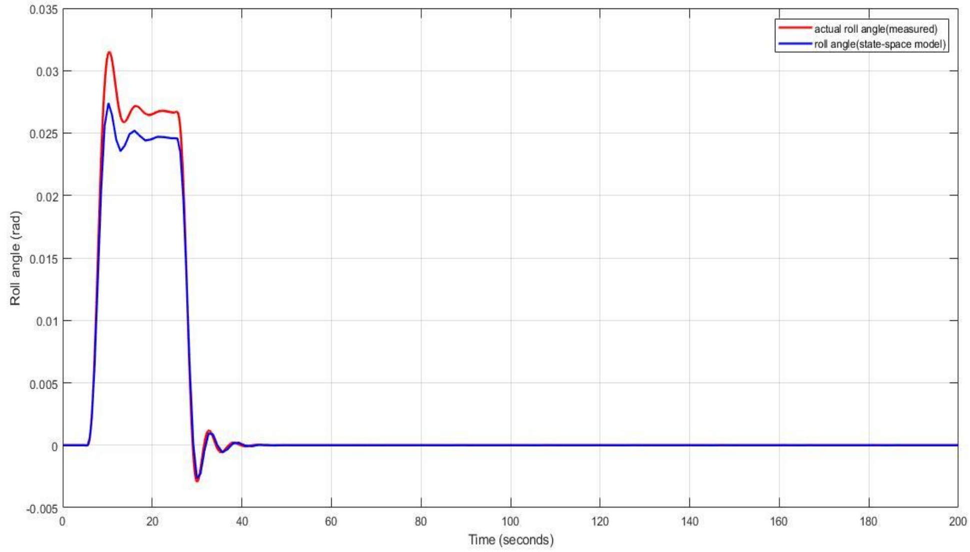

Figure 3.5 : Roll angle vs. time.

Input of a rudder $\delta r = 0.015\, rad$, the sensor measurements and the state-space model measurements are converged to each other very likely to be the same. With respect to the linearization efforts above, now as the linear state-space system can be confirmed and logical to be used with the linear observers in an adequate way.

At any flight case, if the platform parameters take another value, it means that there is a faulty condition and must be detected by state estimation. For example, if not smoothed, a sensor failure will result on false estimation of the matrix A or an actuator failure will result an incorrect value that is gathered by the matrix B. Shortly, the state-space system matrices must not be change at any altering flight conditions to make the steady state safe flight. And another important example is if there is a structure loss at the aircraft, incorrect values can be seen of system matrices A, B, C, D. [34]

3.4.2 System matrix poles

To determine the modes of the system and the poles of the transfer function, the system poles matrix A is computed in MATLAB. By analyzing the poles of, we are able to say that the system is stable due to the fact that the poles have negative values and they are accumulated on the left side region of the y-axis which are show following:

Dutch roll (oscillatory): $-0.2900 + 1.0768\mathrm{i}, -0.2900 - 1.0768\mathrm{i}$

Roll damping (fast real): $-0.6507 + 0.4098\mathrm{i}, -0.6507 - 0.4098\mathrm{i}$

3.4.3 Established subsystems in Simulink

Various analysis operations are examined to gain the residual. The threshold concept is done by a fine framed -n process to analyze residual transferred by assigned observers to identify the fault. A simple approach to threshold method to evaluate the residual value is obtained through:

$$\begin{Bmatrix} \|t_i(t)\| < t; & healthy\ case \\ \|t_i(t)\| \geq t; & faulty\ case \end{Bmatrix}$$

Here, $t_i(t)$ refers the online time and t refers to the time of detect and given an equation Eq. (26) used to perform simulation cases.

$$t = Nx\ dt \tag{3.24}$$

To acknowledge measurement fault of sideslip angle (β) sensor, fault indicator subsystem is practiced.

As to fault indication, sideslip angle (β) is reached from other states with the help of Demux. β sensor is conveyed through fault introducer and then, we got the faulty signal β which is multiplexed with other healthy sensor states using Mux in Fault indicator subsystem. By this way, we establish the faulty state vector as $xFaulty$. And then, reconfiguration is done by reconfiguration subsystem. The reconfiguration subsystem is maintained by reconfiguring $faulty\ (\beta)$ signal and then we gather the reconfigured signal as $\beta\ (\beta_{out})$ which is utilized to amend the faulty state vector $xFaulty$ in a failure situation. After the corrected signal is rearranged as β_{out}, it is multiplexed with the remaining three states of $xFaulty$ and the remaining thirty-six auxiliary healthy states to embodiment the right state vector fed through nonlinear Boeing 747 aircraft model. β sensor state is terminated with the use of Terminator block [14].

Fault Introducer is executed by N -Sample Switch as a Simulink block. In our case, continuous bias fault is introduced at $t = 40\ s$, of the faulty condition in the model. Sensor measurement bias fault is defined by if-else condition, output signal is equal to healthy signal if $t\ < 40$ s, else if $t\ \geq 40$ s, the output signal is equal to faulty signal. N-sample switch block engenders the signal connected to the healthy signal gate and N is implied in Switch count variable. Fault applied till 60th second and after that t > 60 and continuous bias is extracted from measurement channel [19].
At the time the fault indicator signal is come up instantaneously, the verge amount of the sensor fault signal is actuated in the detection time. For reconfiguration process, fault indicator signal is utilized as if the estimated signal exceeds the foreknown, predefined threshold value, the signal(s) must be corrected. To avert from false alarms, not only the threshold value must be larger than the normal diversity in fault estimation signals, but also not be to high because it can lead to missing of the faults. The threshold value is selected as "0.8" and it fits well as an optimal value during evaluation of the planned filter algorithm in fault schemes [19].

From sensor the estimated value which is gained from mathematical model, is preserved in the reconfiguration block on behalf of the faulty sensor signal in the feedback loop and it is designed as a model in the reconfiguration subsystem for two approaches: Firstly, in Fault Indicator, detect faults and indicate them by figuring out the differences between aircraft sensor output β and observer estimated β_e value which is located in the Reconfiguration subsystem. Secondly, make a decision between the observer estimated value β_e on behalf of faulty sensor output β during the fault indication process. The switch occurs between the lateral states which are estimated by two Kalman Filters in regard of 0.8 threshold value. In Chapter 4, it is discussed more in detail.

The fault detection and reconfiguration is succeeded by the cooperation of an observer and Canberra metric in the Reconfiguration subsystem. With utilization of Canberra metric fact, stuck fault is detected by Fault detection model. Here, the Canberra metric is a method that evaluates a distance metric to point out affinity analysis. In Eq. (3.25), the generalized equation is given. The difference is taken in the nominator and it is normalized in the denominator.

$$Canberra\ Metric = \frac{|observed - measured|}{|observed| + |measured|} \tag{3.25}$$

So, β signal from Fault Indicator subsystem and β_e signal from Observer subsystem are compared in the Canberra metric and an $'\,S\,'$ signal is generated which has a role in the reconfiguration process. Therefore, Canberra metric can come up with a solution that how much affinity between β and β_e are close to each other. The input is created by an 'S' signal and goes into transfer function block of Simulink that acts like a filter, and this way signal is smoothened. Related to sideslip angle β, the mathematical formula is represented in Eq. (3.27) [14].

$$S(t) = \frac{|\beta(t) - \beta_e(t)|}{|\beta(t) + \beta_e(t)|} \tag{3.26}$$

If $\beta = \beta_e = 0$ then it is assumed to be $S(t) = 0$

Reconfiguration subsystem is facilitated in Simulink by implying Eq. (3.27) done by using "$Switch$" and "Abs" block. The output of the “Abs" block take absolute value of input data and smooths signal 'S' and the value demonstrate fault appearance. If the value is equal to or exceeds the threshold value, in our case it has a magnitude of '0.8', this means there is an error.

There is another area of utilization of the fault indicator which is the a control signal value necessary for the switch mechanism in the Reconfiguration subsystem. This control signal of Switch is gathered from Abs block. Switch performs the equation as shown [14].

$$\beta_{out} = \begin{cases} \beta, & |Control\ signal| < 0.8 \\ \beta_e, & |Control\ signal| \geq 0.8 \end{cases} \tag{3.27}$$

It is performed by logical if-else statements located in Switch block in Simulink. While a fault is detected, instantly reconfiguration issue the decision of taking β_e from the observer with the switch mechanism.
Kalman filter is founded in observer subsystem and it estimates the aircraft' s sensor states of sideslip angle (β), yaw rate (r), roll rate (p) and roll angle $(\emptyset)$ and to be able to estimate those states, our observer subsystem gets healthy sensor outputs from the non-linear model.

Correlated with the subsystems shown on top, the whole integrated aircraft closed-loop model architecture, including fault detection and reconfiguration and observer based estimation subsystems, established in MATLAB Simulink is illustrated in Figure 5.1 for Kalman Filter.

3.4.4 Residual generation

Observer-based method is available and comprehensible merely in systems working on the same instant time, which disables and requires design restrictions. Fault detection with observer based method purposes a residual generation. The residual is generated by subtracting state value from actual system and model system and reach a difference value. This process is given in Figure 3.2.

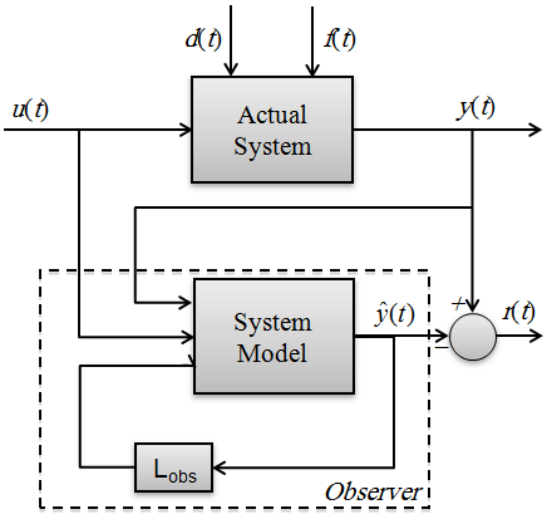

Figure 3.2 : An observer utilizing process for establishing residual [35].

3.5 Kalman Filter

Beyond the filters, the Kalman filter is very famous in industry applications and it was first introduced by Rudolf Kalman. After its function utilized by NASA project, it become a reputed filter. There are several engineering systems that Kalman filter took part in such image processing, computer vision, navigation, aircraft tracking with radar, etc.. It is a looping filter that fits online real-time digital processing and have simple to embed [25]. Related to indirect, inaccurate and uncertain observations, Kalman filter performs as an optimal observer by minimizing the estimated parameter error value due to Gaussian noise. By focusing the difference of the signal values of true measurements and estimated output values, and the difference is called a 'residual signal' and this way, Kalman filters looks at the residual value and notice faults or failures and behaves as an observer.

For a Kalman filter, it is essential to accomplish the mission of estimate variables whereas it is not possible to measure straight. Kalman filter has an algorithm embed with two stages as estimation and enhancing the states and it has the ability to measure instant states because it has a looping-recursive measuring property yet, it requires a foreknown computer variables and uncertainty matrices for accurate calculations. In prediction stage, anterior information of how the system acts as time continues is utilized. For example, beyond variable values come nearly to current values by multiplying with appropriate system matrices. System matrices are adjusted on the view of convenient designed system model. The estimated values have new values by a weighted average as the outcome of consequent measure is taken care. Continued weight is given to the predicted data results precision on the system model. In the correction stage(enhancing), actual measurements are used and it can be defined that the actual measurements and estimated measurements interact.

There comes a residual with the difference of those two notions and it is multiplied with Kalman gain matrix and necessary values are summed up to estimation variables. To assume that the designed system model is nearly acceptable to a level of additive Gaussian noise which has a known variance, regardless of initial conditions, the Kalman filter manage to reach a convergence with the steady state condition. This means that a focus on estimation of the noise variance is required because noise variance matrices and covariance matrices are related to the state and measurement model.

Kalman filter is superior on remaining observers from sight of optimal calculation of Kalman filter gain. The Standard Kalman filter does not automatically adjust Kalman gain matrix due to standing error statistics match in the designed model, so, it is not an adaptive filter. What makes it preferable along with the other observers is it minimizes the estimation error variance and it is performed whenever there is a control system with lack of estimations of the process variables that must be known formerly for control action.

Due to system model linearity characteristics, assumed distribution and computational cost value, there are several types of Kalman filters. The linear Kalman filter has Gaussian distribution and it has the lowest computational cost. The Extended Kalman filter is locally linear and has a Gaussian distribution and has low computational cost and the last one is the Unscented Kalman filter which is for nonlinear models, again it has Gaussian ditribution and hast the highest calculation memory.

Table 3.2 : Variety of Kalman filters.

Input Sensor	Model	Assumed Distribution	Computational Cost
Kalman Filter	Linear	Gaussian	Low
Extended Kalman Filter	Locally Linear	Gaussian	Low (if Jacobians need to be analytically computed)
Unscented Kalman Filter	Nonlinear	Gaussian	Medium

A linear system' s state-space model is described in Eq. (3.28). Here we add a Gaussian white noise with a zero mean and unit covariance matrix, because that pretend like the behavior of the measurement uncertainty that is caused by the model mismatch or input data is not convenient. In Eq. (3.28) we add the Gaussian white noise and equation becomes a new equation in Eq (3.29). System output equation is in Eq (3.30).

$$x_k = Ax_{k-1} + Bu_{k-1} \tag{3.28}$$

$$x_k = Ax_{k-1} + Bu_{k-1} + w_k \tag{3.29}$$

$$y_k = Cx_k + z_k \tag{3.30}$$

Here k is for time, A is transition matrix that relates former time step, B is input matrix for control input, x means state of the system, u is known control input, y is the measurement output, w means the process noise and the last z means the measurement noise. Generally thw whole quantitatives are in vector form so at least 2 components they are made of. System' s instant value is in (x) – state. Measured output (y) is diverted by measurement noise (z) and the (y) is playing a role on gain estimation of the state (x) by this way, the gain value enhances the state x condition.

Measurement output (y) value is not pure because of the impulses it exposed to noise. The value of the variance is not known therefore it is estimated. The measurement noise (z) is a Gaussian white noise and it has a zero mean and unit covariance matrix.

The residual gathered by the actual states and the estimated states, makes it possible to use conventional Kalman filter. Unknown data variables are ignored in model as to diminish the complexity of the model. From real aspect, the values of noise covariances R and Q are can not be known from an exact point but in our study it is presumed to be known. Kalman filter diverges or converges to a limit value whenever the residuals deny the actual process due to noise data [36].

3.5.1 Kalman filter algorithms

Two properties are expected to be exist in an estimator. The fundamental key specific is ensuring that the substitution between the actual state value and estimation value is not diverge and be equal to zero. Next property is to ensure the least possible convergence of state estimation compared to real states which implies that minimal error potential of variance exist. The Kalman filter meets the demands of an estimator formerly mentioned and it facilitate estimation of a linear and time-invariant model. This filter can be utilized only if the system model has exact noise specifics like process noise covariance matrix (Q) and measurement noise covariance matrix (R) in Eq. (3.31) and Eq. (3.32) respectively.

$$Q = E(w_k w_k^T) \tag{3.31}$$

$$R = E(z_k z_k^T) \tag{3.32}$$

Here w^T and z^T are the transpose matrix of noise matrices and E is the needed expectation value. Prediction and Update correction stages are owned by Kalman filter.

If we look into the prediction stage, prediction of observer states and covariance matrix are performed. The performance of the estimation or estimation error, is dedicated by the covariance matrix. K is the value of the Kalman filter gain matrix also P is considered as estimation error covariance. The equations are established for prediction stage as in Eq. (3.33), Eq. (3.34) and Eq. (3.35).

$$\hat{x}_k = A\tilde{x}_{k-1} + Bu_{k-1} \tag{3.33}$$

$$\hat{P}_k = A\tilde{P}_{k-1}A^T + Q \tag{3.34}$$

$$K_k = \hat{P}_k C^T \left(C\hat{P}_k C^T + R\right)^{-1} \tag{3.35}$$

Here $-1, T, \wedge$ symbols are imply inversion, transpose and estimate value. $(\hat{x}_k)$, state estimation refreshes its value as time spend and it is based on sentient. In correction stage, correction function presents the value to enhance the regained state estimation comes from measurement. The noise covariance is directly proportional to the measurement noise and Kalman gain matrix (K) is going to diminish at the moment reliability is not steady on the measured output (y) during the new iteration to compute the next state $\hat{x}$.
To describe the residual, it is given in Eq. (3.36).

$$residual = y_k - C\hat{x}_k \tag{3.36}$$

Inside the correction section, updated state estimate of the observer is given in Eq. (3.37).

$$\hat{X}_{k+1} = \hat{x}_k + K_k(y_k - C\hat{x}_k) \tag{3.37}$$

And updated error covariance matrix is given in Eq. (3.38).

$$\hat{P}_{k+1} = \hat{P}_k - (K_k C\hat{P}_k) \tag{3.38}$$

Acquiring a great success from the Kalman filter, the values that are given, dynamic model and probabilistic data values, must be right. Therefore, a convenient model must match probabilistic model to reveal alterations in dynamics of the aircraft and environment circumstances. Kalman filter desires to have civil aircraft' s initial true value of state and initial covariance and this property of Kalman filter that differs from other types of filters.

3.5.2 Statistical test for fault detection

The states of the Boeing 747 model are estimated throug a linear optimum OKF. Following two hypotheses may be introduced:

$$H_0: No\ sensor\ fault, nominal\ case$$

$$H_1: Sensor\ fault\ observed\ on\ the\ system$$

Innovation approach is utilized on the detection of sensor fault conditions. Establishing detection of sensor failure by altered mean of the innovation sequence of Kalman filter can be gathered as the statistical function below,

$$\beta_k = \sum_{j=k-M+1}^{k} \tilde{\Delta}_j^T \tilde{\Delta}_j \tag{3.39}$$

$\tilde{\Delta}_j$ = normalized innovation sequence of the OKF and M = width of the sliding window.

The Kalman Filter normalized innovation is gained by,

$$\tilde{\Delta}_k = [CP_{k-1}C^T + R_k]^{-1/2}\Delta_k \tag{3.40}$$

P_{k-1} is the covariance matrix of the extrapolation error and R_k is the covariance matrix of measurement error, Δ_k is OKF innovation sequence.

This statistical function has χ^2distribution with s degree of freedom where s is the dimension of the state vector.

If the level of significance, α is selected as,

$$P\{\chi^2 > \chi^2_{\alpha,s}\} = \alpha; \; 0 < \alpha < 1 \tag{3.41}$$

the threshold value, $\chi^2_{\alpha,s}$can be determined from quantiles table of the χ^2 distribution. So, during the hypothesis H_1 is correct, the statistical value of η_k will have higher value compared to the threshold value $\chi^2_{\alpha,s}$, i.e.,

$$H_0: \; \beta_k < \chi^2_{\alpha,s}, \forall k \tag{3.42}$$

$$H_1: \; \beta_k > \chi^2_{\alpha,s}, \exists k \tag{3.43}$$

Fault isolation case is to bring out which sensor is faulty. The algorithm defined by two following equations 3.45 and 3.46 has been implemented for fault isolation.

$S_{\tilde{\Delta}}$ is the selection covariance matrix, and S_k^* is the selection covariance matrix multiplied by all the elements$(M-1)$. The dimensions of S_k^* are adjusted as *nxn*, here *n* is the number of states.

Based on the statistics of the faulty sensor is assumed to have affected more compared to remaining sensors. Meanwhile the fault has an influence on the variance of the innovation system arise, the statistics v_i surpasses the threshold value $\chi^2_{\alpha,Ms}$, that is judged to related on the confidence probability and degrees of freedom $(M-1)$. v_i is the i diagonal element of the S_k^* matrix [37].

$$\tilde{\Delta}_k = \frac{1}{M} \sum_{j=k-M+1}^{k} \tilde{\Delta}_j \tag{3.44}$$

$$S_{\tilde{\Delta}_k} = \frac{1}{M-1} \sum_{j=k-M+1}^{k} \left[\tilde{\Delta}_j(i) - \bar{\tilde{\Delta}}_k(i)\right]\left[\tilde{\Delta}_j(i) - \bar{\tilde{\Delta}}_k(i)\right]^T \tag{3.45}$$

$$S_k^* = \sum_{j=k-M+1}^{k} \left[\tilde{\Delta}_j(i) - \bar{\tilde{\Delta}}_k(i)\right]\left[\tilde{\Delta}_j(i) - \bar{\tilde{\Delta}}_k(i)\right]^T \tag{3.46}$$

3.5.3 Sensor fault isolation algorithm

The time as the fault is detected, it is neccessary to is detect which sensor is faulty. To make it possible, the $\boldsymbol{s}$-dimensional sequence $\tilde{\Delta}$ is reduced into $\boldsymbol{s}$ one-dimensional sequences for isolation process. So, each of the sequences becomes one-dimensional as $\tilde{\Delta}_k(i), i = 1,2, \dots, s$ a corresponding monitoring algorithm executes. Therefore we can observe that the statistics of the failured sensor set supposed to have affected higher compared to the other sensors. If we show the statistics by $S_k(i)$. It can be implied from the calculations that, $\max\{S_k(i) \mid k = 1,2, \dots, s\} = S_k(m)$ for $i \neq j$, and $S_k(i) \neq S_k(j)$, therefore the mth sensor set is diagnosed as faulted.

The process of decision making is run to isolate the faulty sensor is demonstrated as:

$$if \qquad S(k)_{z,z}^* > \chi_{\alpha,Ms}^2 \rightarrow zth\ \ sensor\ is\ faulty \quad z = 1,2,3,4.$$

In this study, the fault accommodation algorithms practiced are robust Kalman filter (RKF) and the reconfigured Kalman filter.

3.5.4 Robust Kalman filter

Sensor faults can be detected and isolated in adequate method yet, the estimation of the filter is not satisfying due to the faults. To overcome this problem, fault accommodation approach is compatible for enhancement of the fault.

A method called RKF is utilized to have better results in estimation of the states that are closer to the actual values even if a sensor fault is observed on the system. The RKF performs by analyzing the actual and theoretical values of the covariance of the innovation sequence. The RKF algorithm succeeds two missions that one is giving a tolerance to the fault and the other is to improve better and accurate estimation values at the moment that a fault appears and measurement values are rough without influencing the past fine characteristics. And this process achieved by detraction the weight of the faulty measurement channel. By doing this, the KF gain will take recent values related to the differentiaton of innovation sequence covariance matrix the moment the operational condition of the system output values are incompatible the models utilized in the establishment of the filter.

3.5.4.1 Rkf with smnsf

As just an error seen in the measurements, the adaptation of KF is actualised by raising S_k to lower the Kalman gain K_k. More elaborately, the Kalman gain is reassessed at the time the estimation of the measurement $[C_k * \hat{x}_k]$ is noticeably differs from the actual measurement y_k. Upon these terms, the Kalman gain value turns into:

$$K = P_k C_k^T [C_k P_k C_k^T + S_k R_k]^{-1} \tag{3.47}$$

Where S_k is the single measurement noise scale factor (SMNSF). S_k is calculated from the formula below:

$$S_k = \frac{\tilde{\Delta}_k{}^T \Delta_k - tr\{C_k P_k C_k^T\}}{tr\{R_k\}} \tag{3.48}$$

Fault detection process is practised by thr statistical funtion named quadratic innovation function, which is determined as:

$$\beta^*(k) = \Delta_k^T \, [C_k \, P_{k-1} C_k^T + R_k]^{-1} \, \Delta_k \tag{3.49}$$

This statistical distribution has χ^2 distribution along with s degrees of freedom, that s is the dimension of the innovation vector.

3.5.4.2 Rkf with mmnsf

The RKF embeeded with multiple measurement-noise scale factor (MMNSF) method, the target is correcting solely the correlated parts of the measurement noise-covariance and eventually, the Kalman gain. The MMNSF scale factor S_k can be designated through the formula:

$$S(k) = \left(\frac{1}{\mu} \sum_{j=k-\mu+1}^{k} \Delta_j {\Delta_j}^T - C_k P_{k-1} C_k^T \right) R_k^{-1} \tag{3.50}$$

Here μ denotes as the width of the moving window. In this case rather than $S(k)$, a matrix $S^*(k)$ is utilized. To establish the scale matrix $S^*(k)$, the following caulculation is performed [38]:

$$S^*(k) = diag(s_1^*, s_2^*, \dots, s_n^*)$$

In which

$$s_i^* = \max\{1, S_{ii}\} \quad i = 1, \dots, n$$

In here the sign S_{ii} serve as the diagonal element of the matrix S_k.

Just in moment, the Kalman filter gain should be run and re-evaluated by the equation:

$$K = P_k C_k^T [C_k P_k C_k^T + S_k^* R_k]^{-1} \tag{3.51}$$

In case of varying malfunction , the correlated element value of the scale matrix raises, therefore a smaller Kalman gain carried out, that diminishes the impulse of the innovation on the state estimation process. By this way, more satisfying and proper estimation values are gathered. A MMNSF is more judicious compared to SMNSF that solely the diagonal elements that relate to faulty states are adjusted.

3.6 Rkf Algorithm Results

Two types of Robust Kalman filters are examined and the results are assesed and the supreme algorith is selected as to embeed inside fault detection algorithm.

3.6.1 Rkf with smnsf

The RKF simulations include just measurement noise-increment malfunction solely. The figure demonstrates that RKF with SMNSF algorithm makes it possible to enhance smooth estimated value and near to actual value.

3.6.2 Rkf with mmnsf

In the figure, it is obvious that MMNSF algorithm runs and gathers estimations with less oscilliations compared with measurement values, thus close near to the actual value. To assess the performance of RKF with SMNSF and RKF with MMNSF whether the malfunction is considered as measurement noise-increment fault, it can be inferred that the RKF with MMNSF gets finer results with fewer oscilliations which means closer to the actual values.

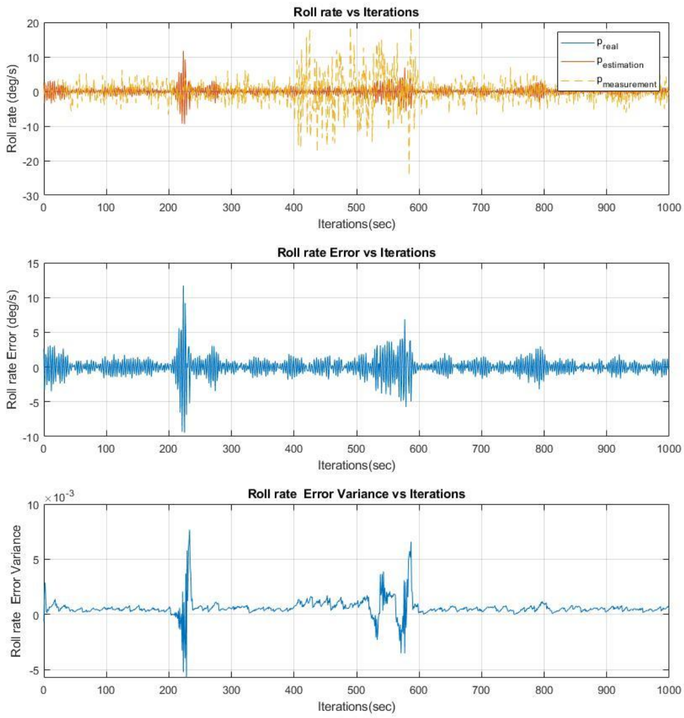

Figure 3.3 : Roll rate estimation, error and error variance with smnsf implemented.

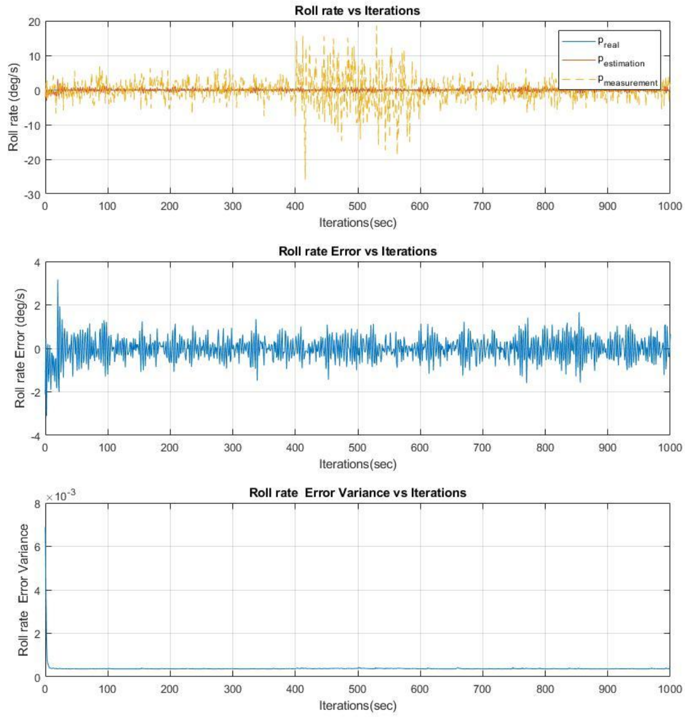

Figure 3.4 : Roll rate estimation, error and error variance with mmnsf implemented.

3.7 Reconfigured Kalman Filter

Final inspected method is the reconfigured Kalman filter. The reconfigurable Kalman filter is regarded as an active fault-tolerant control system as in a reconfigurable control system, the faulty measurement channels are ignored and disabled so, its data is not practiced by filter algorithm. The issue is the filter has to predict N states which is the full state yet, there is just $N-1$ measurement channels are available to catch the incoming data for calculations. In this study, the simulations performed with basic cases and reconfigurable Kalman filter is analyzed. The algorithm starts with ignoring the faulty measurement channel by deleting it. As a result, there is $N-1$ states remaining at the moment simulation proceeds, the algorithm estimates N states.

Adjustments are required inside the OLKF algorithm to analyze the reconfigurable technique. When a fault occurs, one channel is diasbled and the corresponding row has to be deleted from the C_k $s\,x\,n$ dimensional system measurement matrix. Therefore, C_k dimensions are altered as to $(s-1)\,x\,n$. Further, the correlated element of the faulty state has to be deleted from the $v(k)\,s$ -dimensional measurement noise vector. Thus, $v(k)$ changes to $(s-1)$ -dimensional. After those adjustments, as a result the normalized innovation too reduces its measurement channel number from 4 to 3 elements.

3.8 Fault Detection

From the figures it can be seen clearly that the detection of both continuous bias and measurement noise-increment faults are accommplished.

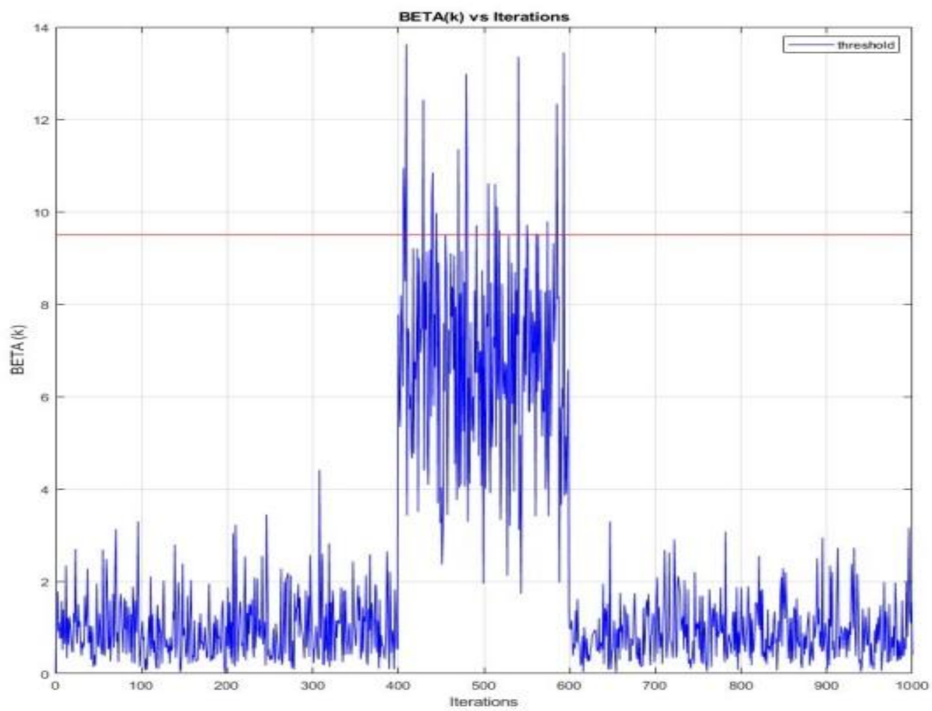

Figure 3.5 : Fault detection for continuous bias fault.

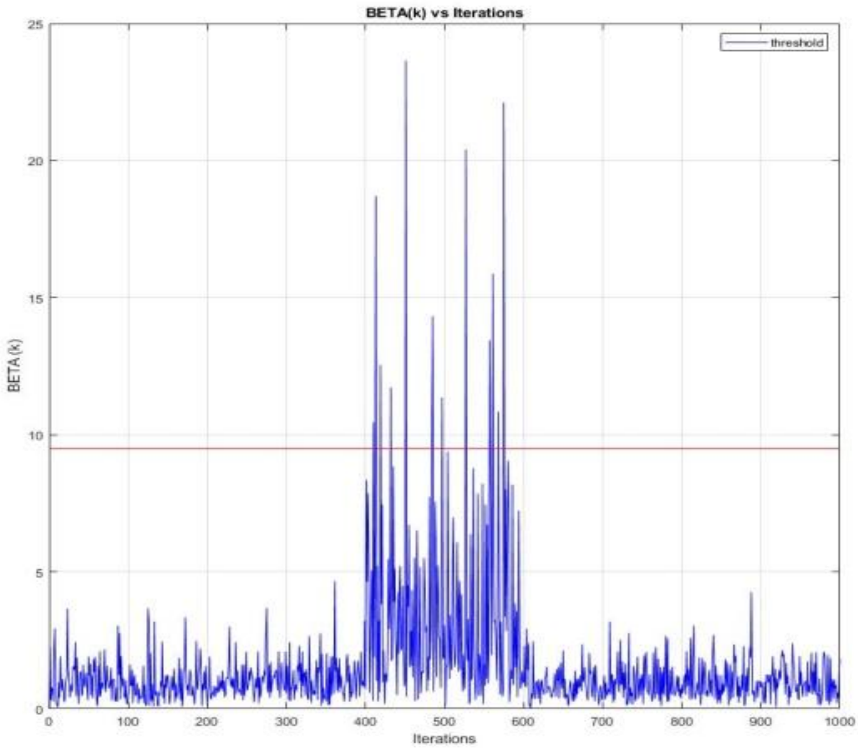

Figure 3.6 : Fault detection for measurement noise-increment fault.

β_k parameter is the decision criteria for fault detection. There is no time delay on the continuous bias fault just as β_k surpasses the threshold level at the iteration 401. However, in the measurement noise-increment fault condition, delay of 408 iterations is observed on detection.

4. MATLAB LATERAL DYNAMICS MODEL RESULTS

As the lateral dynamics are computed, the model is exposured to no sensor faults in the first, therefore OKF tracks actual values of the measurements. In the second case lateral faults are implied to all sensors as sideslip angle, yaw rate, roll rate and roll angle. The faults are isolated through a threshold value with respect to statistics chi square distribution. And for the third case, the faulty sensors are accomodated through reconfiguring the Kalman filter and illustrated satisfying results for converging to the actual values unless s-1 dimension measurement states are fed back to Kalman filter and it estimates the faulty sensor output via the remaining state measurement values.

Aileron input is added as 0.1 radians at time t=1 to t=10 seconds. A continuous bias term and measurement noise increment fault is implied at time interval t = 400 to t = 600 seconds at lateral sensors. The first two faults are continuous bias fault at sideslip angle for 7.5 degrees and yaw rate fault for 10.5 degrees per second and the remaining faults are both measurement noise increment faults of 10 degrees per second and 20 degrees per second on roll rate and roll angle sensors respectively.

An Optimal KF and Robust Kalman filter is used to detect and isolate the sensor faults. The first part of the figures Show the Kalman filter state real values, estimation values and the actual values comparatively. Second part illustrates the error estimation process related to the actual state values of the B-747. The last part indicates the variance value of the estimation.

Clearly it can be seen from figure that OKF is not accurate after the fault is occured at t =400 to t=600 s to end of the simulation time period (where a fault in the side-slip angle sensor exist).

4.1 Sensor Fault Results with Optimal Linear Kalman Filter

4.1.1 Sideslip angle continuous bias sensor fault

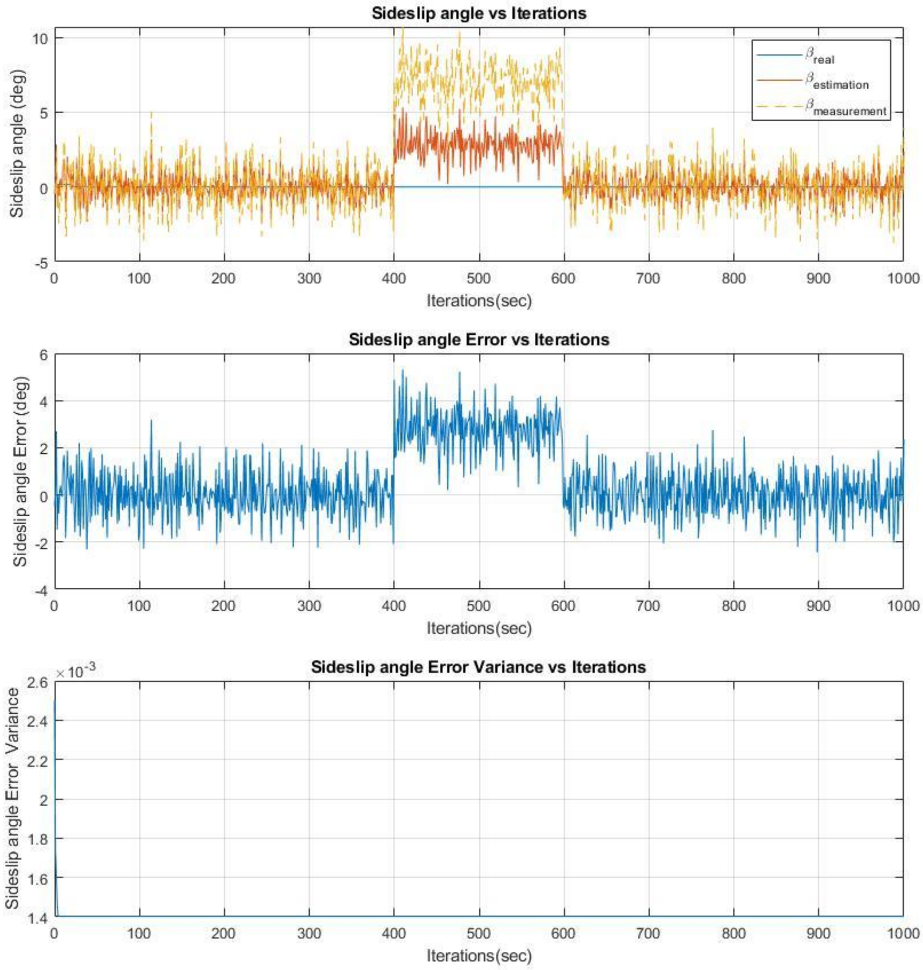

Figure 4.1 : Sideslip angle estimation, error and error variance with olkf implemented in case of sideslip angle sensor fault.

In the first case, a continuous bias fault of 7.5 degrees is implied on the sideslip angle sensor at t = 400 s to t = 600 s time interval and from the graph we can clearly observe that sideslip angle measurements are invalid due to the fault. Our OKF estimates the states close to actual value even if there is a fault on sensor.

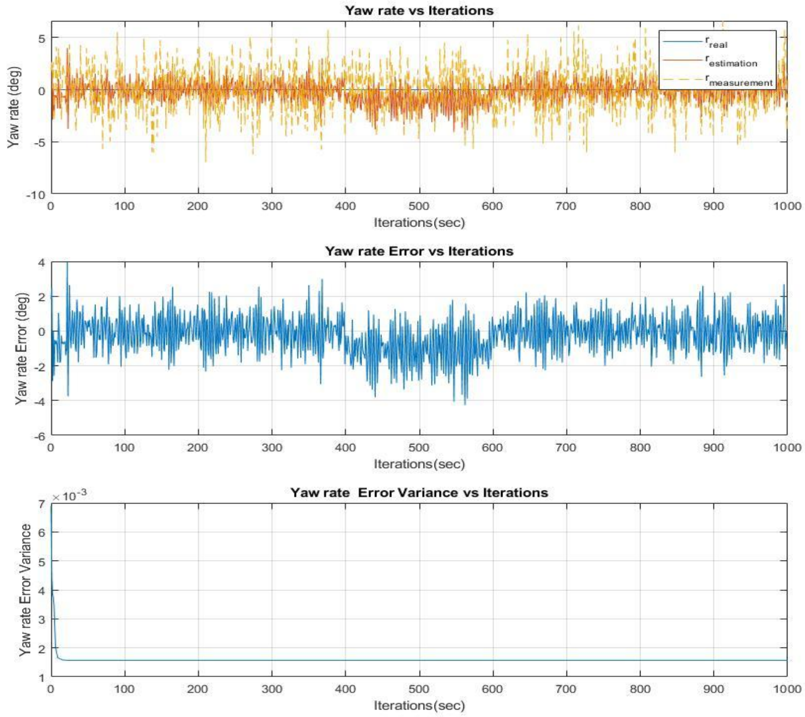

Figure 4.2 : Yaw rate estimation, error and error variance with olkf implemented in case of sideslip angle sensor fault.

Here the Figure shows, there is a minor effect on yaw rate sensor values that are affected by faulty sideslip angle sensor.

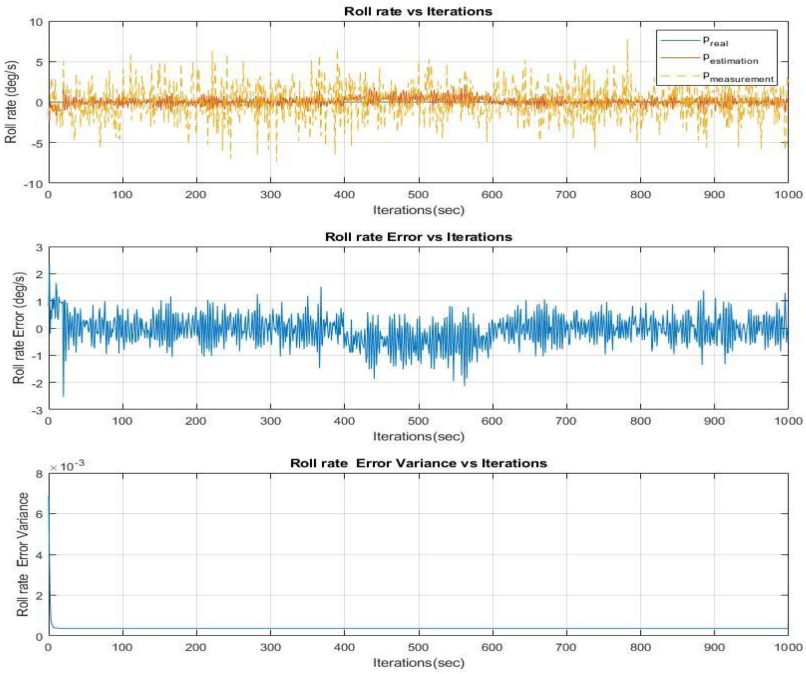

Figure 4.3 : Roll rate estimation, error amd error variance with olkf implemented in case of sideslip angle sensor fault.

In Figure the roll rate and roll angle sensor outputs are almost not affected by faulty sensor.

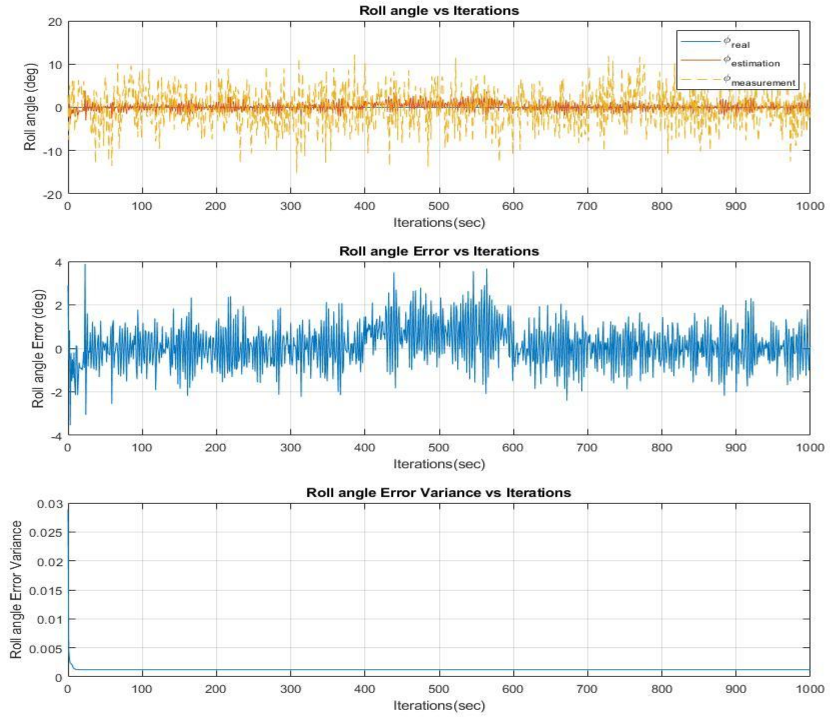

Figure 4.4 : Roll angle estimation, error amd error variance with olkf implemented in case of sideslip angle sensor fault.

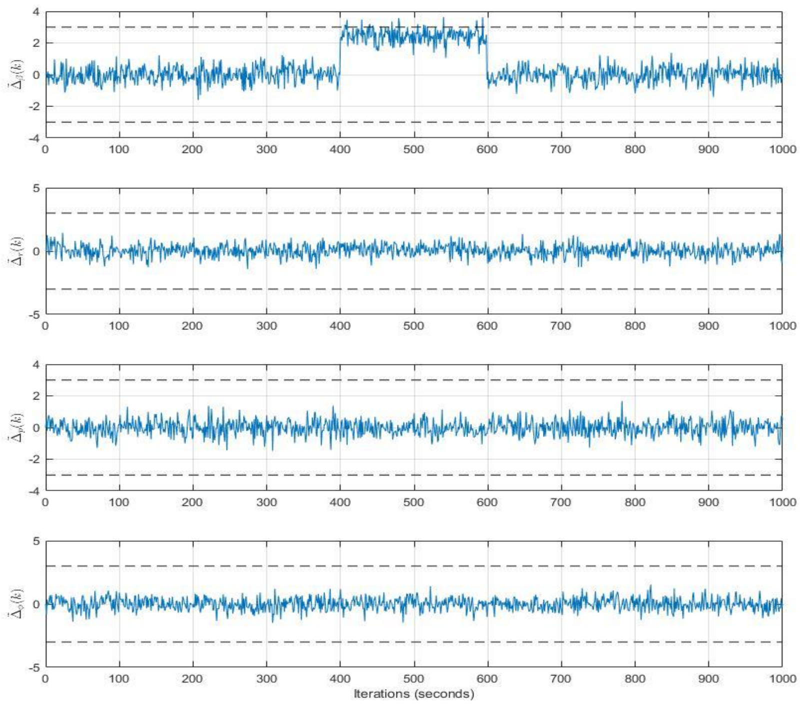

Figure 4.5 : Normalized innovations of olkf for $\boldsymbol{\beta}, \boldsymbol{r}\ \boldsymbol{p}, \boldsymbol{\varphi}$ measurement channels in case of sideslip angle sensor fault.

The graph of the normalized innovations demonstrate that the innovation sequences related to the sideslip angle measurement channel exceeds the threshold value 3σ. Therefore, it is obvious that there is an error at sideslip angle β measurement channel and the remaining channels are not faulty. From this graph the faulty sensor channel is isolated.

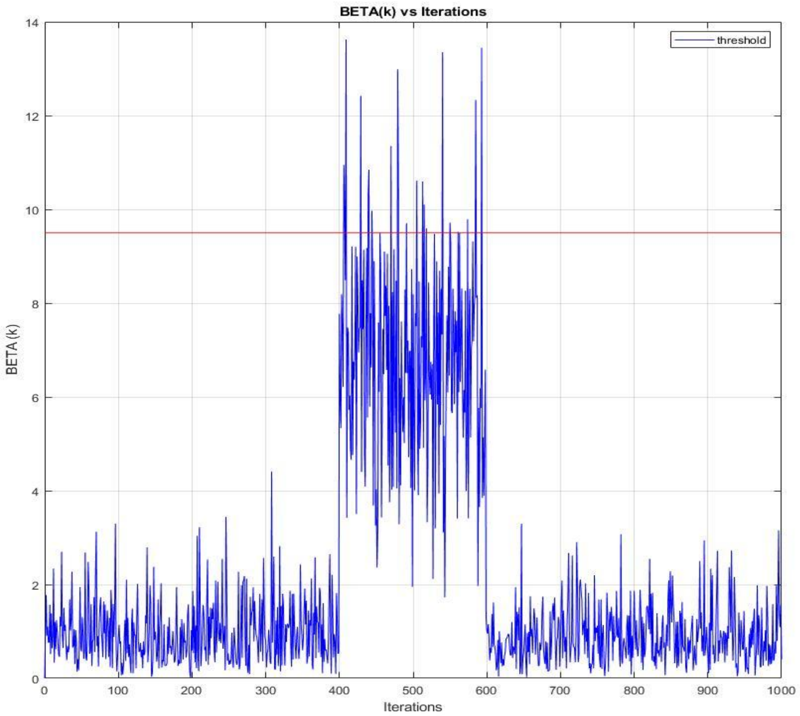

Figure 4.6 : $\boldsymbol{\beta(k)}$ evolution for the case of continuous bias fault at beta measurement in case of sideslip angle sensor fault.

Continuing sensor fault detection, the judgement performed for sensor fault isolation appears by the statistics given by Eq. as follows: $v_k(i) \neq v_k(j), i \neq j$ and $\max\{v_k(i) \mid i = 1,2,3,4\} = v_k(1)$; then it is implied that there is a fault in the first measurement channel which is sideslip angle (β) sensor. It has exceed the threshold value of 9.5 from t = 400 till t = 600 seconds.

4.1.2 Roll rate measurement noise increment sensor fault

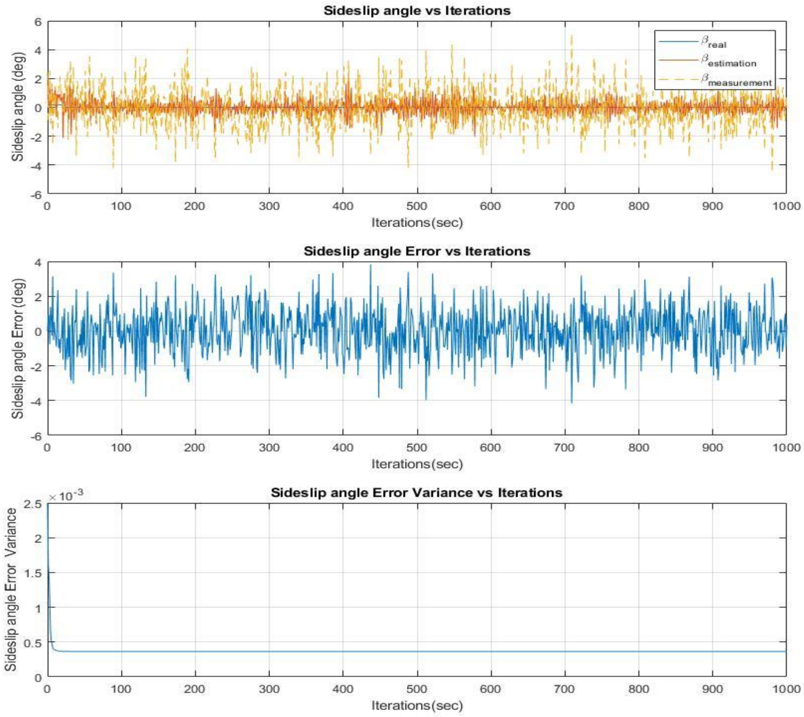

Figure 4.7 : Sideslip angle estimation, error and error variance with olkf implemented in case of roll rate sensor fault.

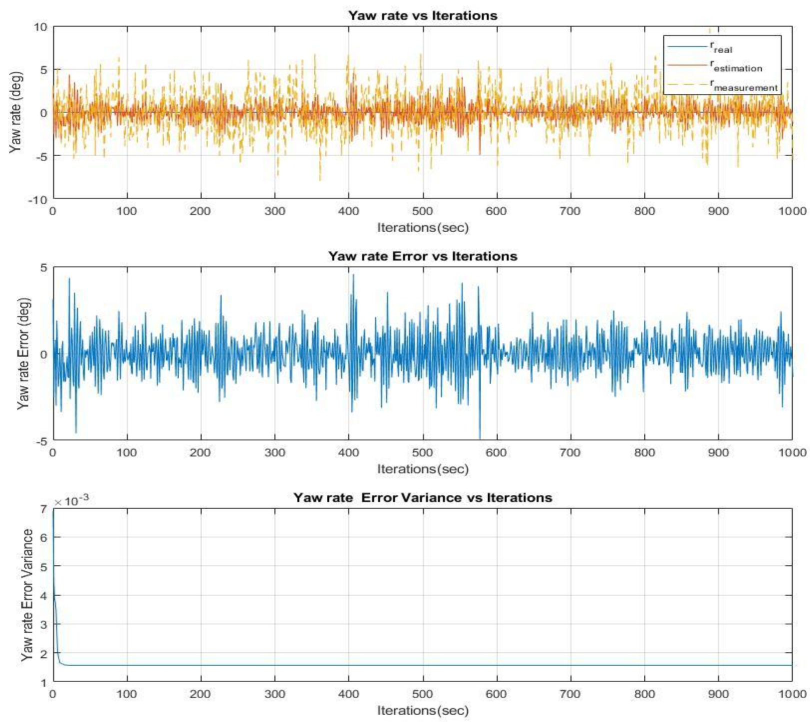

Figure 4.8 : Yaw rate estimation, error and error variance with olkf implemented in case of roll rate sensor fault.

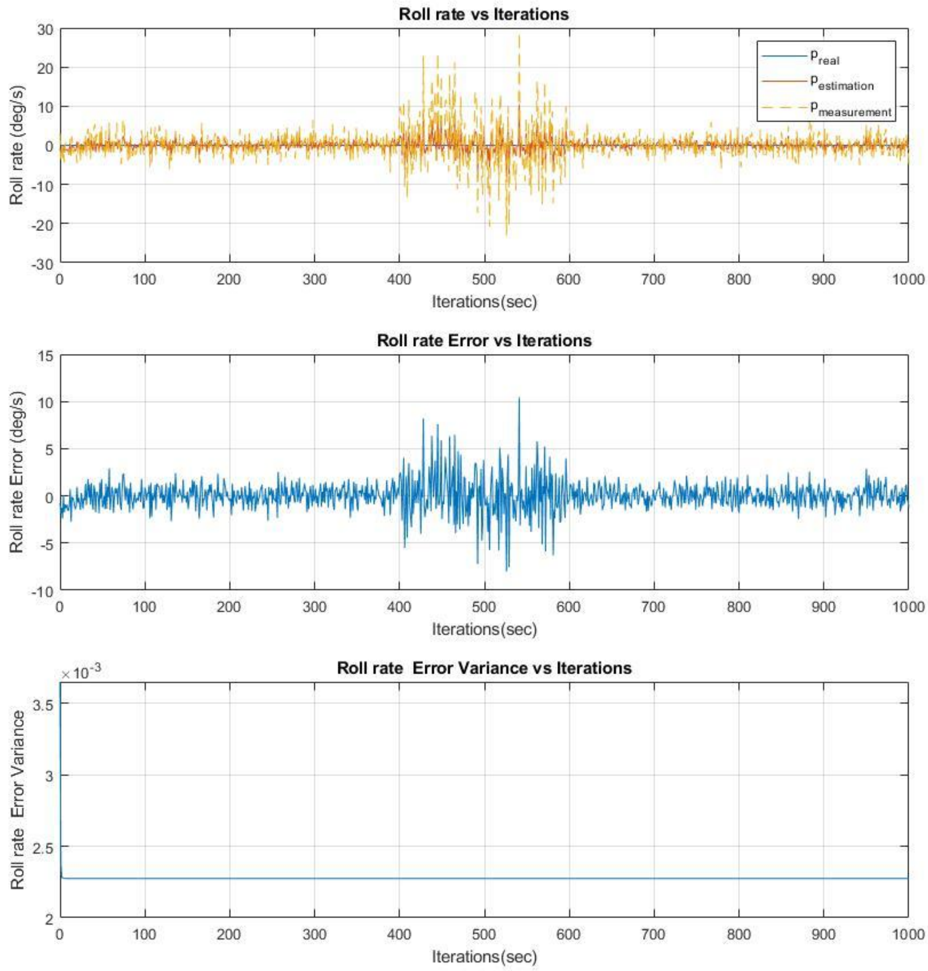

Figure 4.9 : Roll rate estimation, error and error variance with olkf implemented in case of roll rate sensor fault.

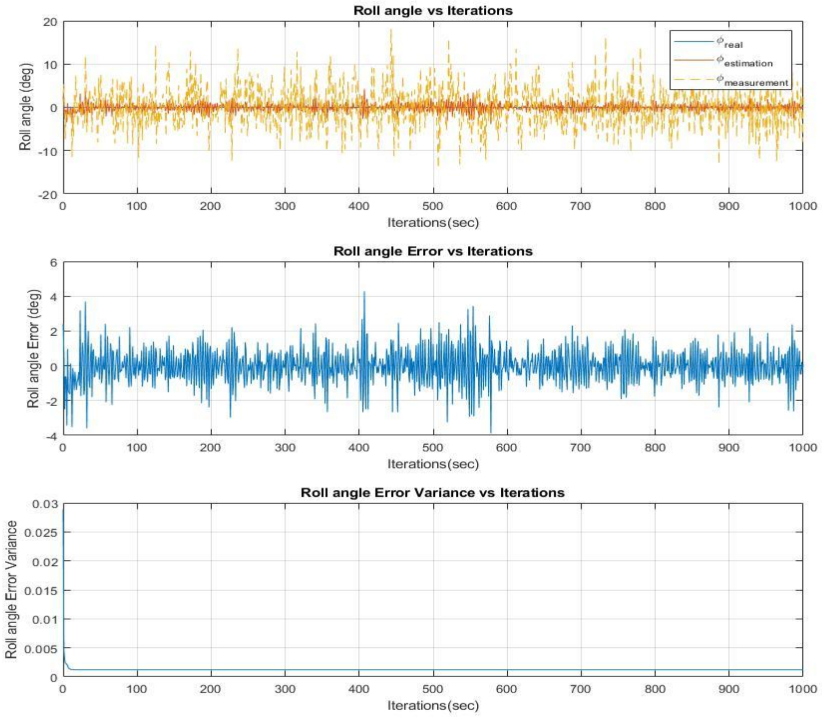

Figure 4.10 : Roll angle estimation, error and error variance with olkf implemented in case of roll rate sensor fault.

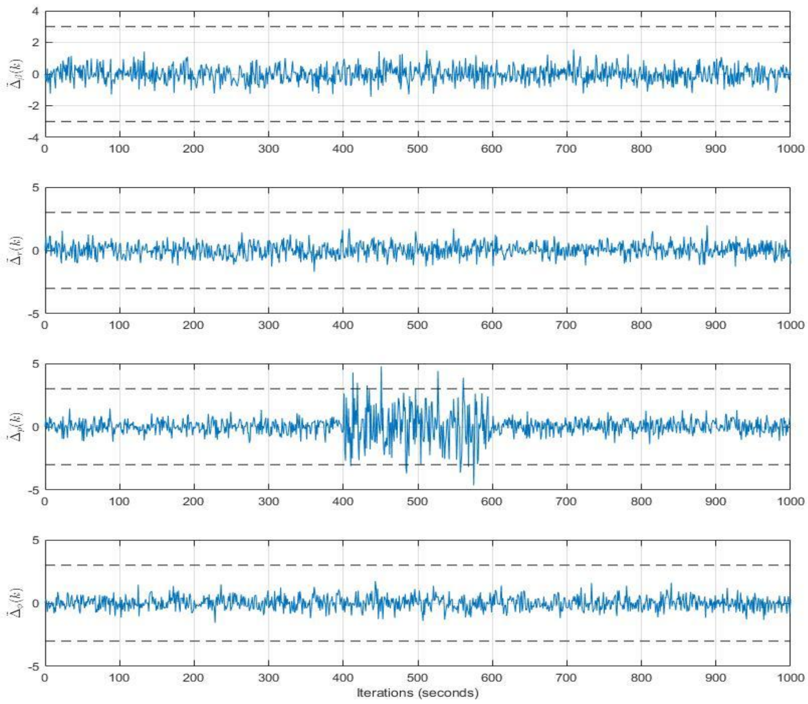

Figure 4.11 : Normalized innovations of olkf for $\boldsymbol{\beta}, \boldsymbol{r}\ \boldsymbol{p}, \boldsymbol{\varphi}$ measurement channels in case of roll rate sensor fault.

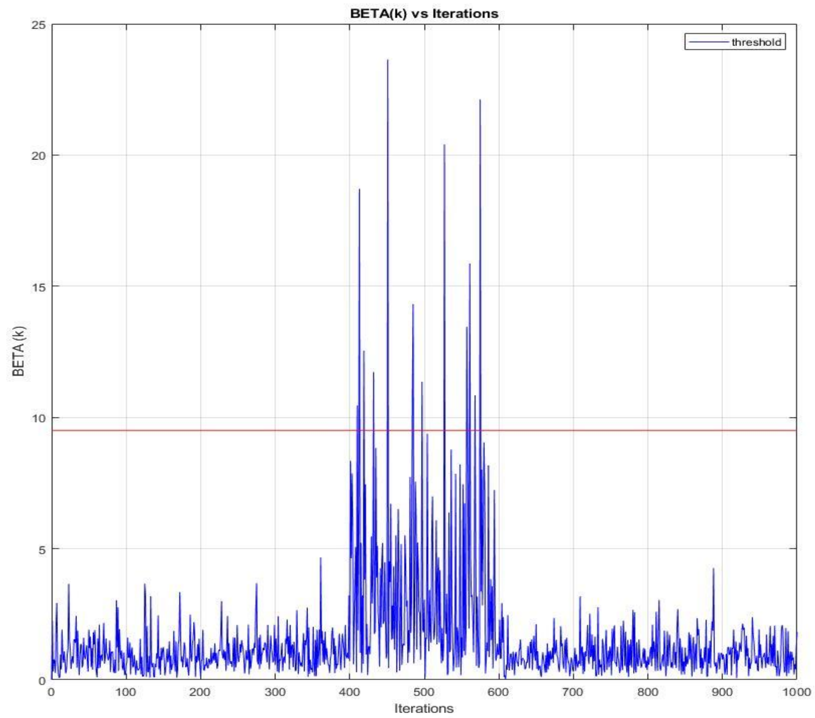

Figure 4.12 : β(k) evolution for the case of continuous bias fault at beta measurement in case of roll rate sensor fault.

4.1.3 Measurement noise increment double sensor fault

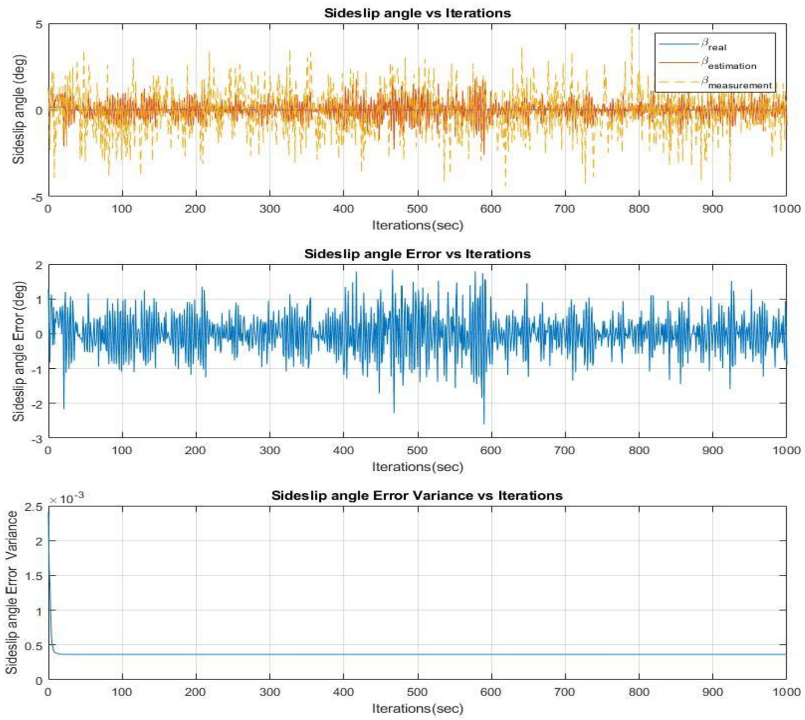

Figure 4.13 : Sideslip angle estimation, error and error variance with olkf implemented in case of roll rate & roll angle sensor fault.

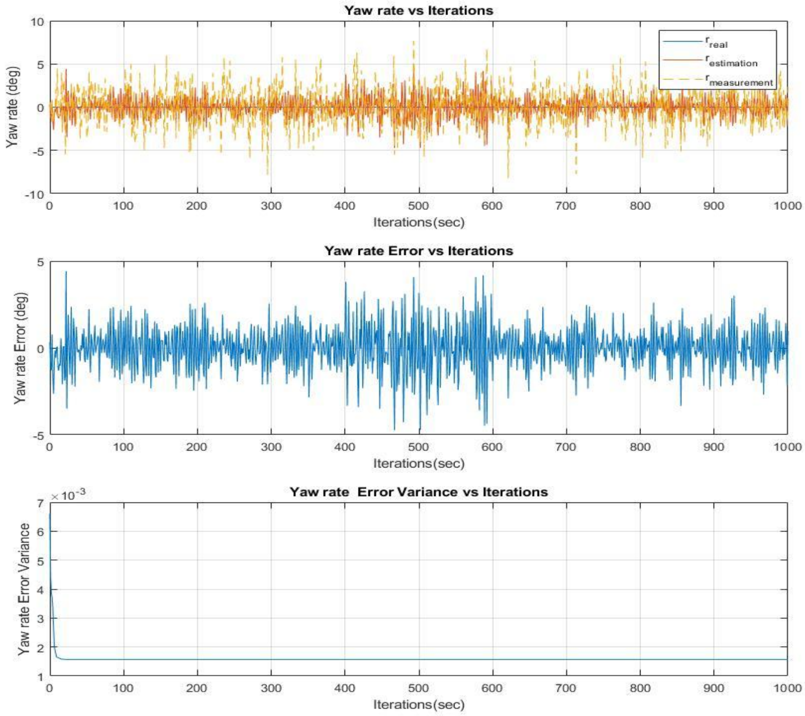

Figure 4.14 : Yaw rate estimation, error and error variance with olkf implemented in case of roll rate & roll angle sensor fault.

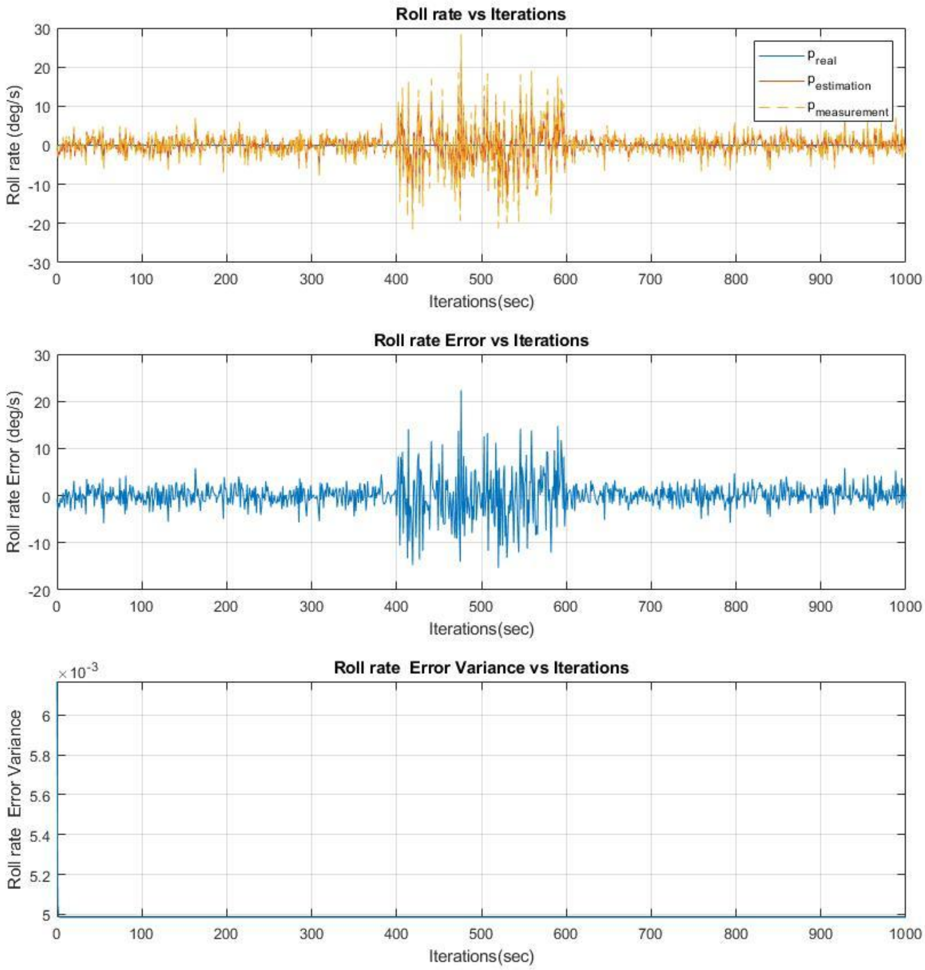

Figure 4.1 : Roll rate estimation, error amd error variance with olkf implemented in case of roll rate & roll angle sensor fault.

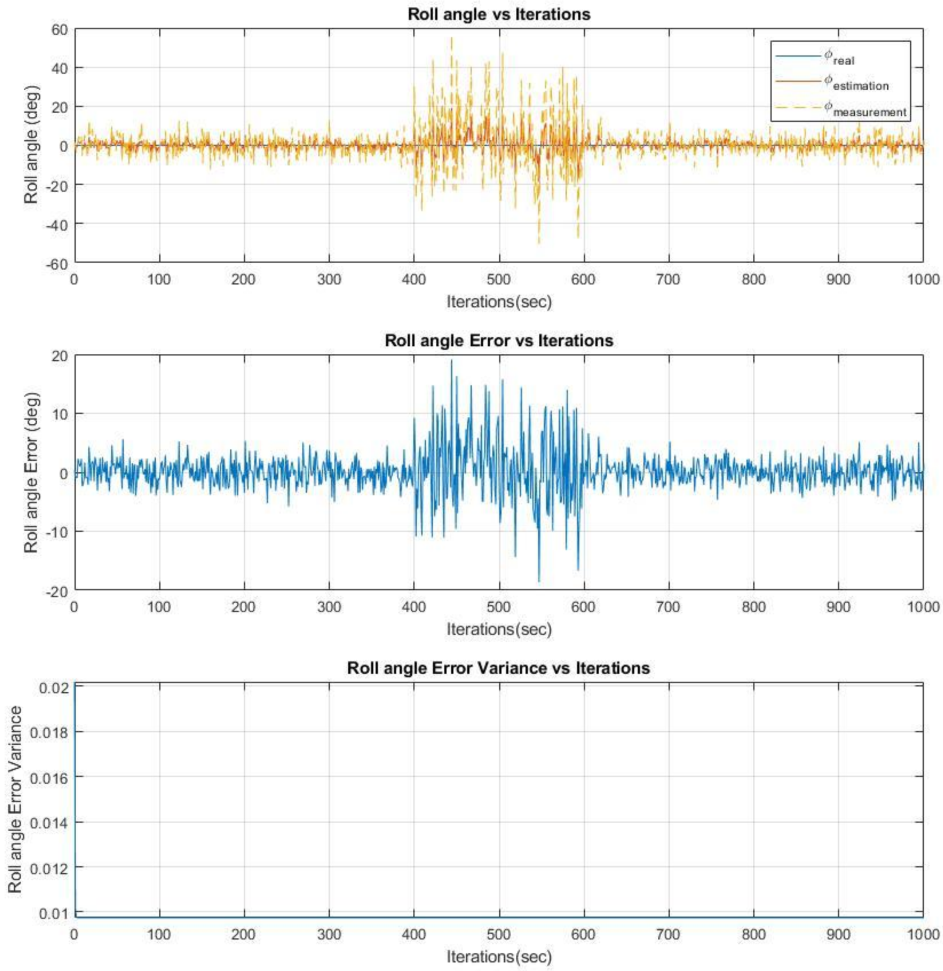

Figure 4.2 : Roll angle estimation, error amd error variance with olkf implemented in case of roll rate & roll angle sensor fault.

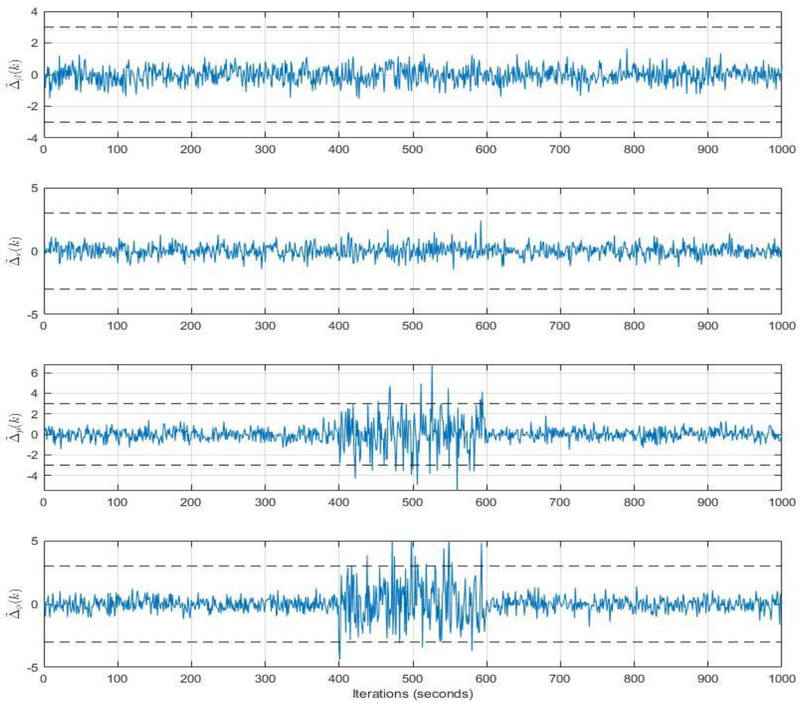

Figure 4.3 : Normalized innovations of olkf for $\boldsymbol{\beta}, \boldsymbol{r}\ \boldsymbol{p}, \boldsymbol{\varphi}$ measurement channels in case of roll rate and roll angle double sensor fault.

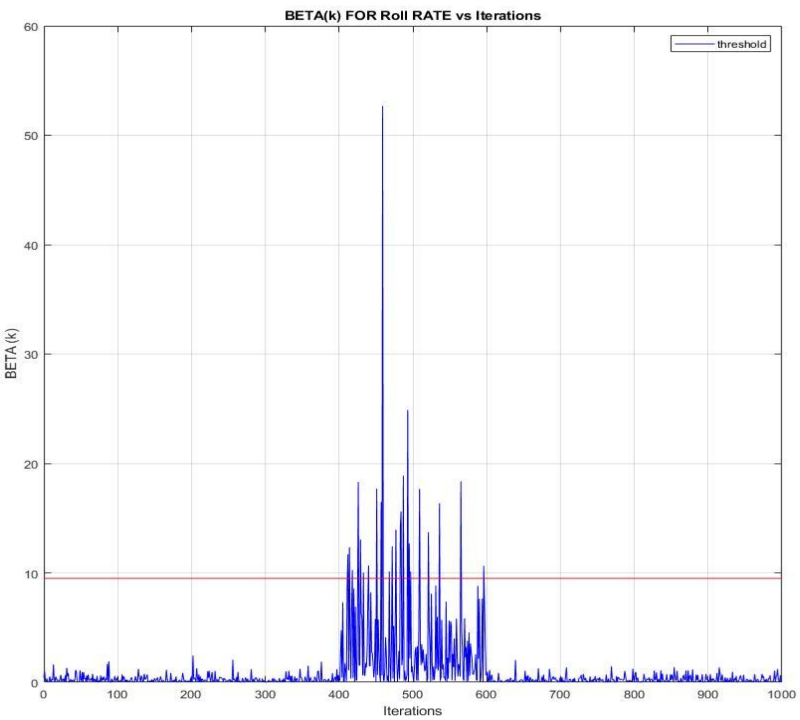

Figure 4.4 : β(k) evolution for roll rate in case of measurement noise-increment double sensor fault.

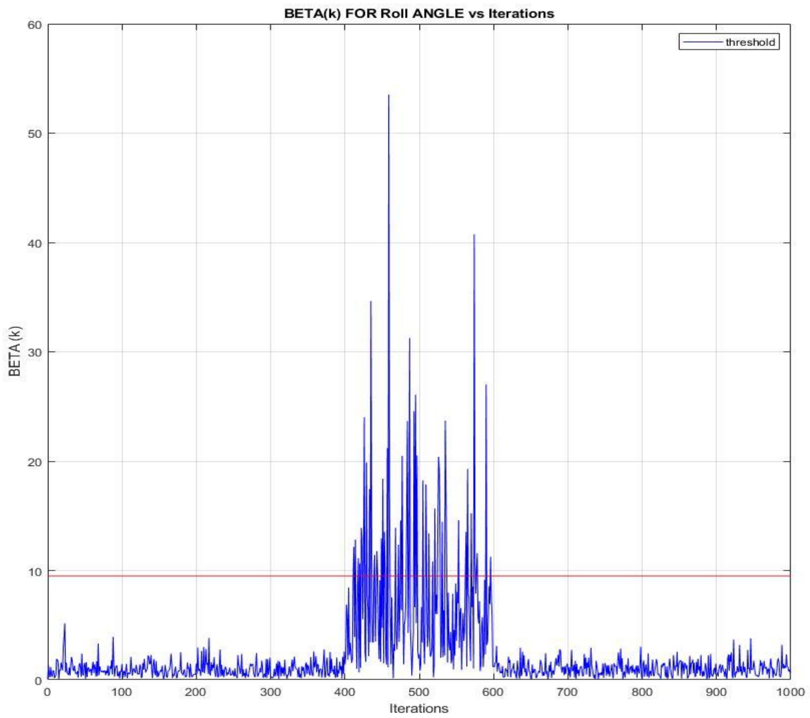

Figure 4.5 : β(k) evolution for roll angle in case of measurement noise-increment double sensor fault.

4.2 Sensor Fault Results with Robust Kalman Filter

4.2.1 Sideslip angle continuous bias sensor fault

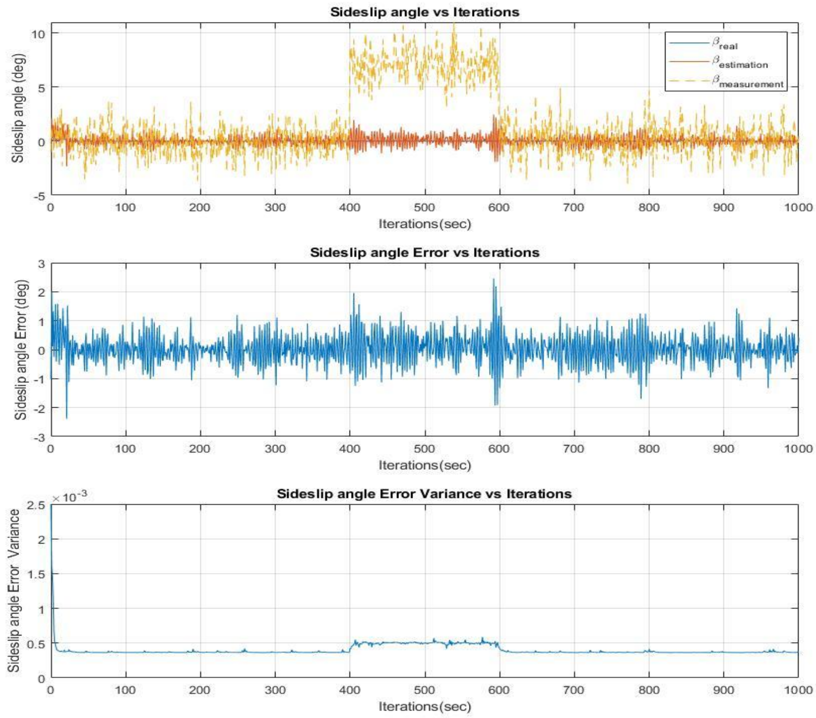

Figure 4.6 : Sideslip angle estimation, error and error variance with rkf implemented in case of sideslip angle sensor fault.

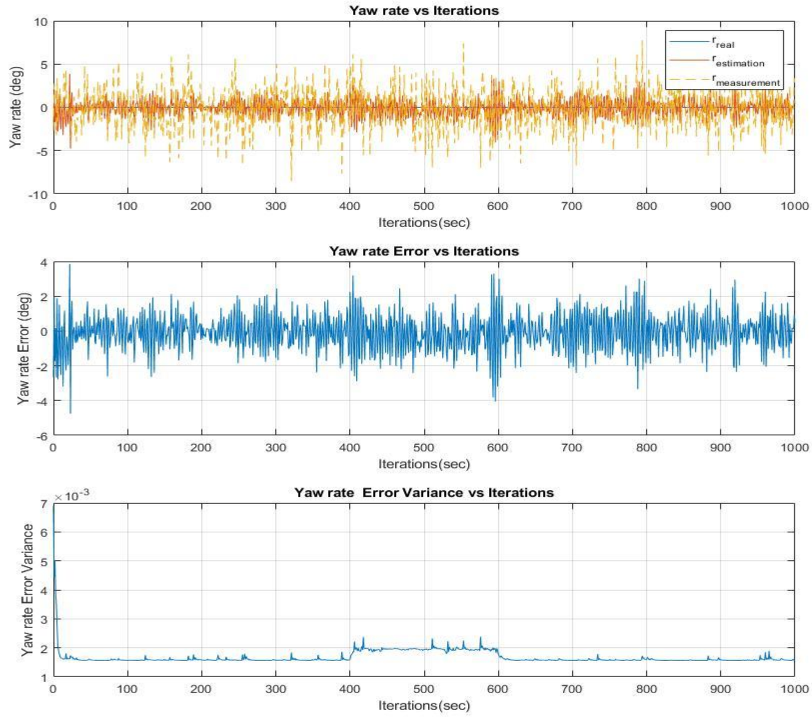

Figure 4.7 : Yaw rate estimation, error and error variance with rkf implemented in case of sideslip angle sensor fault.

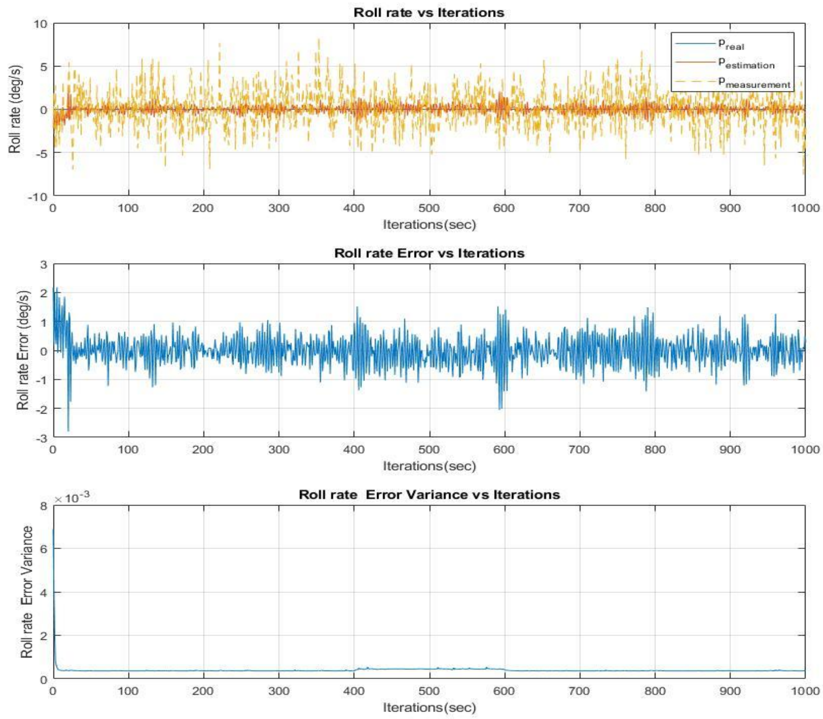

Figure 4.8 : Roll rate estimation, error and error variance with rkf implemented in case of sideslip angle sensor fault.

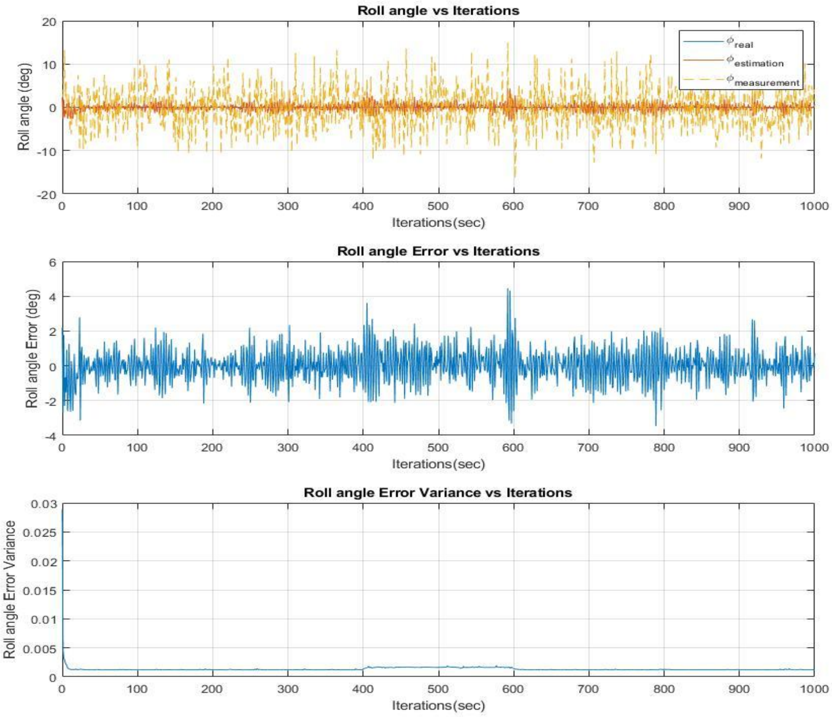

Figure 4.9 : Roll angle estimation, error and error variance with rkf implemented in case of sideslip angle sensor fault.

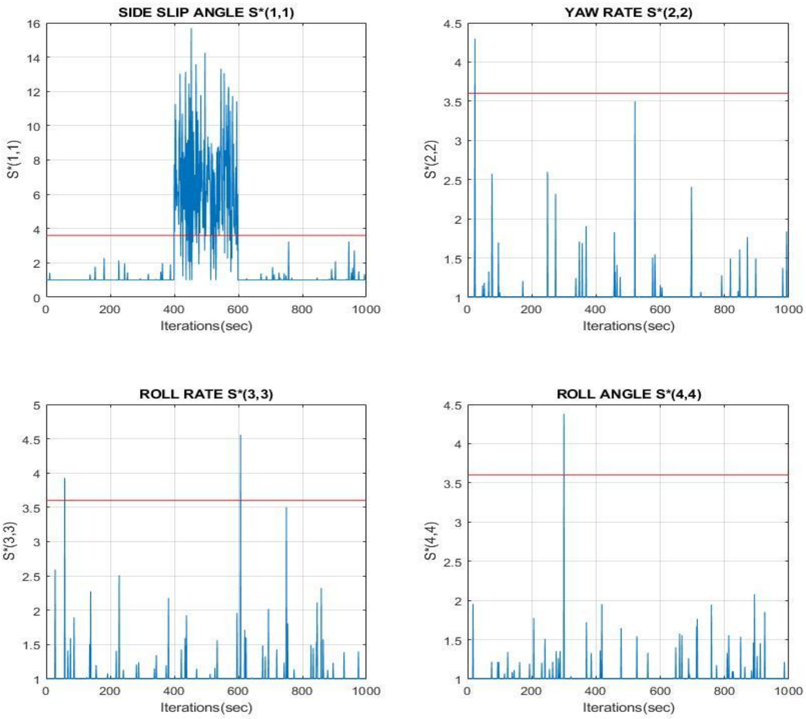

Figure 4.10 : Sensor fault isolation with continuous bias fault at $\boldsymbol{\beta}$ measurements.

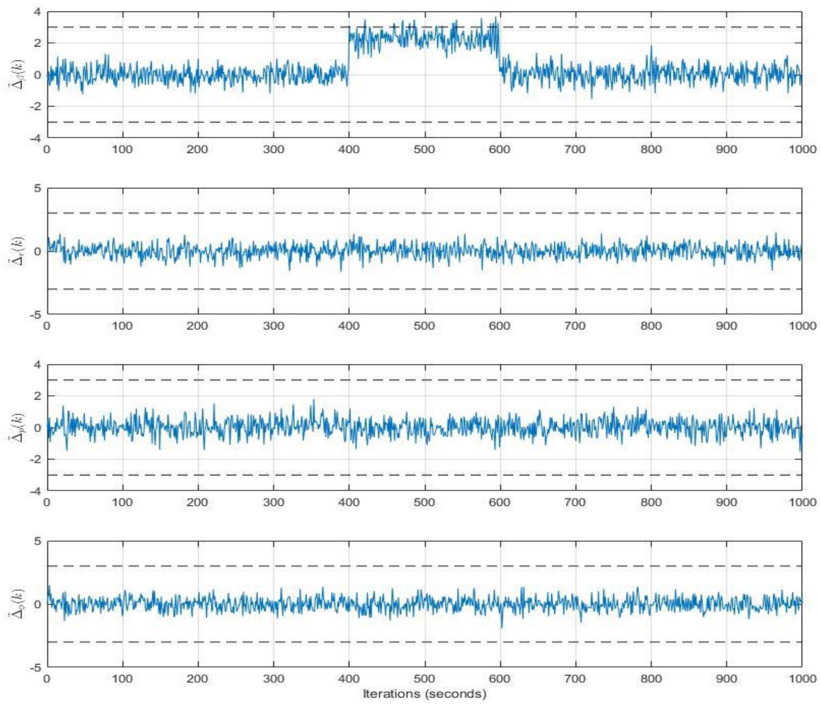

Figure 4.11 : Normalized innovations of rkf for $\boldsymbol{\beta}, \boldsymbol{r}, \boldsymbol{p}, \boldsymbol{\varphi}$ measurement channels.

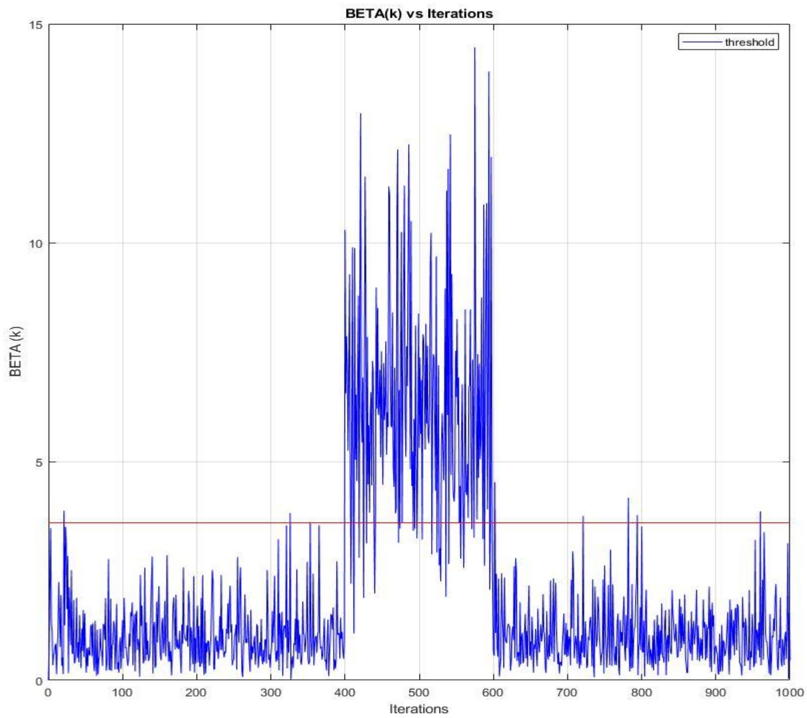

Figure 4.12 : β(k) evolution for sideslip angle continuous bias sensor fault.

4.2.2 Roll rate measurement noise increment sensor fault

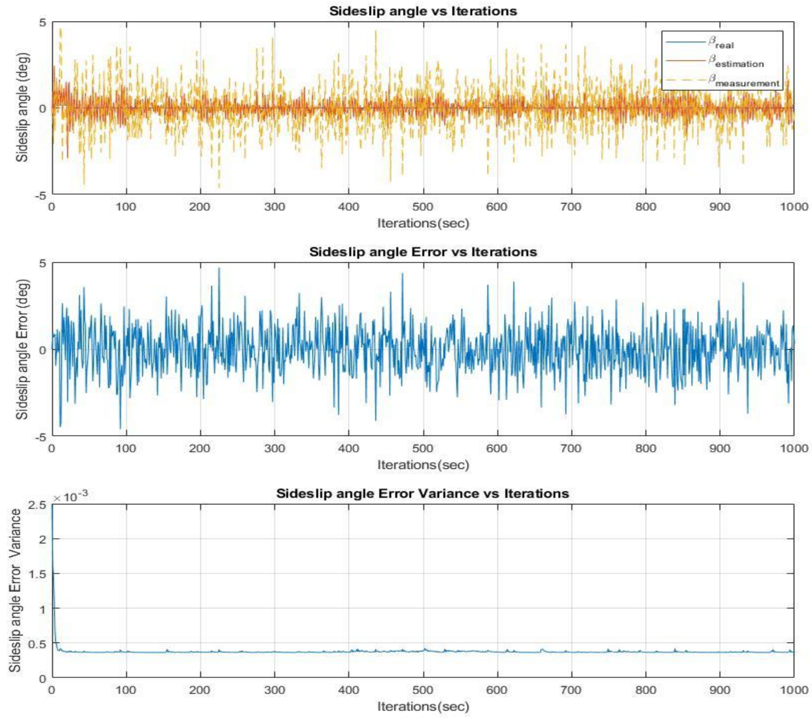

Figure 4.13 : Sideslip angle estimation, error and error variance with rkf implemented in case of roll rate sensor fault.

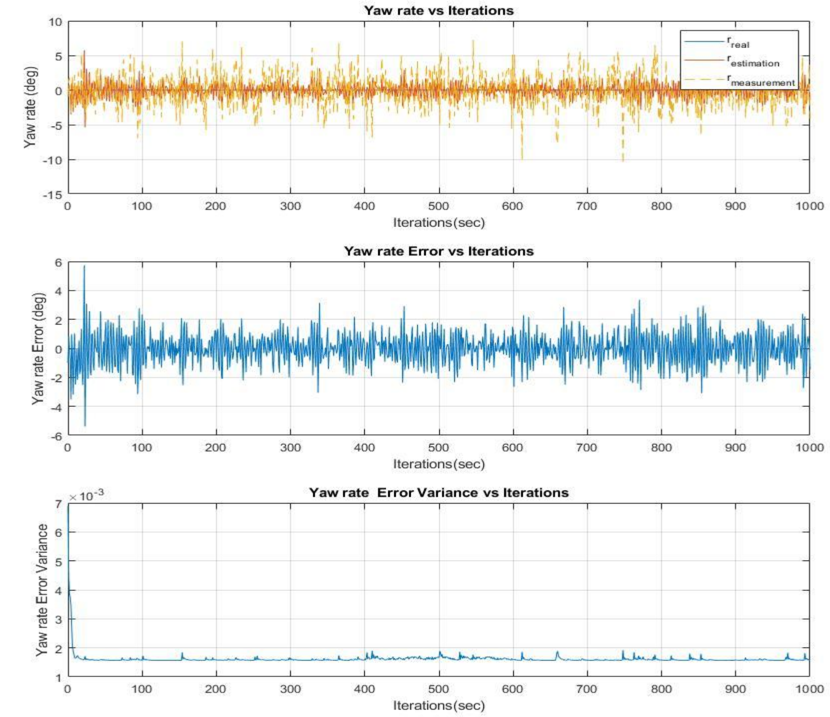

Figure 4.14 : Yaw rate estimation, error and error variance with rkf implemented in case of roll rate sensor fault.

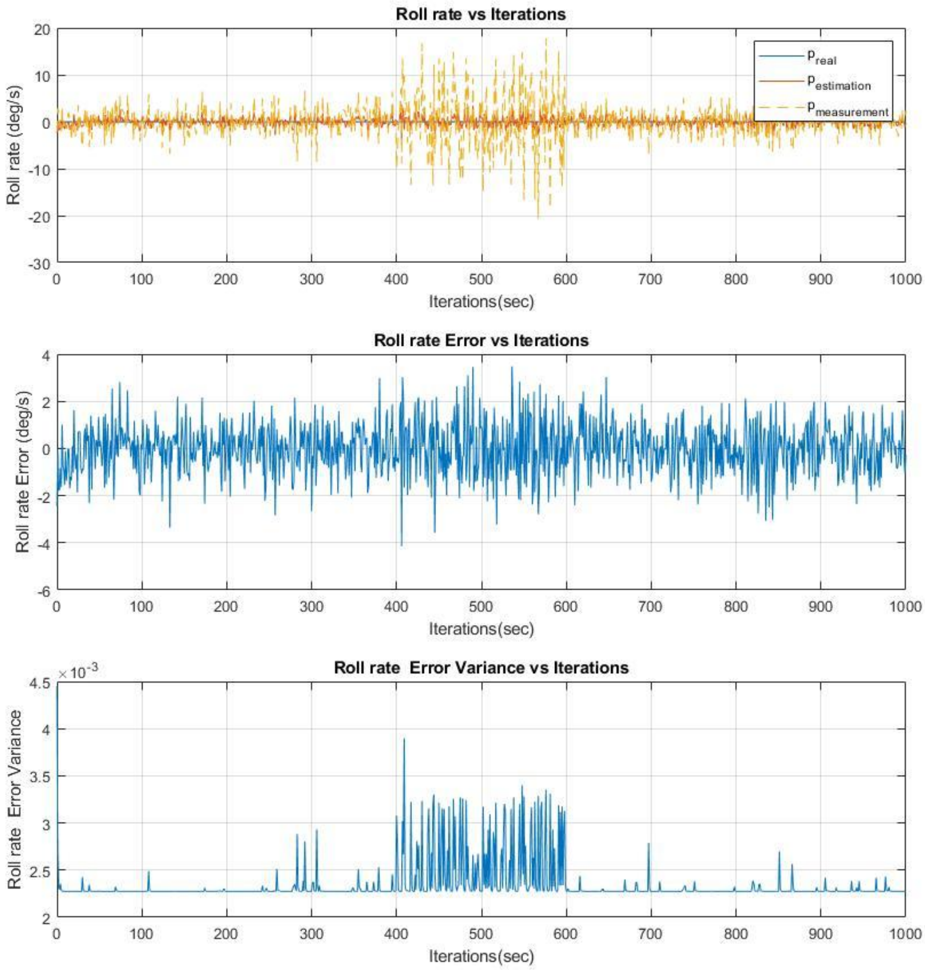

Figure 4.15 : Roll rate estimation, error and error variance with rkf implemented in case of roll rate sensor fault.

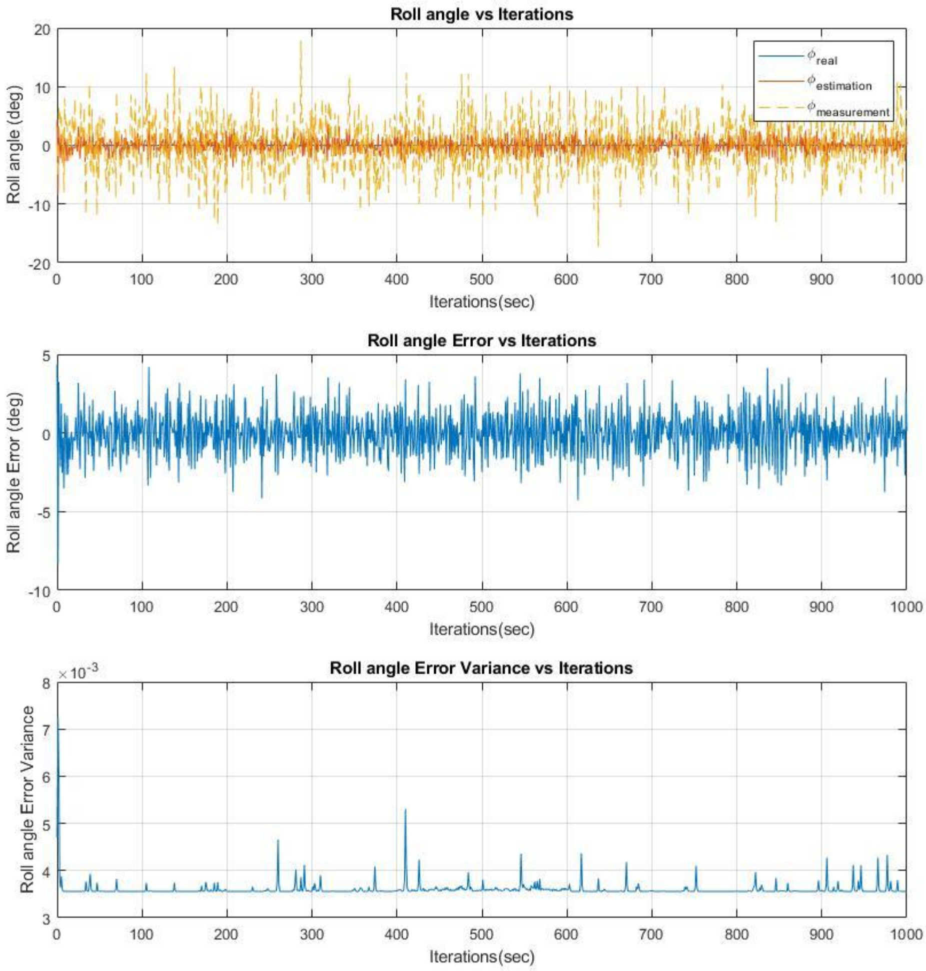

Figure 4.16 : Roll angle estimation, error and error variance with rkf implemented in case of roll rate sensor fault.

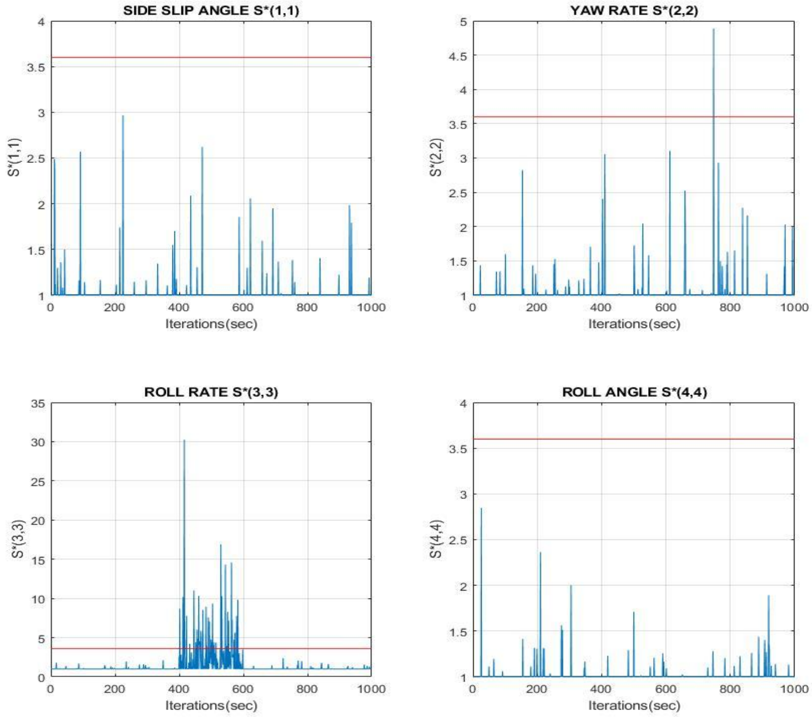

Figure 4.17 : Sensor fault isolation with measurement noise-increment fault at roll rate (p) measurements.

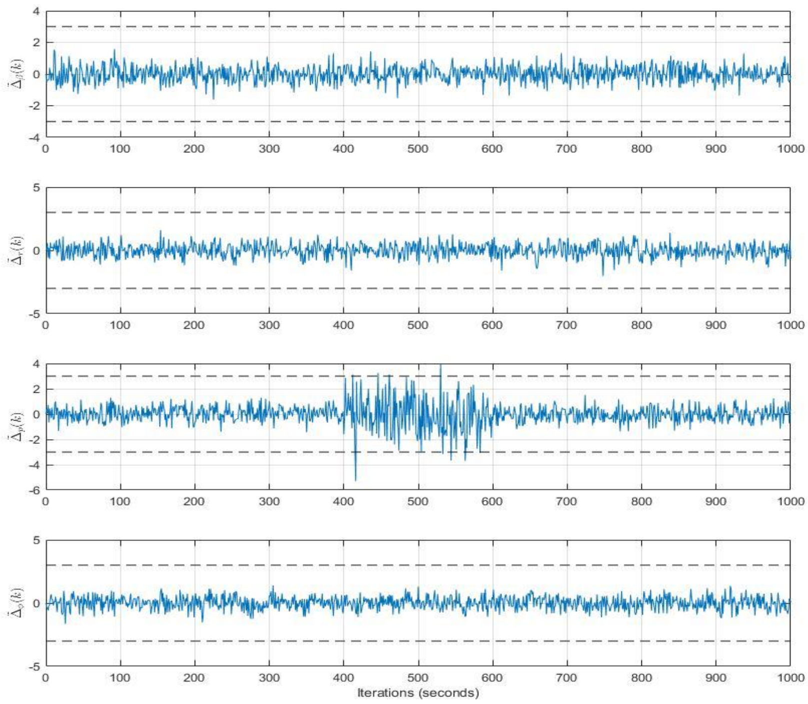

Figure 4.18 : Normalized innovations of rkf for $\boldsymbol{\beta}, \boldsymbol{r}, \boldsymbol{p}, \boldsymbol{\varphi}$ measurement channels.

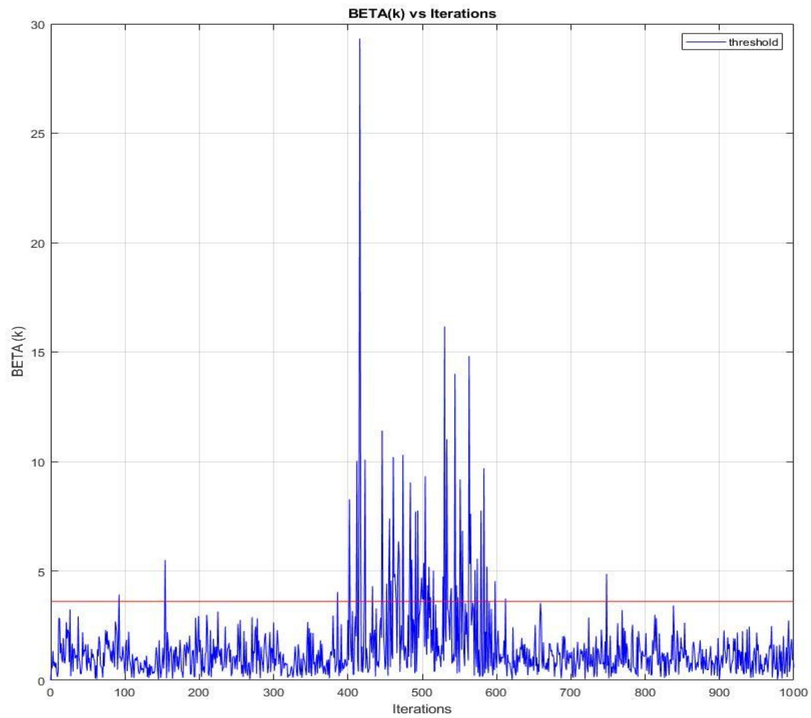

Figure 4.19 : β(k) evolution for roll rate measurement noise-increment sensor fault.

4.2.3 Measurement noise increment double sensor fault

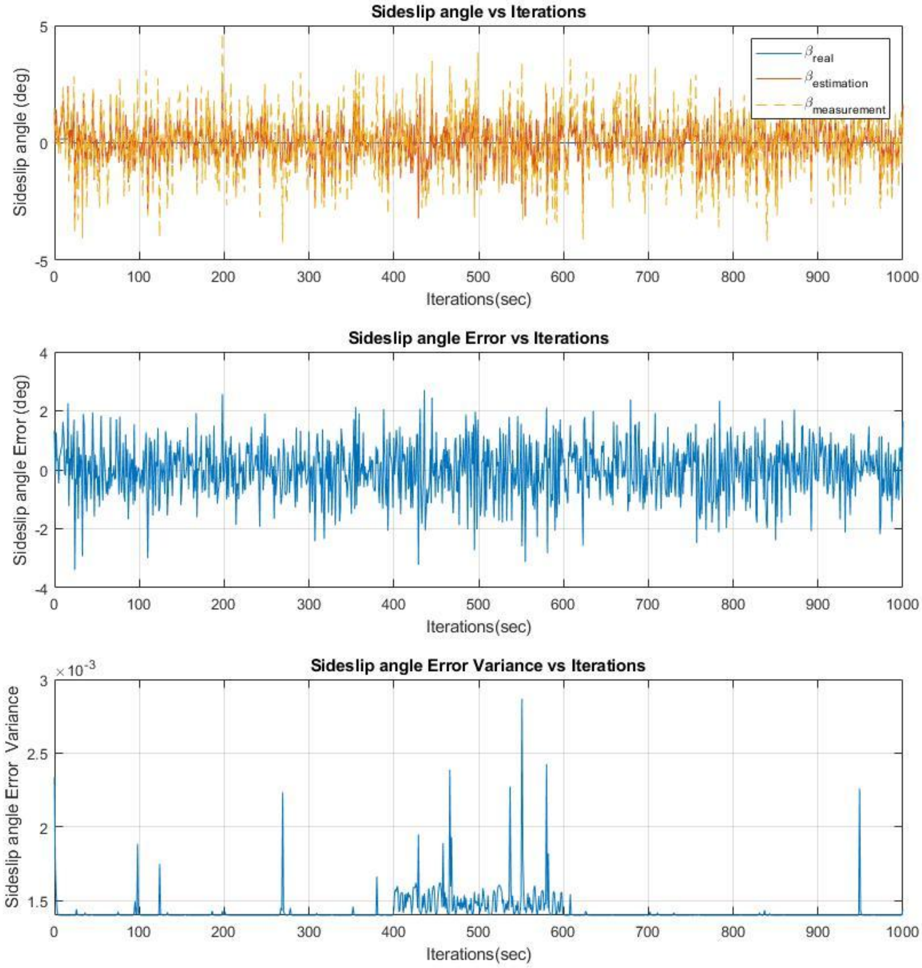

Figure 4.20 : Sideslip angle estimation, error and error variance with rkf implemented in case of roll rate & roll angle double sensor fault.

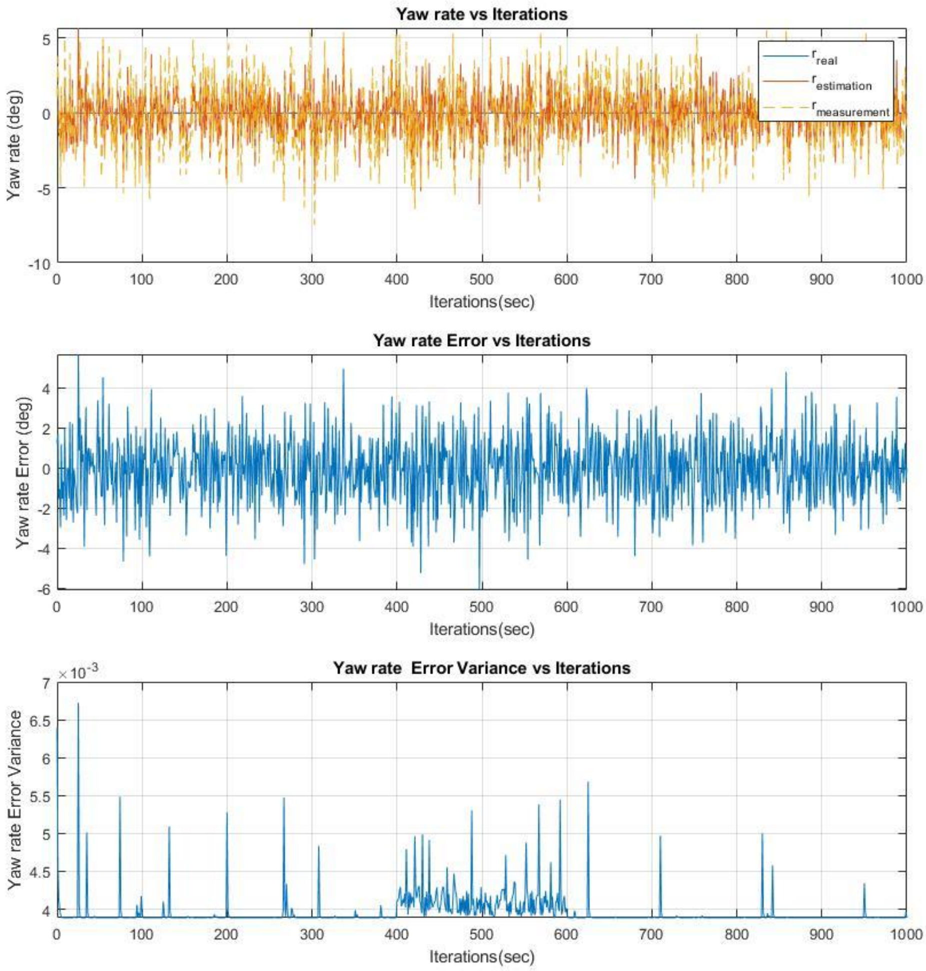

Figure 4.21 : Yaw rate estimation, error and error variance with rkf implemented in case of roll rate & roll angle double sensor fault.

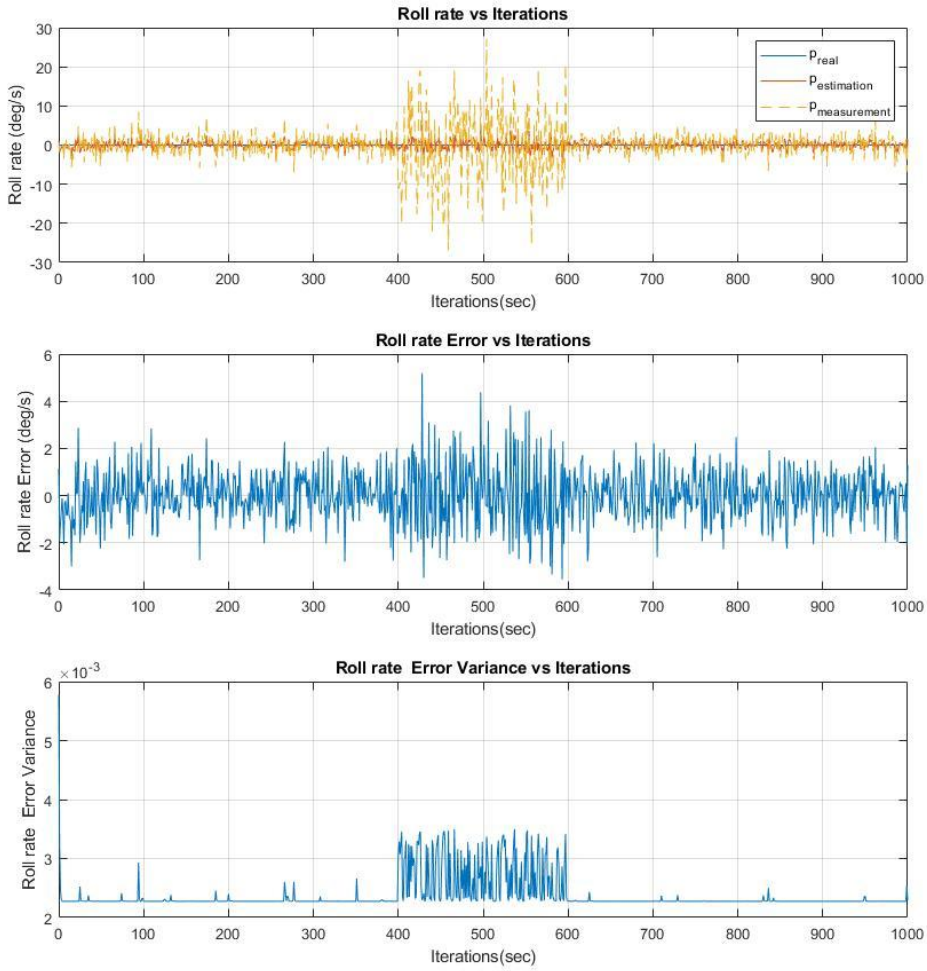

Figure 4.22 : Roll rate estimation, error and error variance with rkf implemented in case of roll rate & roll angle double sensor fault.

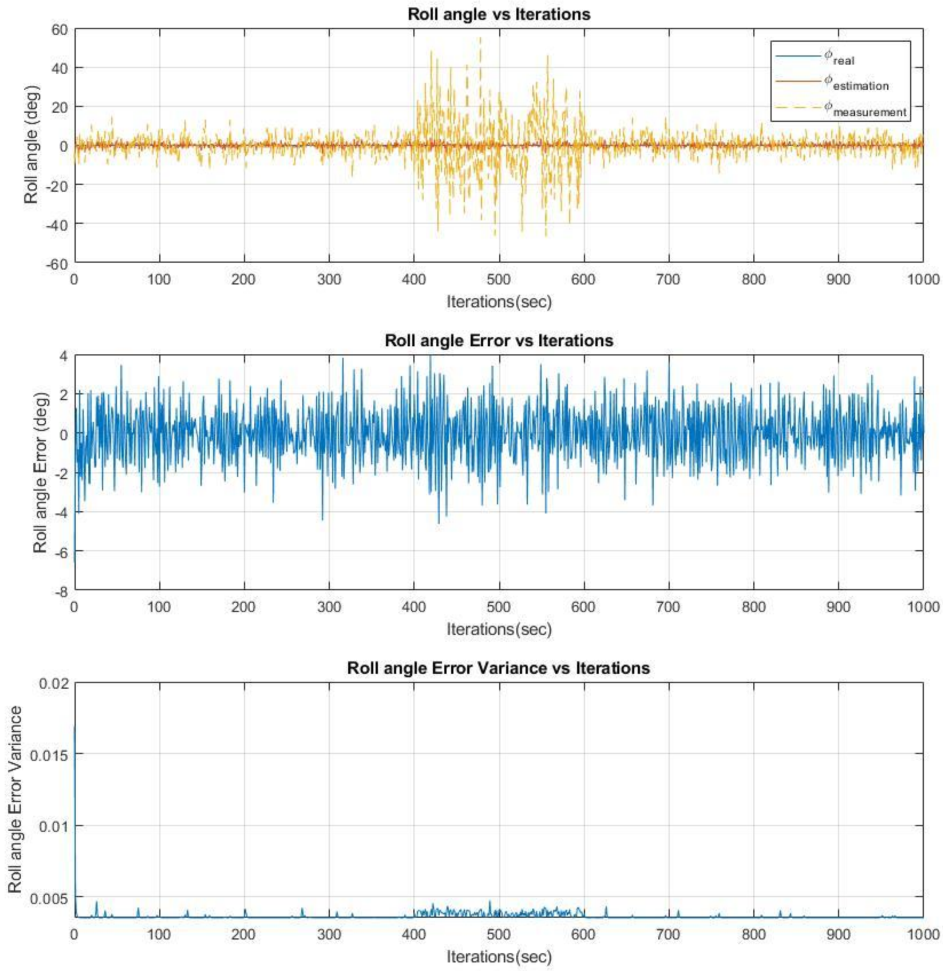

Figure 4.23 : Roll angle estimation, error and error variance with rkf implemented in case of roll rate & roll angle double sensor fault.

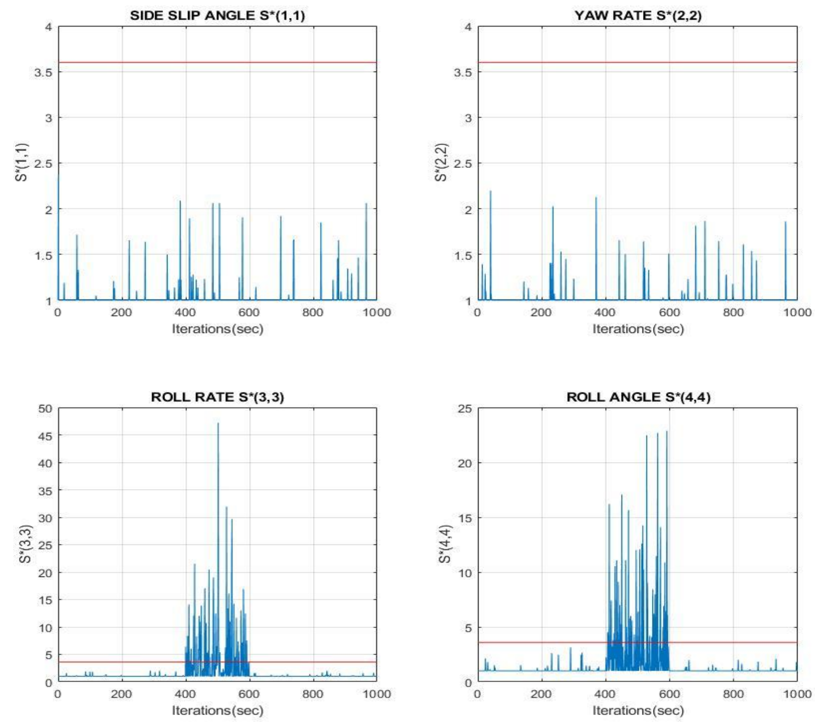

Figure 4.24 : Sensor fault isolation with measurement noise-increment fault at roll angle (φ) measurements.

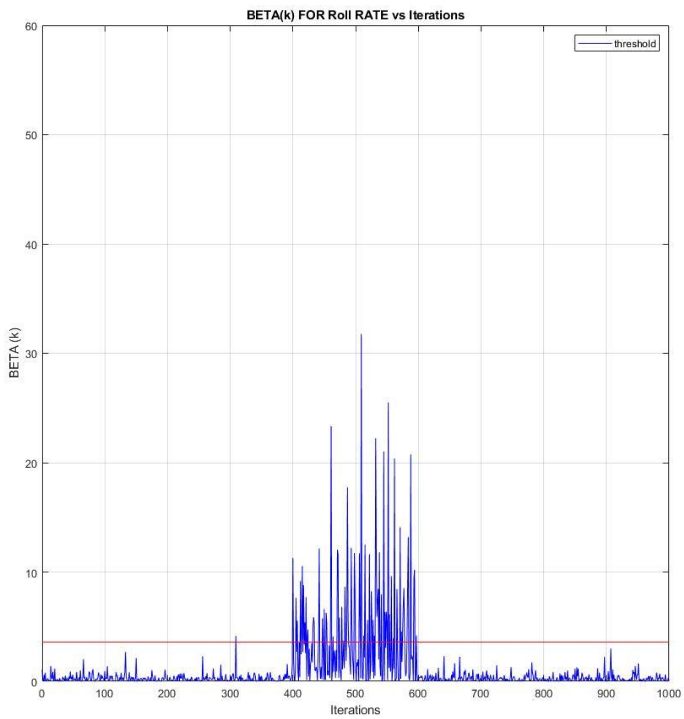

Figure 4.25 : β(k) evolution for roll rate measurement noise-increment sensor fault

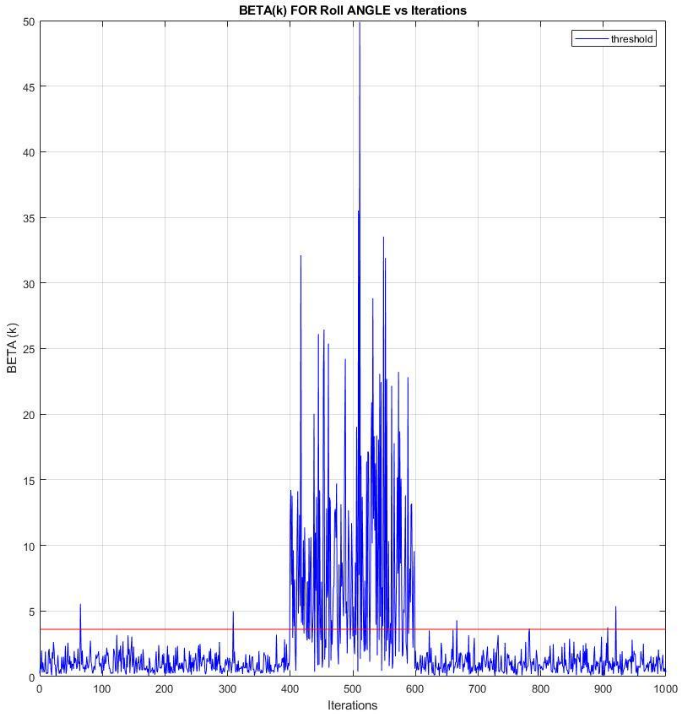

Figure 4.26 : β(k) evolution for roll angle measurement noise-increment sensor fault

4.3 Sensor Fault Results with Reconfigured Kalman Filter

The technique has been executed in 1 state parameter faulty (sideslip angle, yaw rate, roll rate and roll angle) and also in double state parameter faulty (roll rate, roll angle). It is proposed that there has been a fault from the begining of the iterations and thus, faulty measurement channels are out of order over entire simulations. Figures below have both real and estimated value for development of all lateral faults along with their error and variances, for the single and double parameter disabled conditions.

4.3.1 Reconfigured okf for sideslip angle beta sensor fault

From the Figure it can be implied that, when just one parameter diasbled, the reconfigurable Kalman filter estimates with non- remarkable error of the sideslip angle, beyond any input measurement data. Essential parameters to assess estimation performance are velocity of the error convergence, the evolution of the error absolute value and the error variance along with the iteratins nad the absolute value of the stationary error. In Fig. 4.27 it can be imferred that until 20 th iteration that the estimation accomplish to reach stationary value.

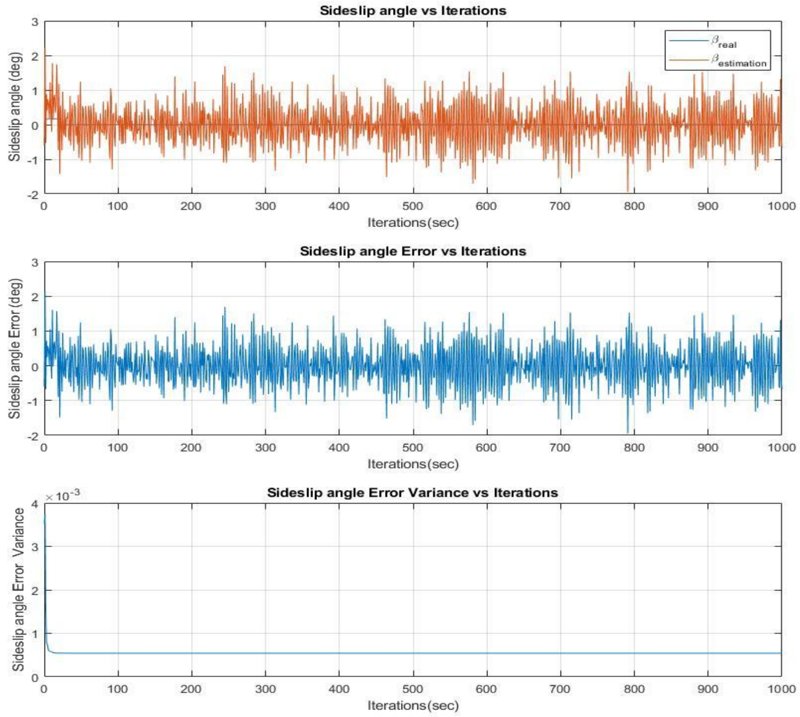

Figure 4.27 : Sideslip angle evolution, error and error variance in reconfigured Kalman filter (1 parameter (beta) estimated).

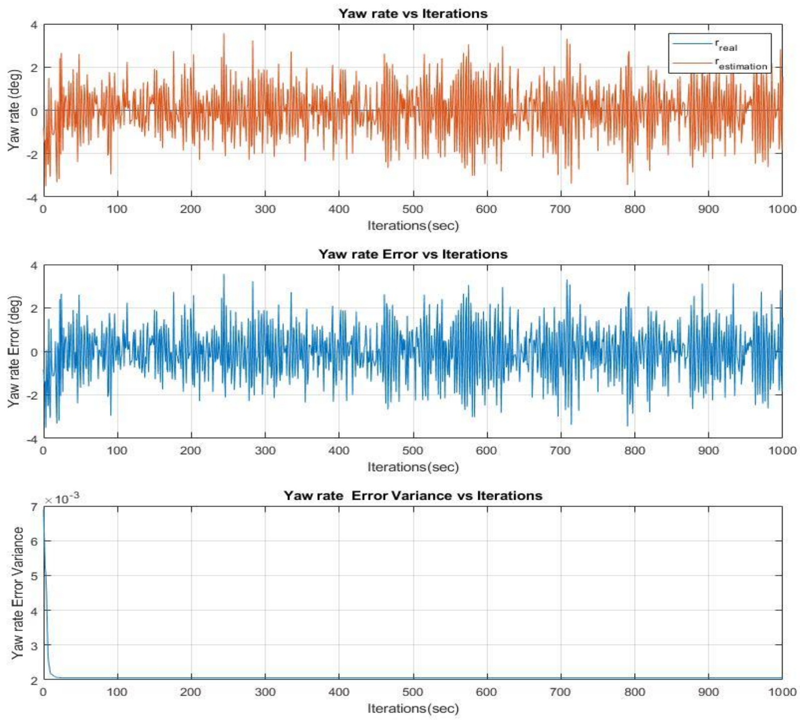

Figure 4.28 : Yaw rate evolution, error and error variance in reconfigured Kalman filter (1 parameter (beta) estimated).

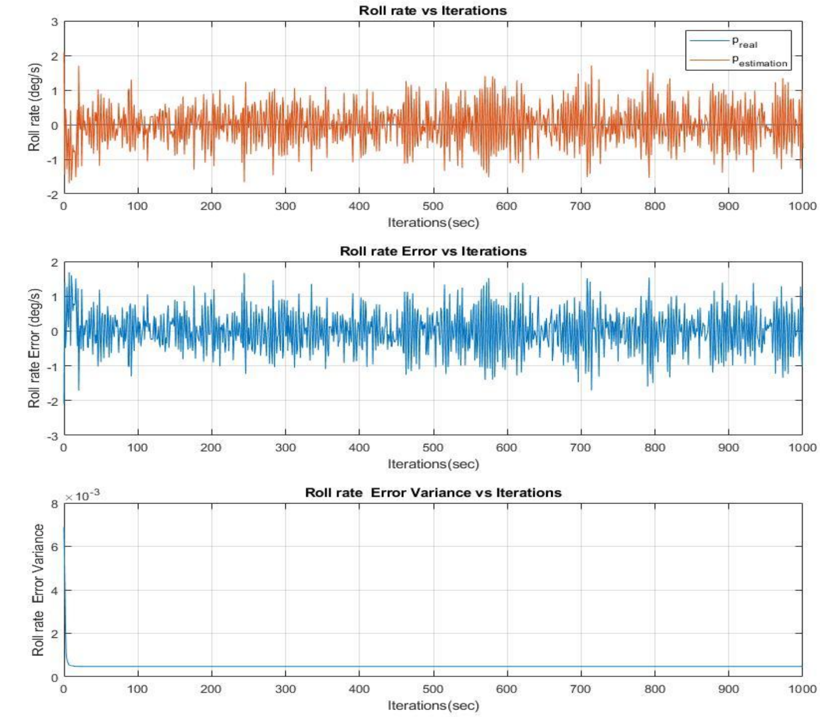

Figure 4.29 : Roll rate evolution, error and error variance in reconfigured Kalman filter (1 parameter (beta) estimated).

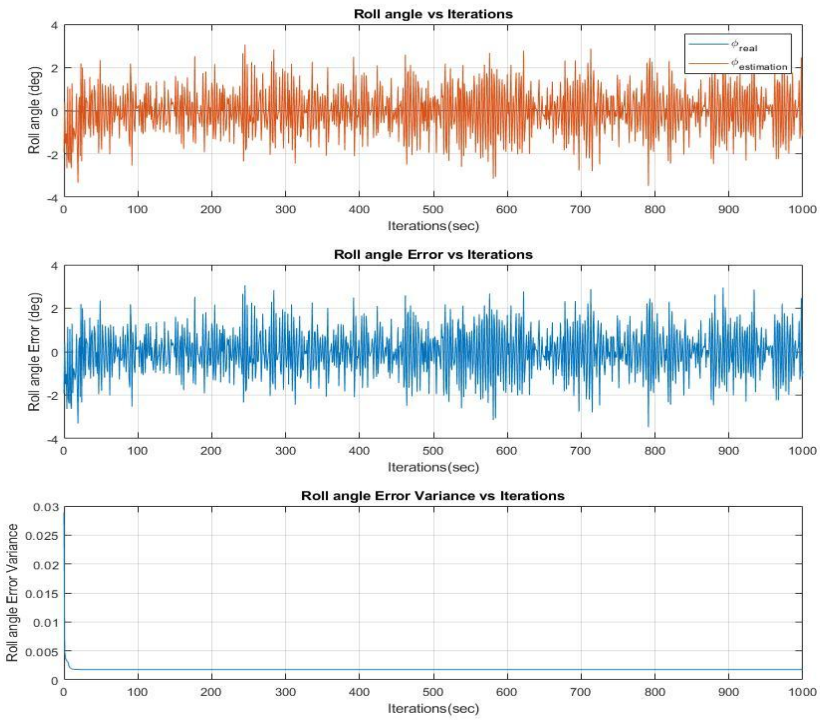

Figure 4.30 : Roll angle evolution, error and error variance in reconfigured Kalman filter (1 parameter (beta) estimated).

4.3.2 Reconfigured kf for roll rate sensor fault

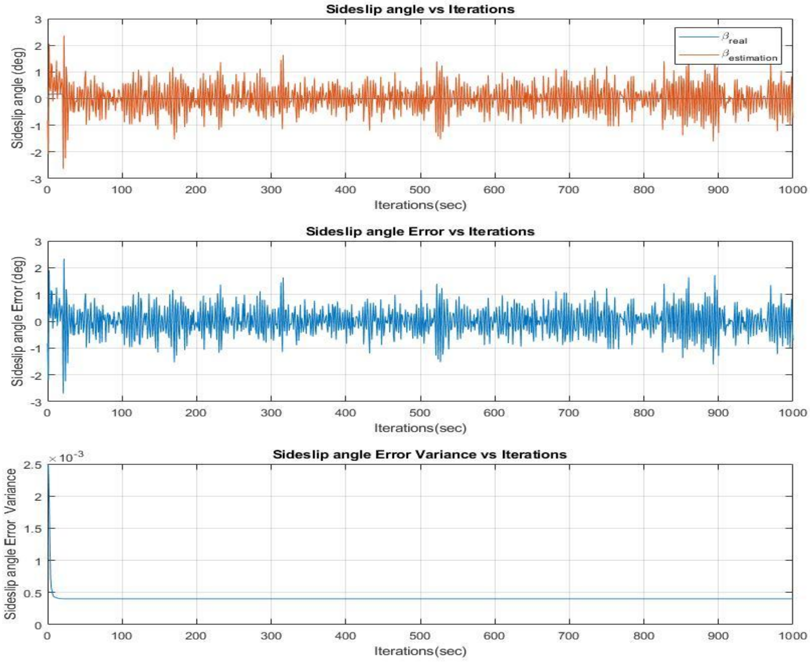

Figure 4.31 : Sideslip angle evolution, error and error variance in reconfigured Kalman filter (1 parameter (roll rate) estimated).

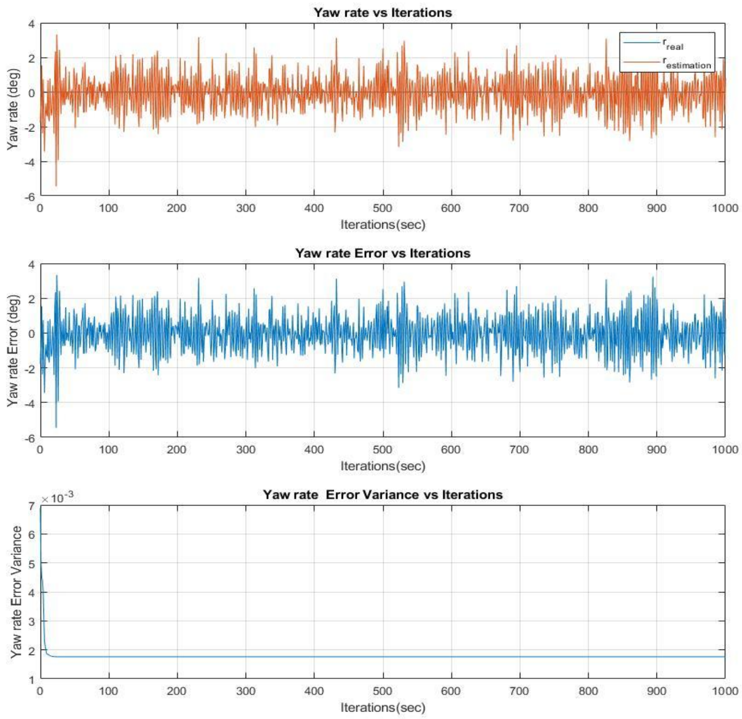

Figure 4.32 : Yaw rate evolution, error and error variance in reconfigured Kalman Filter (1 parameter (roll rate) estimated).

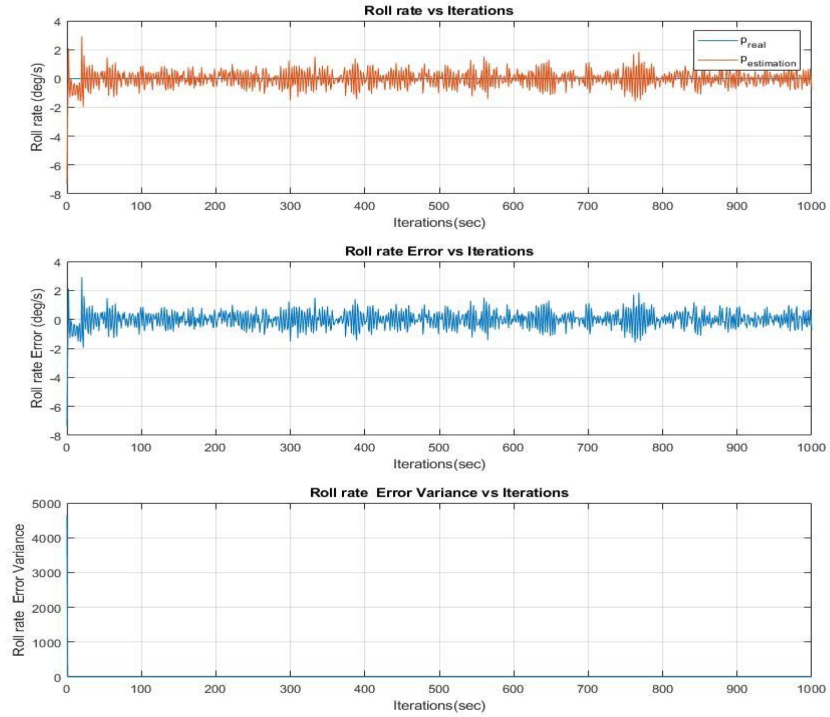

Figure 4.33 : Roll rate evolution, error and error variance in reconfigured Kalman filter (1 parameter (roll rate) estimated).

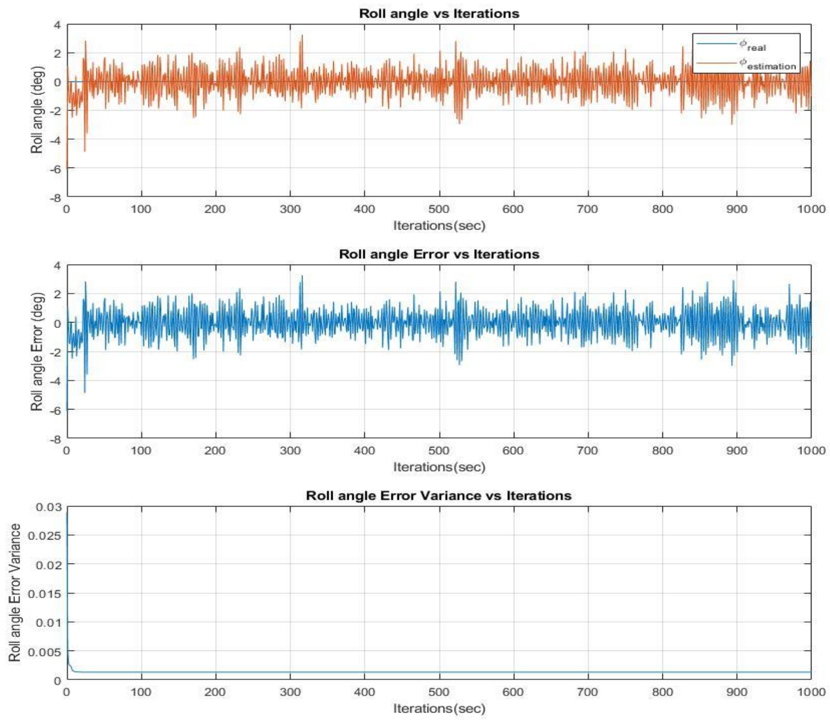

Figure 4.34 : Roll angle evolution, error and error variance in reconfigured Kalman filter (1 parameter (roll rate) estimated).

4.3.3 Reconfigured Kf for roll rate and roll angle double sensor fault

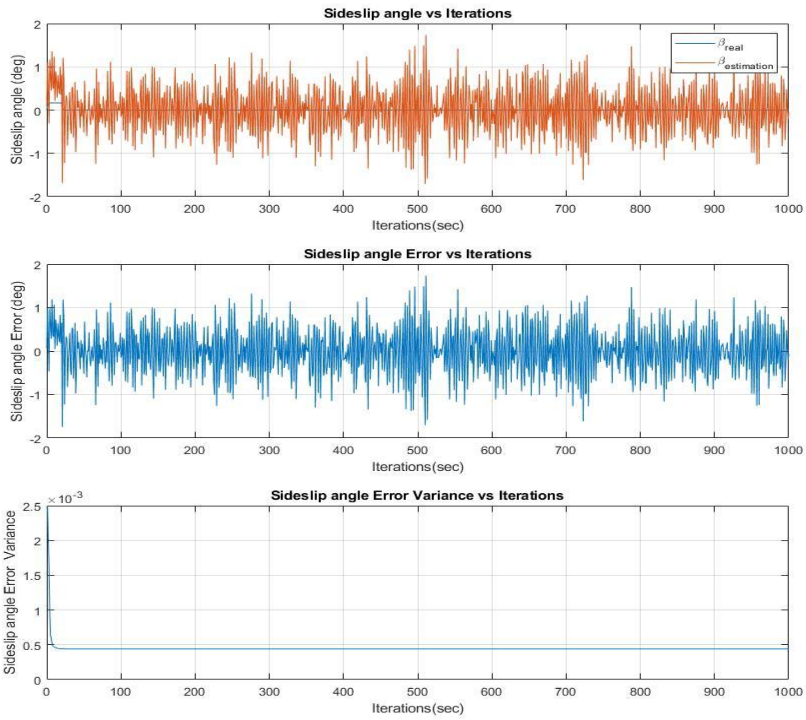

Figure 4.35 : Sideslip angle evolution, error and error variance in reconfigured Kalman filter (2 parameters (roll rate & roll angle) estimated).

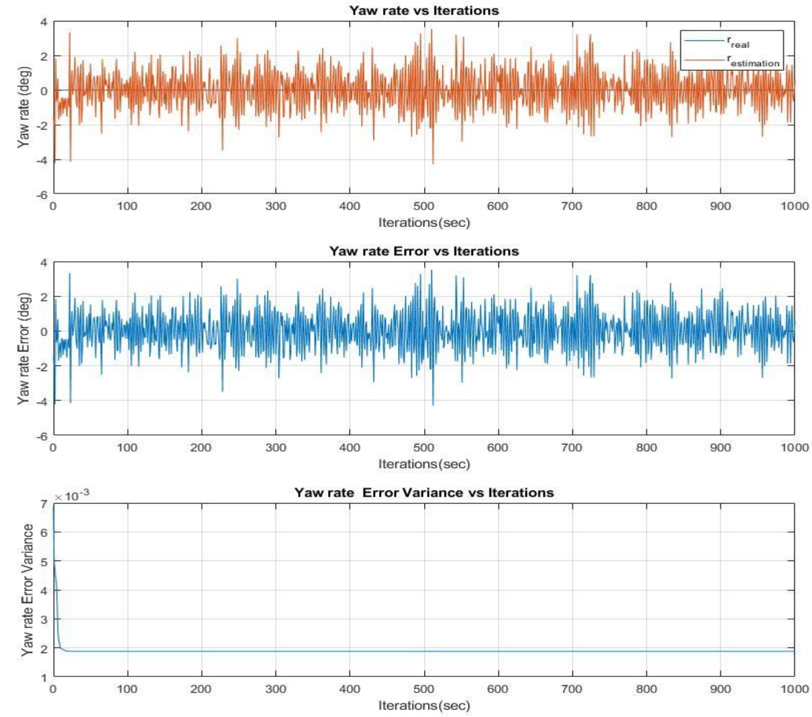

Figure 4.36 : Yaw rate evolution, error and error variance in reconfigured Kalman filter (2 parameters (roll rate & roll angle) estimated).

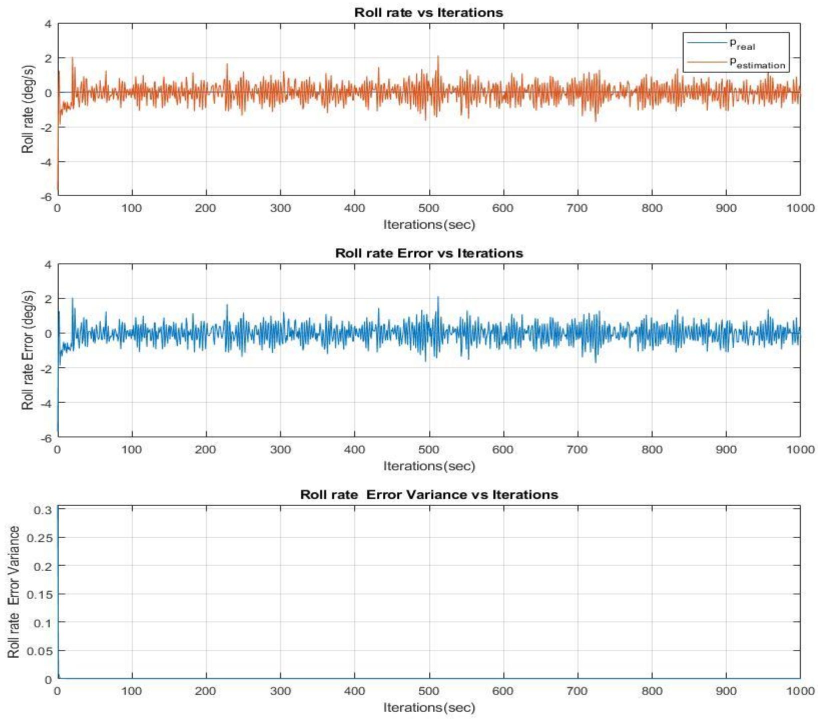

Figure 4.37 : Roll rate evolution, error and error variance in reconfigured Kalman filter (2 parameters (roll rate & roll angle) estimated).

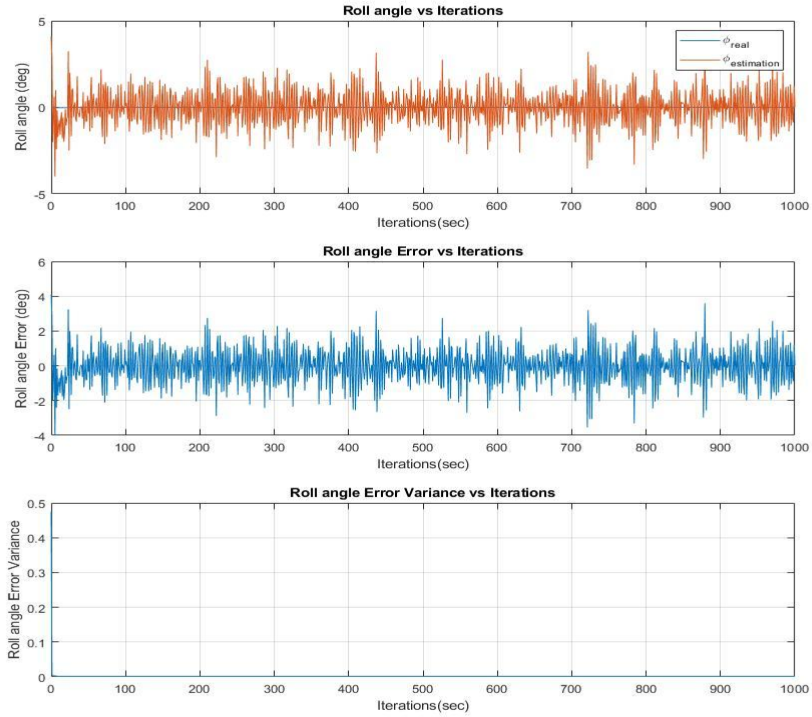

Figure 4.38 : Roll angle evolution, error and error variance in reconfigured Kalman filter (2 parameters (roll rate & roll angle) estimated).

4.4 Rmse Value Comparison in Case of Sideslip Angle SF

Table 4.1 : Root mean square value comparison.

Lateral States	No Fault Case RMSE Value	OLKF RMSE Value	RKF RMSE Value	Reconfigured KF RMSE Value
Sideslip angle (β)	0.8934	0.5816	0.5518	0.6093
Yaw rate (r)	1.6262	1.1766	1.0974	1.2045
Roll rate (p)	1.0219	0.5704	0.5394	0.5947
Roll angle (φ)	1.3540	1.0243	1.009	1.1202

In case of a sideslip angle sensor fault,

RKF gives the best estimation results that are close to actual value for yaw rate, roll rate and roll angle value.
For Yaw rate sensor, there is a 0.0792 degree error between Robust KF and OLKF value and much more close to the real value.

For Roll rate sensor, OLKF and RKF are more close to each other however, RKF has more close value to real vaue with 0.031 degrees less error.

For Roll angle sensor, the RKF estimation value is finer with 0.0153 error difference against OLKF.

4.5 Rmse Value Comparison in Case of Roll Rate SF

Table 4.2 : Root mean square value comparison in roll rate sensor fault case.

Lateral States	No Fault Case RMSE Value	OLKF RMSE Value	RKF RMSE Value	Reconfigured KF RMSE Value
Sideslip angle (β)	0.8934	1.0391	0.9588	1.0173
Yaw rate (r)	1.6262	1.8337	1.7740	1.8028
Roll rate (p)	1.0219	1.5770	1.1168	1.0066
Roll angle (φ)	1.3540	1.4672	1.3861	1.4241

In case of a roll rate sensor fault,
RKF gives the best estimation results that are close to actual value for remaining sensors.

For Sideslip angle sensor, the RKF has better result with 0.0585 degrees less error than closest Reconf. KF estimation value.

Again for Yaw rate sensor, the RKF has better result with 0.0288 degrees less error than closest Reconf. KF value.

And last for Roll angle sensor, the RKF has better result with 0.038 degrees less error than closest Reconf. KF value.

4.6 Rmse Value Comparison in Case of Double SF

Table 4.3 : Root mean square value comparison in double sensor fault case.

Lateral States	No Fault Case RMSE Value	OLKF RMSE Value	RKF RMSE Value	Reconfigured KF RMSE Value
Sideslip angle (β)	0.8934	1.1169	0.9447	1.0224
Yaw rate (r)	1.6262	1.9365	1.6918	1.8595
Roll rate (p)	1.0219	1.7616	1.1289	0.9512
Roll angle (φ)	1.3540	1.8693	1.4689	1.5193

In case of a roll rate & roll angle double sensor fault,

Robust KF gives the best estimation results that are close to actual value for sideslip angle and yaw rate sensor value.

For Sideslip angle sensor, the RKF has better result with 0.0777 degrees less error than closest Reconf. KF estimation value.

Again for Yaw rate sensor, the RKF has better result with 0.1677 degrees less error than closest REconf. KF value which means that very close to each other method value.

We can easily imply from the table that in case of a Double sensor fault, reconfigured Kalman filter has poor estimation values compared to RKF algorithm due to double faulty sensor channel.

5. SIMULINK SIMULATION RESULTS

5.1 Design and Simulation Tool

MATLAB is shortened for Matrix Laboratory and is generally used for engineering and academic aims, and speared to on broad world. Matlab makes it possible to use many several algorithms and tools to examine and analyze the problems for engineers and it utilizes matrix adjustment as to modify the matrix as required and uses matrix for basic element to display data results also the vector for special status. Those specifications makes Matlab easy to facilitate modelling systems and added to that, it performs well on behalf of illustrating graphical results. Further, Simulink is a tool included in MATLAB to calculate complex systems and algorithms and show conclusions [39]. In the light of those properties formerly implied, MATLAB Simulink program is determined to work.

5.2 Boeing 747 Test Bed

For electronic flight control system, construction of a sensor fault detection, it is vital to manipulate a modelling and simulation software. In Simulink, Airlib is a library of wide body type civil aircrafts formed by MATLAB developers and it maintains a trustworthy data source for establishing a high fidelity civil aircraft model and then implying an EFCS sensor fault detection system. Inside this library, two types of nonlinear (discrete time and continuous) aircraft model is included [40].

The aircraft model of Boeing 747 is established to sustain the nonlinear system to input of many data and for this data flow, convenient field is formed that sensors can output data to model sensors. For self-directed autonomous control, an elaborately complex model of true genuine model is necessary so for sensors are performed, suitable data flow is guaranteed. A Boeing 747 civil aircraft is decided to reach this mission and in Simulink, there are several reliable data sources for sensor system and model have been established.

In Airlib toolbox, the main structure of Boeing 747 model in Simulink shown in Figure 5.1 The model in there, takes many adjustments that are input parameters to handle the aircraft in which condition is desired commonly in steady state flight. Commonly, to illustrate a more general type of motion practiced in flight, steady state flight is chosen.

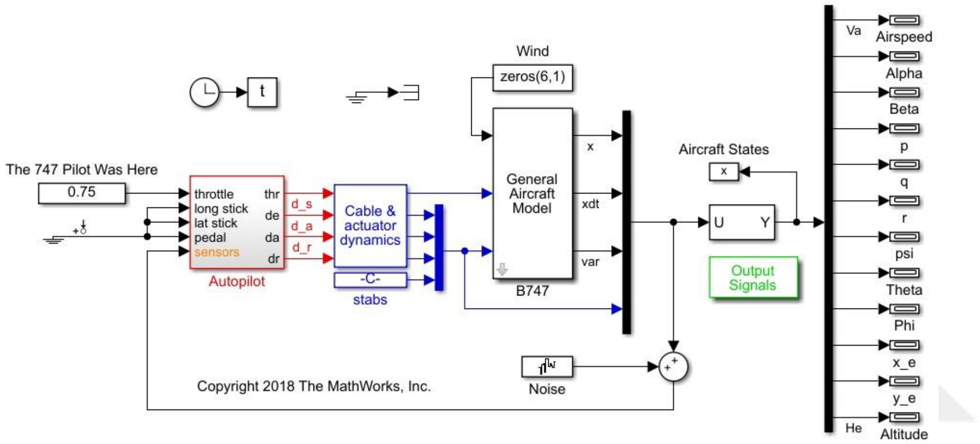

Figure 5.1 : The main structure of Boeing 747 model in simulink [40].

This section, suggested filter algorithm is qualified in this stage as to evaluate the performance of prediction when there are stuck faults tracked in the sensors. The performance of the filter algorithm and the reliability of the design paradigm that are shown in previous sections are demonstrated by many simulation cases. This is done by utilizing the effectiveness of the observer in the closed-loop system and a reliability check of the non-linear state-feedback control way.

In MATLAB Simulink, simulations of Boeing 747 nonlinear model is performed to validate the given observer-based fault detection method. Errors are remarked as residuals, are executed by conveying input data via observer subsystem in the model design. The limit error values, in another name called “thresholds” are selected for the FDD by taking the greatest value gathered by the residuals consequent to many tests. Even a residual value exceeds threshold value, fault alarm is triggered. Fault data parametrization in the simulation model of the filters have a tendency to take the angle when the control capability vanished. Wind units adjusted in the plant frame [41]. The wind effect and turbulence are assumed to be zero because of there is a negligible effect on the simulation cases.

To illustrate the FDD performance and test the fidelity of the assumed FDD method, one steady-state flight scenario is examined with variations in the states.

The simulations are done for faulty case on sideslip angle sensor. Simulation of a civil Boeing 747 aircraft is done which has an altitude of $35,000$ ft and 0.8 Mach true-airspeed for 50 seconds. The sampling time (dt) is assigned to 0.02 seconds. Outcomes are plotted as five graphics for simulation environment conditions. In Appendix A, the result and rate of the altering of the other states of B-747 differ from the lateral states$(\beta, r, p, \emptyset)$ are shown as following.

The feedback controller that is actualized for the simulation scenarios, sideslip angle (β) is given for every iteration. Sensors are the first element of noise occurrence in aircrafts. Turbulence and wind disturbances are neglected in noise subject therefore, the measurement noise (z) comes from sensor noise as it measures. Just as the moment a fault is detected, high tips in roll ange $(\emptyset)$ and yaw rate (r) are regulated by a severe rudder deflection actioned by the controller rapidly. The measurement noise (z) is added to measured sideslip angle (β) which comes from actual nonlinear aircraft model and routed to observer model subsystem.

This method concludes that, Reconfiguration block outputs, the lateral states $\beta, r, p, \emptyset$ attached as feedback to the autopilot system are manageable with a threshold value between two discrete Kalman filters. Following some simulation executes, the noise covariance matrices which are process noise (w), measurement noise (v) and the estimate error covariance (P) are assigned optimum values shown in table 5.1 in the sense of there is no affiliation among each other [42].

Table 5.1 : Process noise, measurement noise and estimate error covariance values for faulty condition.

Noise	Mean	Covariance Matrix
Process Noise (w)	0	$\begin{bmatrix} 1x10^{-3} & 0 & 0 & 0 \\ 0 & 1x10^{-3} & 0 & 0 \\ 0 & 0 & 1x10^{-3} & 0 \\ 0 & 0 & 0 & 1x10^{-3} \end{bmatrix}$
Measurement Noise (v)	0	$\begin{bmatrix} 0.0025 & 0 & 0 & 0 \\ 0 & 0.0069 & 0 & 0 \\ 0 & 0 & 0.0069 & 0 \\ 0 & 0 & 0 & 0.0289 \end{bmatrix}$
Estimate Error Covariance (P)	0	$\begin{bmatrix} 5x10^{-4} & 0 & 0 & 0 \\ 0 & 5x10^{-4} & 0 & 0 \\ 0 & 0 & 5x10^{-4} & 0 \\ 0 & 0 & 0 & 5x10^{-4} \end{bmatrix}$

The simulation process lasted for 50 seconds and an aileron input is added as delta_aileron = 0.05 radians at time t = 1 to 10 seconds. For sideslip angle , bias fault is added at t = 20 seconds and we observe that the results are satisfying for values of Optimal Kalman filter and Reconfigured Kalman filter values either converge to the measurement and actual states respectively.

5.3 Sideslip Angle Continuous Bias SF in Simulink Model

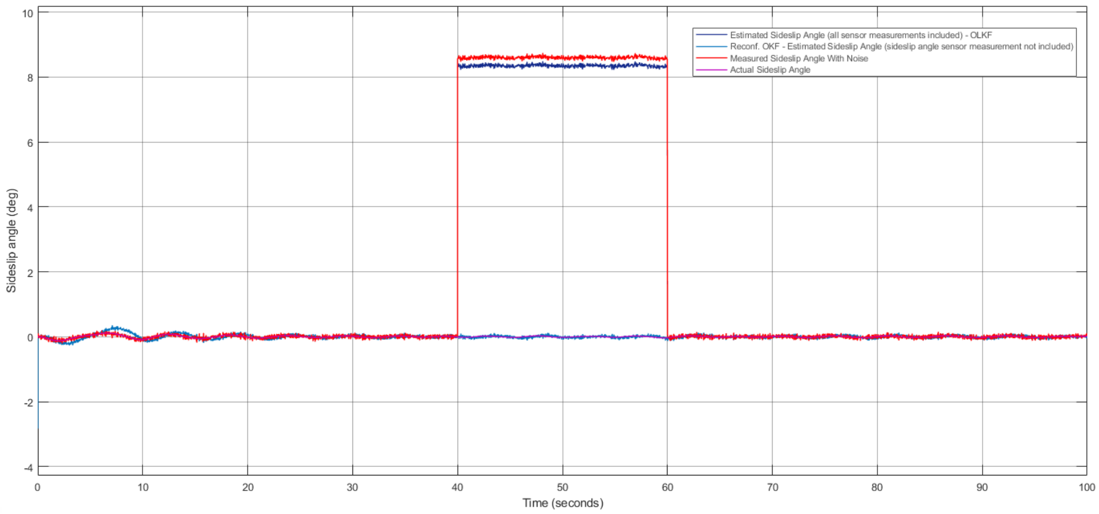

Figure 5.2 : Sidealip angle sensor fault estimations with optimal Kalman filter and reconfigured Kalman filter.

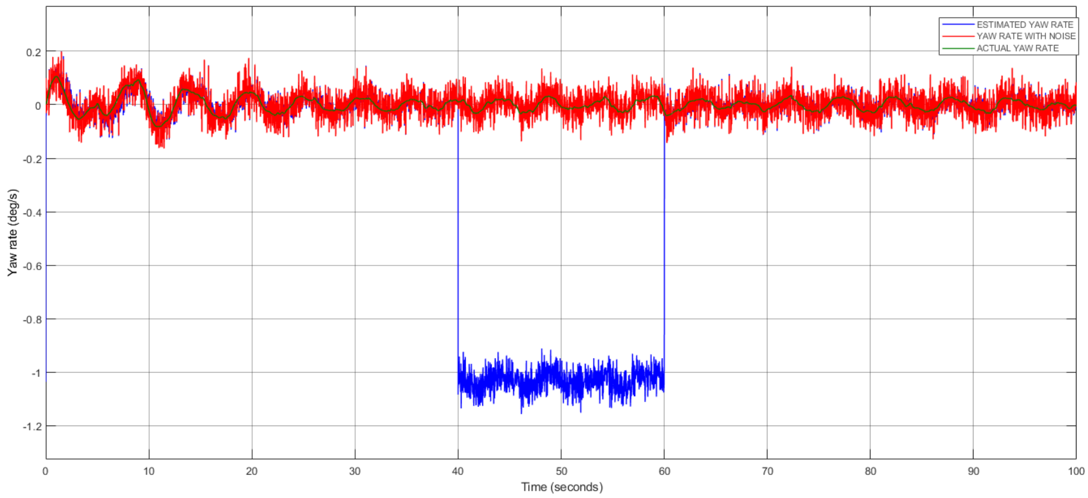

Figure 5.3 : Yaw rate estimations with optimal Kalman filter and reconfigured Kalman filter.

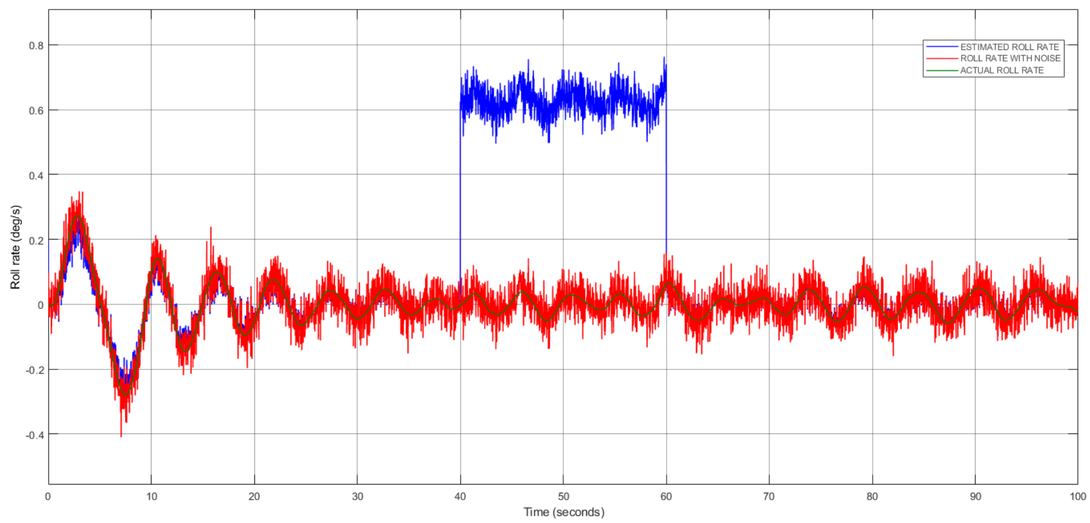

Figure 5.3 : Roll rate estimations with optimal Kalman filter and reconfigured Kalman filter.

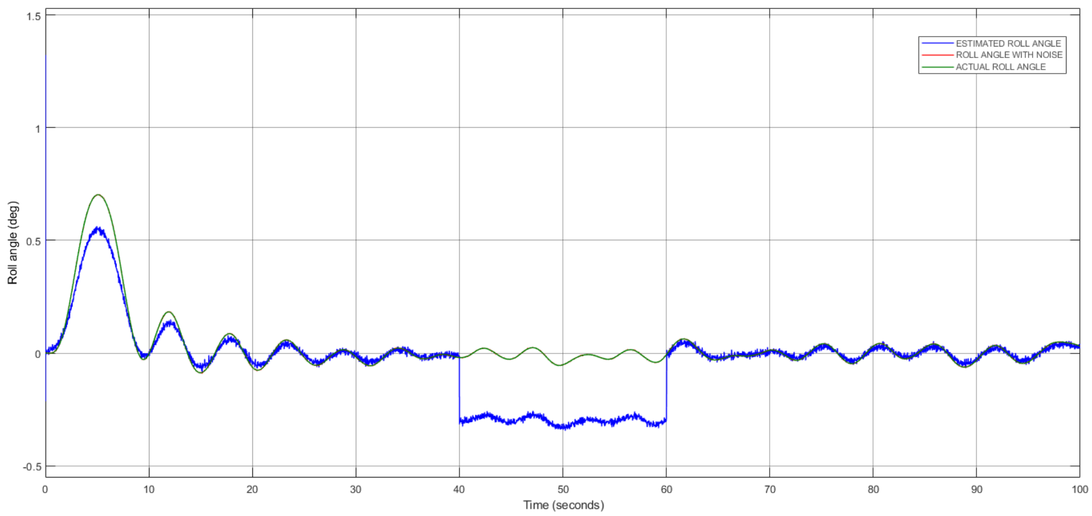

Figure 5.4 : Roll angle estimations with optimal Kalman filter and reconfigured Kalman filter.

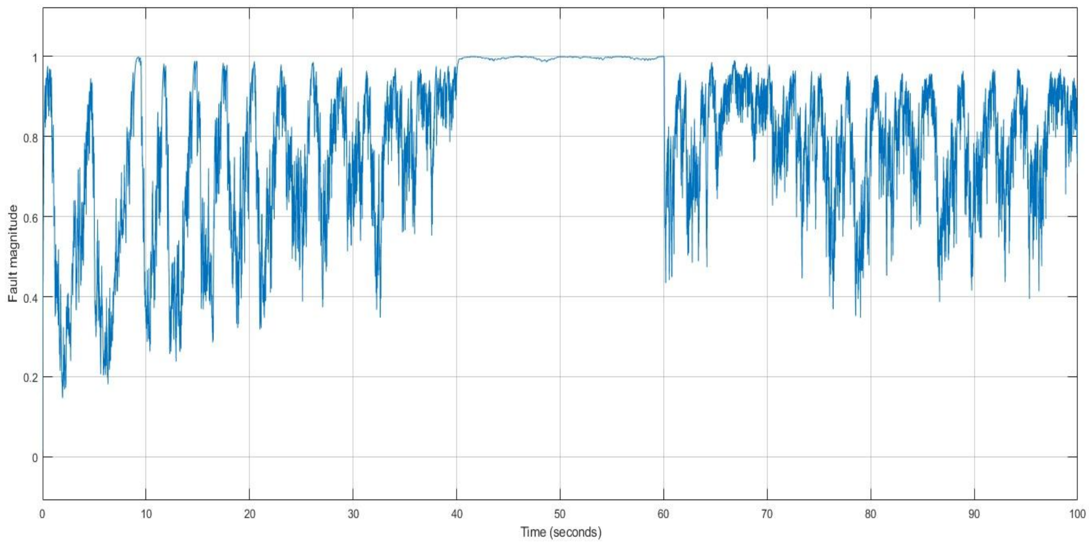

Figure 5.5 : Fault indicator when continuous bias fault.

For the first type of fault is bias fault at sideslip angle sensor. Here on the graph we see that the continuous bias fault of 7.5 degrees on measured state β is implemented at 40 th iteraton and rejected at 60 th iteration.

Here we conclude that our Optimal Kalman filter estimates the states well and values are converging to the real measurement till the fault occurs and during and after the fault, our Reconfigured Kalman filter (second Kalman filter) is selected related to the control signal at the reconfiguration process therefore enhanced estimation shows an adequate tracking of the actual state.

The yaw rate graph shows that there is an error after fault and the estimation results are broken due to the effect of the sideslip angle fault.

For roll rate graph, the measured state roll rate values are similar to the OKF values.

Again for roll angle graph, the measured state roll rate values are close to the OKF values.

6. CONCLUSIONS AND RECOMMENDATIONS

Optimal linear Kalman filter, fault detection, fault isolation, Robust Kalman filter and reconfigurable Kalman filter algorithms have been used on the flight control system of a Boeing-747 aircraft. The proposed fault detection method correctly detect the faults whether it is bias or measurement increment fault conditions. Based on the fault isolation suggested algorithm, the essential outcomes are that the RKF technique have better results compared to the other techniques. Also in case of a measurement-noise increment fault, the MMNSF allows to have estimation values that are more close to the actual value compared to the SMNSF algorithm and the oscilliations on the sensor output values diminishes. Finally, the reconfigurable kalman filter algorithm method shows better results than OLKF. In case of fouble fault the Reconfigured Kalman filter has less performance than the other proposed algorithms to have estimations that are close to real value.
All over, from the results of the simulations, it can be implied that the fault detection, isolation and accomodation algorithms accurately performs and can be embeeded to Boeing-747 flight control system.

The other study represents the concept and results of a Fault Detection and Diagnose method based on state estimations of a stochastic observer model in the continuous-time framework. The introduced design framework includes a flight control law that make an effort to tackle with unwanted faulty cases about the sensors of a transport aircraft. The sensor fault detection issue took place to confirm multi simulation tests and the control effectiveness of a high complexity dynamics systems was verified enlightened by many faulty and nominal non-fault incidents. Related to coupling effect, fault in sensor which measures sideslip angle is also have an influence on the sensor measurements of the roll angle. This situation is resulted from faulty state vector in feedback loop on controller. To succeed real time simulation conclusions, the aircraft should include direct stability derivatives. The simulation implies that the civil aircraft preserve the trim conditions for stabilization of airspeed, altitude and the last, Euler angles.

As the main section of the study utilizing the Kalman filter, the linearization applied again. An FDI scheme was enhanced for analytical backup for primarily the (β) sideslip angle sensor of lateral dynamics model of Boeing 747 civil aircraft. The created subsystems are attached properly in the simulation model to illustrate the entire elaborate architecture of the system. The offered FDI system can perform instantly for stuck faults. Another vital thing to draw attention the nonlinear aircraft model must directly unified to the observer design to gather true and accurate state estimation values even in cases that has higher strict harsh faults.

In the Kalman filter approach, it is clarified that the resultant state estimator is unbiased, stable and minor variance in precise acceptance of assumptions. In the system, on estimate state issues and detecting stuck faults, the Kalman filter performs well. It is observed that even if in the nominal situation, simulation carried out with success. Our FDD operation in the study deals with Boeing 747 civil aircraft yet, it can be modified for other types of civil, military and further on spacecrafts. From the conclusions of the simulations, it is clarified for Kalman filter mathematically overcomes on estimating the system states precisely. From theoretical perspective, the observer gain matrix is adaptive for Kalman filter which is regarded as an optimal observer if there is a such Gaussian noise resourced from sensor [33].

The figures shown in the former sections demonstrate conclusions of many numerical simulation examples for no-fault and stuck fault conditions. Coming from the stuck fault condition case, the difference among the measurements and estimations are generated the residual and the value of it was diminished and fault detection captured at a small residual value. Moreover, nominal case with a selected threshold value and verification time, there is no false alarms triggered and detected.

In conclusion, Kalman filter method is sensitive to faults and carries out via slight detection threshold level, short affirmation time scope and adequate alarm percentage limitation properties. The system model could rapidly detect even minor altering in the measurement channel and fits for real-time fault detection situations. The residuals are demonstrated to be limited in a constrained gap for the developed design method. In case, fault detection and reconfiguration system does not work properly, aircraft will outrun the safe operation region, therefore fault detection is crucial to take place so faults could be identified at instant. If not detected, the aircraft system will run into an instability condition which would result a fatal accident. The conclusions of the experiment enlightened that the offered Kalman filter maintained a remarkable profit and safety for estimation performance. Similar to the use of Kalman filter in this study, it can be confirmed to utilize in expanded applications for similar studies and from industrial dimension, it can help enhancing aircraft performance in flight.

Future studies could center attention on interactive multiple model (IMM) union Kalman filter rather performing one Kalman filter model in the FDI scheme to gather higher precise state estimations. IMM Kalman filter model is formed from two Kalman model that utilizes the model equations and it makes a decision on two and selects one to use by calculations on probability and weight facts on behalf of the measurement value by the model. So, the necessity to calibrate the optimum values of covariances will be autonomously set with filter.

The mission of the study could help real-time flight conditions by regulating and augmenting aircraft system and performance such fuel consumption, reduced noise and boost the range of the aircraft. The educational and research purposes can be followed in the light of this study. For industrial sight, the linearization process can be exerted to several flight conditions instantly with performing the required adjustments on the system and Kalman filter discrete time step simultaneously to the autopilot system and followingly the fault detection, isolation and accommodation algorithms can be run to make the flight preserve its safe operation.

REFERENCES

[1] **Gheorghe, A. & Zolghadri, Ali & Cieslak, Jérôme & Goupil, Philippe & Dayre, R. & LeBerre, H..** (2013). Toward model-based approaches for fast and robust fault detection in aircraft control surface servo-loop: From theory to application. IEEE Control Systems Magazine. 33.

[2] **Fang, H., N. Tian, Y. Wang, M. Zhou, & M.A. Haile.** (2018). "Nonlinear Bayesian Estimation: From Kalman Filtering to a Broader Horizon." *IEEE/CAA Journal of Automatica Sinica.* Vol. 5, Number 2, pp. 401–417.

[3] **Zhang, J., You, K., & Xie, L.** (2018). *Bayesian Filtering with Unknown Sensor Measurement Losses. IEEE Transactions on Control of Network Systems, 1–1.* doi:10.1109/tcns.2018.2802872

[4] **Valade, A., Acco, P., Grabolosa, P., & Fourniols, J.-Y.** (2017). *A Study about Kalman Filters Applied to Embedded Sensors. Sensors, 17(12), 2810.* doi:10.3390/s17122810

[5] **Hajiyev, C. and Caliskan, F.** (2005), *Sensor and control surface/actuator failure detection and isolation applied to F-16 flight dynamic, Aircraft Engineering and Aerospace Technology,* Vol. 77 No. 2, pp. 152-160.

[6] **Jayaram, S.** (2010). *A new fast converging Kalman filter for sensor fault detection and isolation. Sensor Review, 30(3), 219–224.* doi:10.1108/02602281011051407

[7] **Wei, Xiukun & Verhaegen, Michel.** (2011). Sensor and actuator fault diagnosis for wind turbine systems by using robust observer and filter. Wind Energy. 14. 491 - 516. 10.1002/we.438.

[8] **Lim, J. K., & Park, C. G.** (2014). Satellite Fault Detection and Isolation Scheme with Modified Adaptive Fading EKF. *Journal of Electrical Engineering and Technology,* 9(4), 1401–1410. https://doi.org/10.5370/jeet.2014.9.4.1401

[9] **Van Eykeren, Laurens & Chu, Q**.. (2013). Air Data Sensor Fault Detection Using Kinematic Relations. 10.1007/978-3-642-38253-6_12.

[10] **Jesussek, Mathias & Ellermann, Katrin.** (2013). Fault detection and isolation for a nonlinear railway vehicle suspension with a Hybrid Extended Kalman filter. Vehicle System Dynamics. 51. 10.1080/00423114.2013.810764.

[11] **Miao Du, Scott, J., & Mhaskar, P.** (2013). *Actuator and sensor fault isolation of nonlinear systems. 2013 American Control Conference.* doi:10.1109/acc.2013.6580383

[12] **Bolandi, H. & Abedi, M. & Haghparast, Mehran.** (2013). Fault detection, isolation and accommodation for attitude control system of a three-axis satellite using interval linear parametric varying observers and fault tree analysis. Proceedings of the Institution of Mechanical Engineers, Part G: Journal of Aerospace Engineering. 228. 1403-1424. 10.1177/0954410013493230.

[13] **Sercekman, O., & KUTAY, A. T. ,** (2018). *A Model Based Approach for Sensor Fault Detection in Civil Aircraft Control Surface* (Master's thesis).

[14] **Xu, G. X.** (2011). *Nonlinear Fault-Tolerant Guidance and Control for Damaged Aircraft* (Master's thesis).

[15] **Zolghadri, A., Henry, D., Cieslak, J., Efimov, D., & Goupil, P.** (2014). *Fault Diagnosis and Fault-Tolerant Control and Guidance for Aerospace Vehicles. Advances in Industrial Control.* doi:10.1007/978-1-4471-5313-9

[16] **Caliskan, Fikret & Hajiyev, Chingiz.** (1999). Sensor fault detection in flight control systems based on the Kalman filter innovation sequence. Proceedings of The Institution of Mechanical Engineers Part I-journal of Systems and Control Engineering - PROC INST MECH ENG I-J SYST C. 213. 243-248. 10.1243/0959651991540115.

[17] **Bonfè, M., Castaldi, P., Geri, W., & Simani, S.** (2006). *Fault detection and isolation for on-board sensors of a general aviation aircraft. International Journal of Adaptive Control and Signal Processing, 20(8), 381–408.* doi:10.1002/acs.906

[18] **Kim, S., Jung, I., Kim, Y., & Park, C.** (2004). *Hybrid Fault Detection and Isolation Techniques for Aircraft Inertial Measurement Sensors. AIAA Guidance, Navigation, and Control Conference and Exhibit.* doi:10.2514/6.2004-5419

[19] **Jiang, J., & Yu, X.** (2012). *Fault-tolerant control systems: A comparative study between active and passive approaches. Annual Reviews in Control, 36(1), 60–72.* doi:10.1016/j.arcontrol.2012.03.005

[20] **Wang, T.** (2012). Sliding Mode Fault Tolerant Reconfigurable Control against Aircraft Control Surface Failures.Concordia University, Department of Mechanical and Industrial Engineering.

[21] **Blanke, M., Kinnaert, M., Lunze, J., & Staroswiecki, M.** (2016). *Diagnosis and Fault-Tolerant Control.* doi:10.1007/978-3-662-47943-8

[22] **Levesque, Mario J. L.** (1993) *Fault Detection and Isolation for the Bluebird Test Bed Aircraft, Naval Postgraduate School*, Department of Electrical Engineering.

[23] **P. K. Rachinayani.** (2006) Robust Fault-Tolerant Control for aircraft systems, Graduate Faculty of the Louisiana State University and Agricultural and Mechanical College, Department of Electrical and Computer Engineering.

[24] **GNair, Vishnu & v, Dileep & R, Prahalad.** (2012). Design of Fuzzy Logic Controller for Lateral Dynamics Control of Aircraft by Considering the Cross-Coupling Effect of Yaw and Roll on Each Other. International Journal of Computer Applications. 47. 44-48. 10.5120/7252-0368.

[25] **Alwi, H., Edwards, C., & Pin Tan, C.** (2011). *Fault Detection and Fault-Tolerant Control Using Sliding Modes. Advances in Industrial Control.* doi:10.1007/978-0-85729-650-4

[26] **Hong, J., Laflamme, S., Dodson, J., & Joyce, B.** (2018). *Introduction to State Estimation of High-Rate System Dynamics. Sensors, 18(2), 217.* doi:10.3390/s18010217

[27] **Vepa, R., & Caliskan, F.** (1995). Application of Observers to Monitoring, Failure Detection and Fault Diagnosis in Aircraft Flight Control. Proceedings of the Institution of Mechanical Engineers, Part G: Journal of Aerospace Engineering, 209(1), 65–73. https://doi.org/10.1243/PIME_PROC_1995_209_271_02

[28] **Han, Y., Kim, Y., Choi, B., Kim, H. J., Oh, S., & Kwak, D.** (2012). *Fault detection and identification of aircraft control surface using adaptive observer and input bias estimator. IET Control Theory & Applications, 6(10), 1367–1387.* doi:10.1049/iet-cta.2010.0724

[29] **J. George.** (2005). Lateral Directional Approximations to Aircraft, Indian Institute of Science, Department of Aerospace Engineering.

[30**] Akmeliawati, R., & Mareels, I.** (2002). *Flight control systems, practical issues in design and implementation. Automatica, 38(12), 2191–2193.* doi:10.1016/s0005-1098(02)00132-2

[31] **L. Tian.** (1999). A study of nonlinear flight control system designs, Iowa State University, Department of Aerospace Engineering.

[32**] Etkin, B. and L.D. Reid.** (1996). *Dynamics of Flight; Stability and Control*, Third Edition, John Wiley & Sons, Inc., New York.

[33] **V. Sridhar, H. S. Sheshadri and M. C. Padma.** (2014). "Emerging Research in Electronics, Computer Science and Technology," *Proceedings of International Conference*, vol. 248, pp. 801–810.

[34] **Kumar M G, Ravi & Ramamurhy, Dr.T.** (2016). Fault Detection of Aircraft Plant Using KALMAN FILTER. 8. 923-932.

[35] **E. I. E. Madbouly I. A. Hameed and M. I. Abdo.** (2017). Reconfigurable Adaptive Fuzzy Fault-hiding Control for Greenhouse Climate Control System, *International Journal of Automation and Control.*, vol. 11, no. 2, pp. 164–187.

[36] **Sasiadek, J. Z., & Hartana, P.** (2000). *Sensor data fusion using Kalman filter. Proceedings of the Third International Conference on Information Fusion.* doi:10.1109/ific.2000.859866

[37] **Hajiyev, C., & Soken, H. E.** (2012). *Robust Estimation of UAV Dynamics in the Presence of Measurement Faults. Journal of Aerospace Engineering, 25(1), 80–89.* doi:10.1061/(asce)as.1943-5525.0000095

[38] **Robinson, C.R.** (2008). Decentralised Data Fusion Using Agents.

[39] **G. Campa,** Airlib version 1.11.0.0, The Aircraft Library. Available from https://www.mathworks.com/matlabcentral/fileexchange/3019-airlib. Accessed: 2018-06-01.

[40] **Samara, P. A., Sakellariou, J. S., Fouskitakis, G. N., & Fassois, S. D.** (2003). Detection of sensor abrupt faults in aircraft control systems. Proceedings of 2003 IEEE Conference on Control Applications, 2003. CCA 2003. doi:10.1109/cca.2003.1223211

[41] **A. Gelb, A.** (1974). Applied Optimal Estimation, Eleventh Edition.

APPENDICES

APPENDIX A:

APPENDIX B:

APPENDIX A

A.1. OLKF for Yaw Rate Continuous Bias Sensor Fault

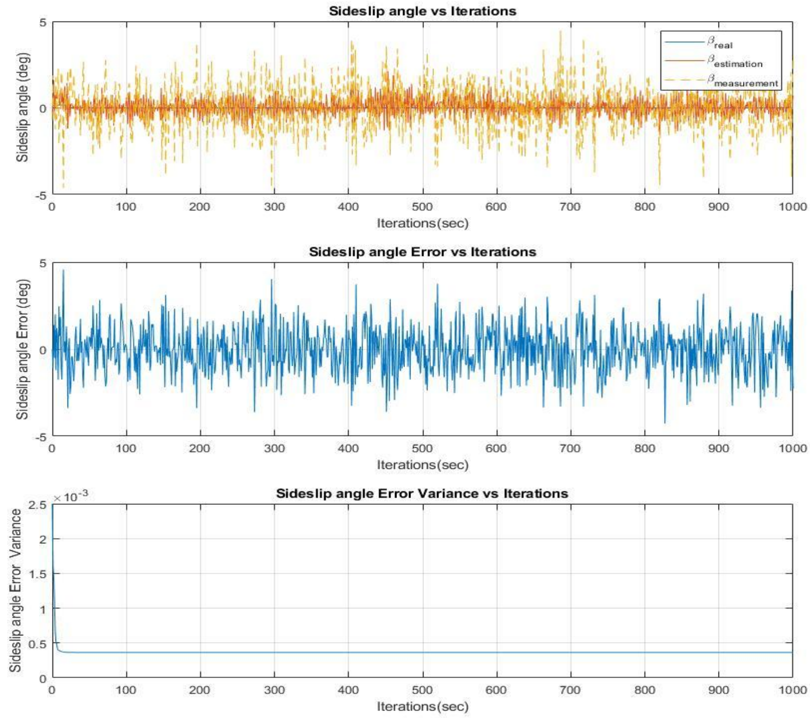

Figure A.1.1 : Sideslip angle estimation, error amd error variance with olkf implemented in case of yaw rate sensor fault.

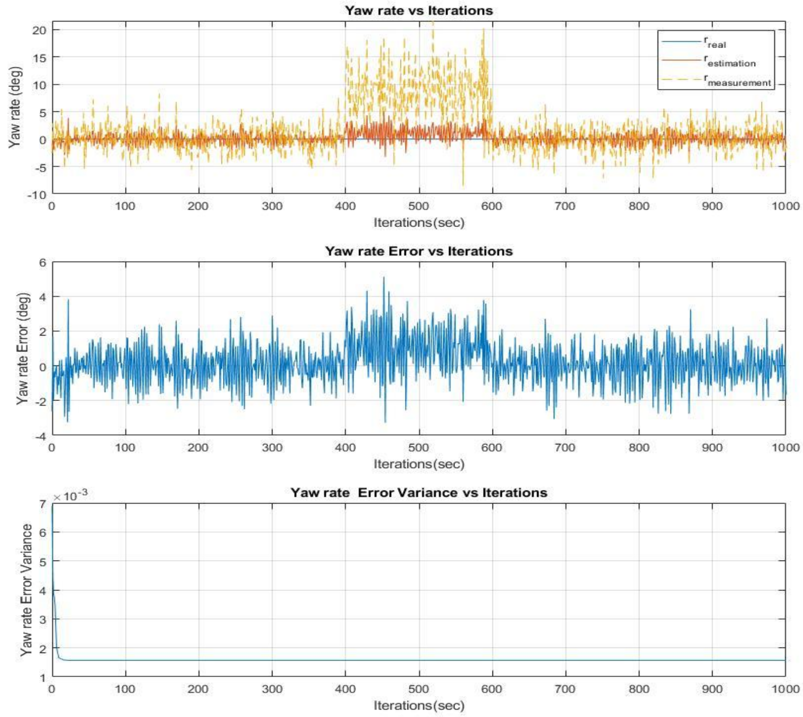

Figure A.1.2 Yaw rate estimation, error amd error variance with olkf implemented in case of yaw rate sensor fault.

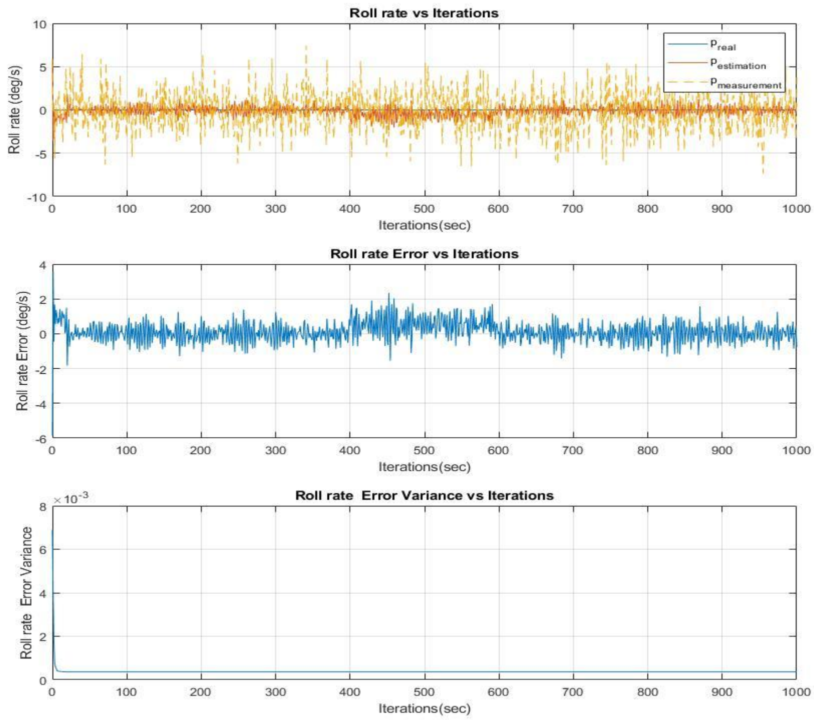

Figure A.1.3 : Roll rate estimation, error amd error variance with olkf implemented in case of yaw rate sensor fault.

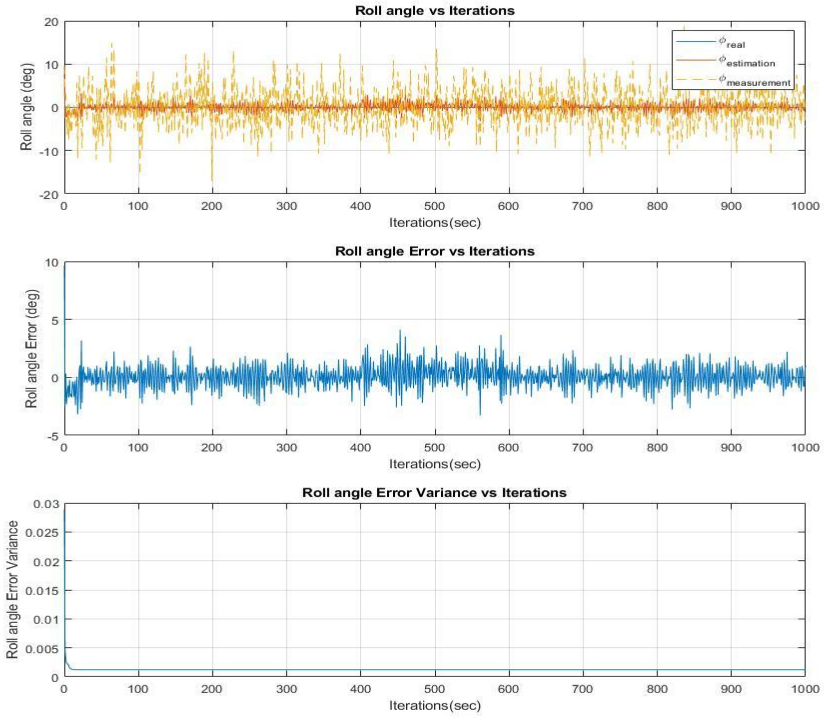

Figure A.1.4 : Roll angle estimation, error amd error variance with olkf implemented in case of yaw rate sensor fault.

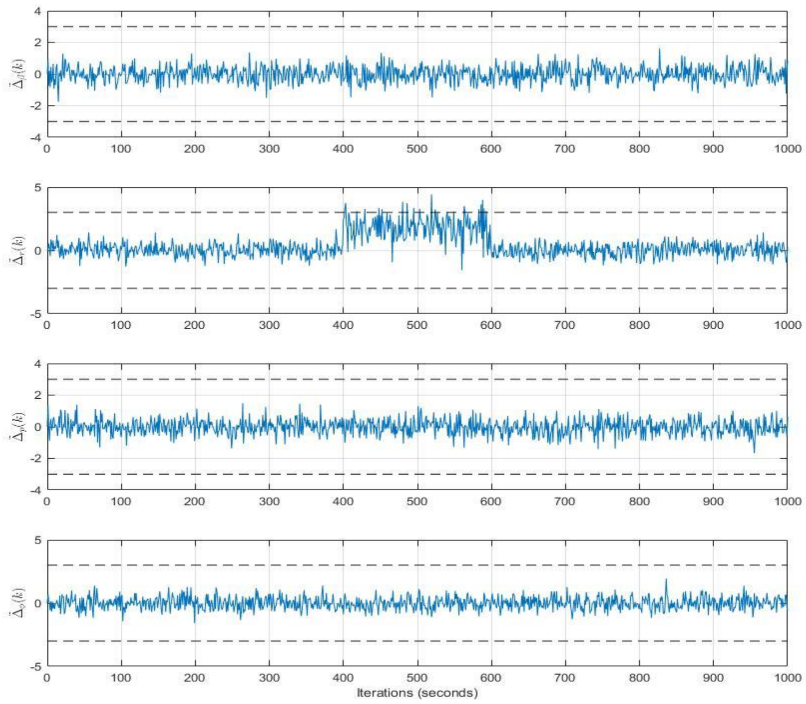

Figure A.1.5 : Normalized innovations of olkf for β,r p,φ measurement channels in case of yaw rate sensor fault.

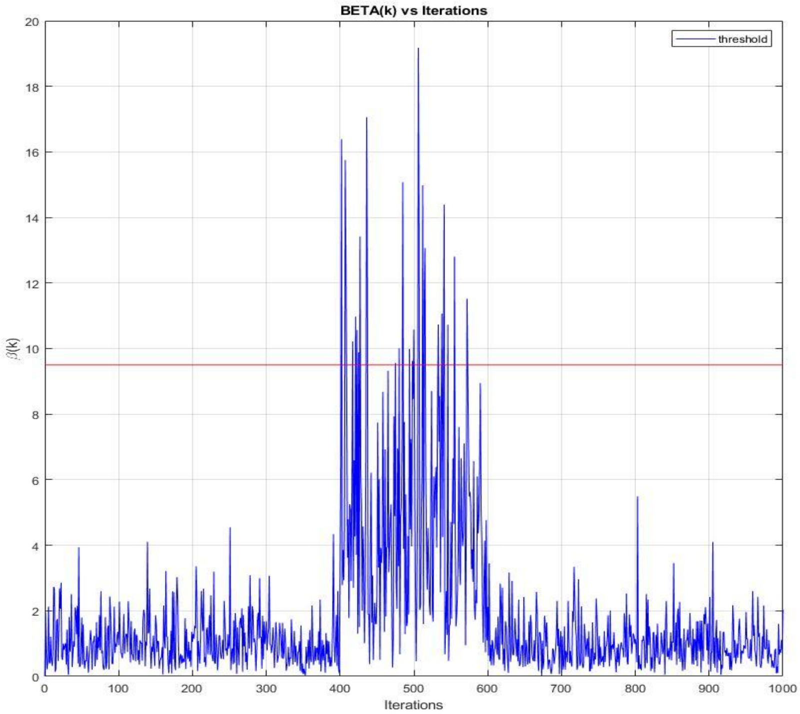

Figure A.1.6 : β(k) evolution for the case of continuous bias fault at beta measurement in case of yaw rate sensor fault.

A.2. RKF for Yaw Rate Continuous Bias Sensor Fault

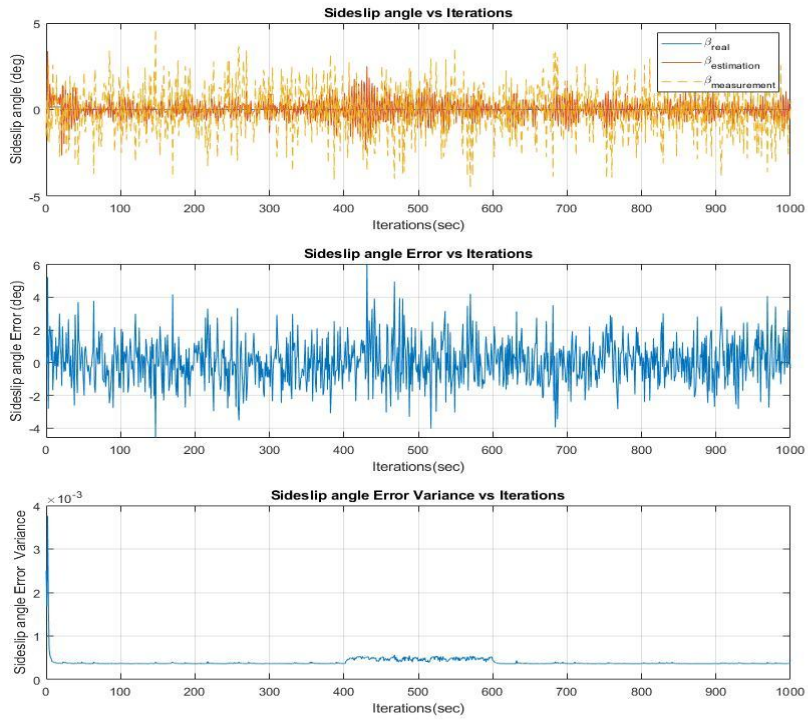

Figure A.2.1 : Sideslip angle estimation, error and error variance with rkf implemented in case of yaw rate sensor fault.

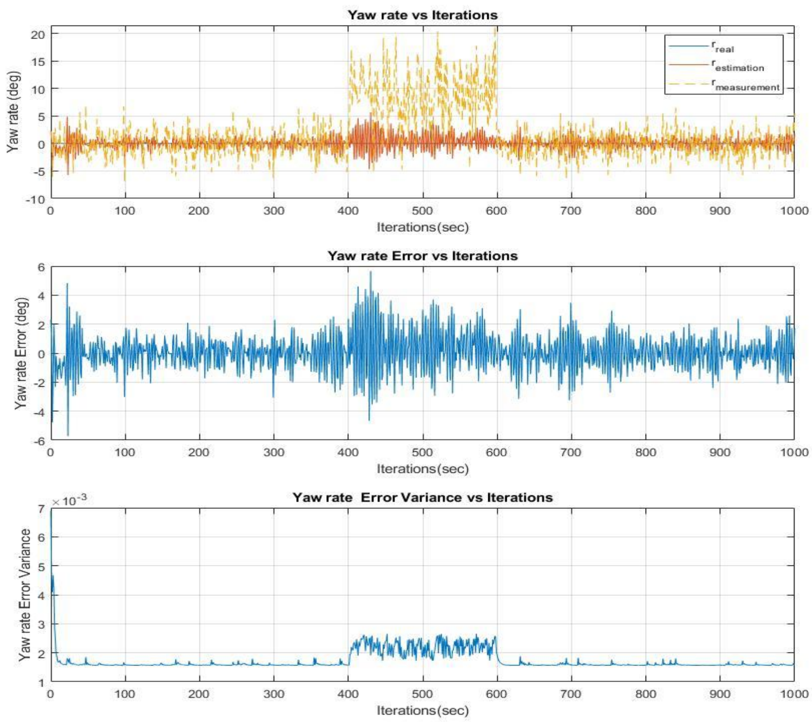

Figure A.2.2 : Yaw rate estimation, error and error variance with rkf implemented in case of yaw rate sensor fault.

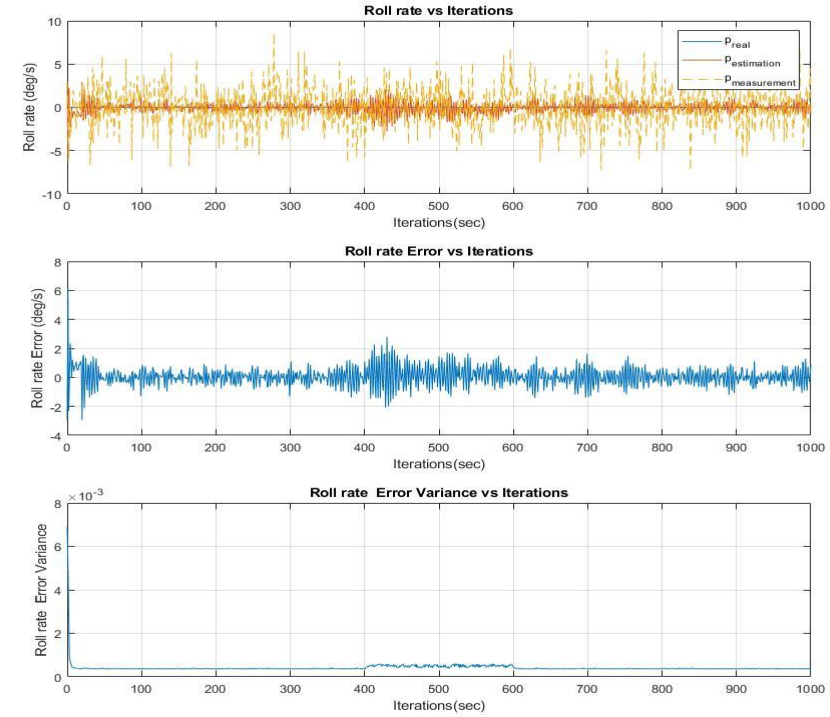

Figure A.2.3 : Roll rate estimation, error and error variance with rkf implemented in case of yaw rate sensor fault.

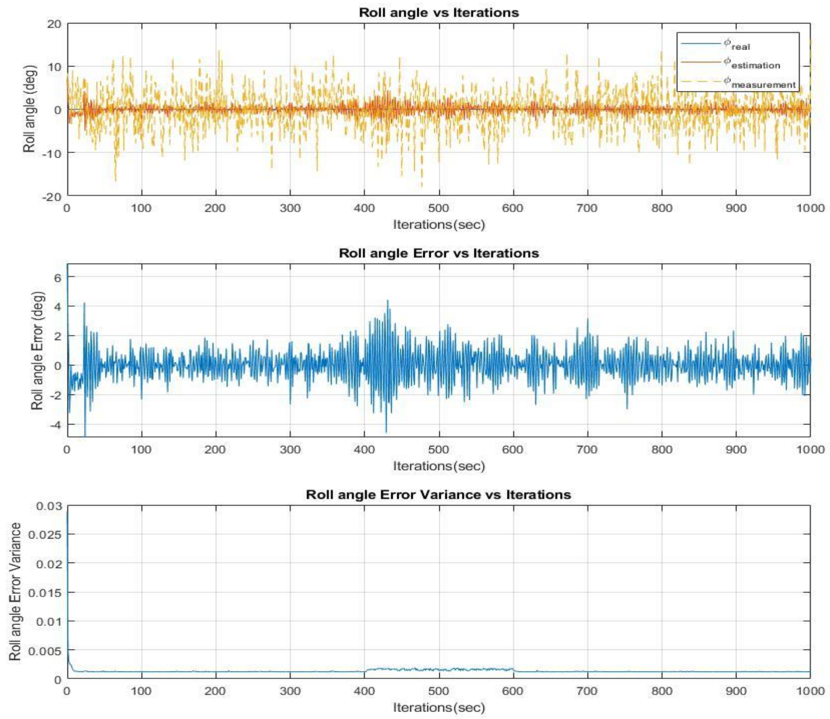

Figure A.2.4 : Roll angle estimation, error and error variance with rkf implemented in case of yaw rate sensor fault.

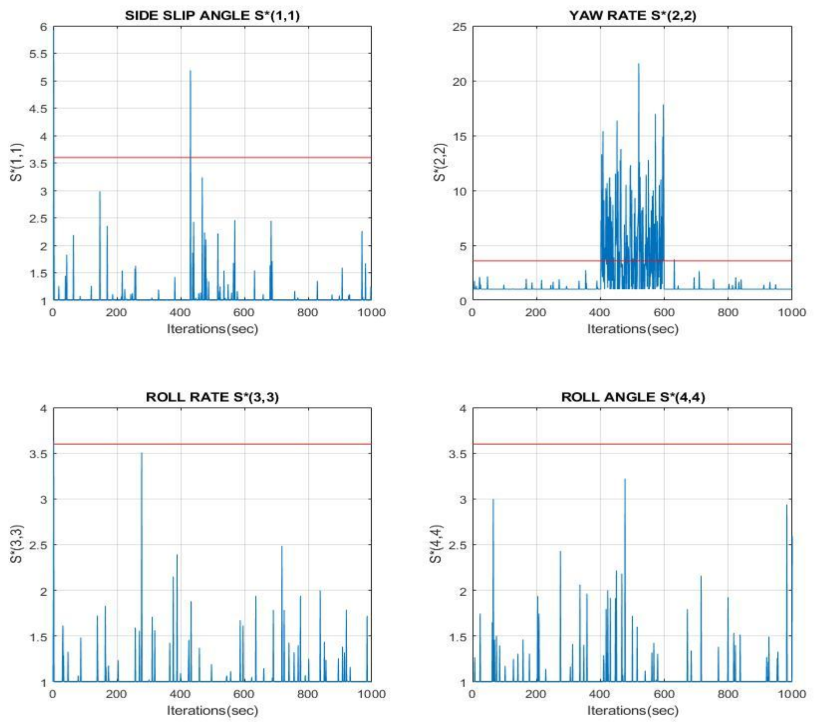

Figure A.2.5 : Sensor fault isolation with continuous bias fault at yaw rate measurements.

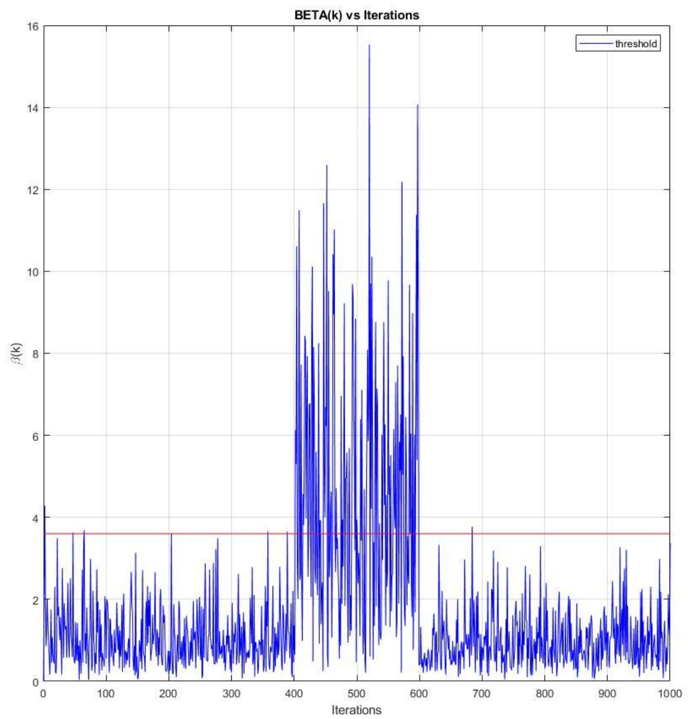

Figure A.2.6 : β(k) evolution for yaw rate continuous bias sensor fault.

A.3. Reconfigured KF for Yaw Rate Sensor Fault

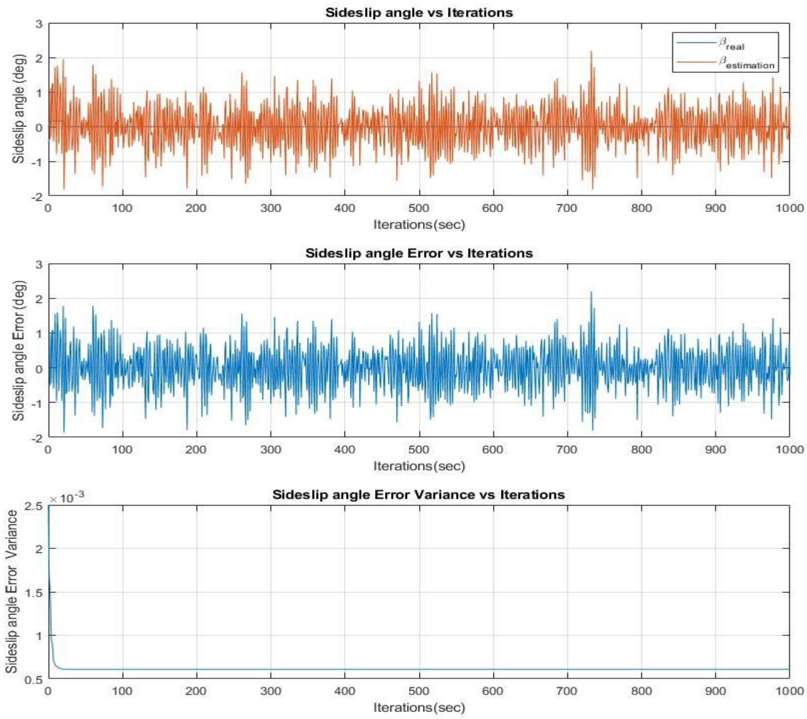

Figure A.3.1 : Sideslip angle evolution, error and error variance in reconfigured Kalman filter (1 parameter (yaw rate) estimated).

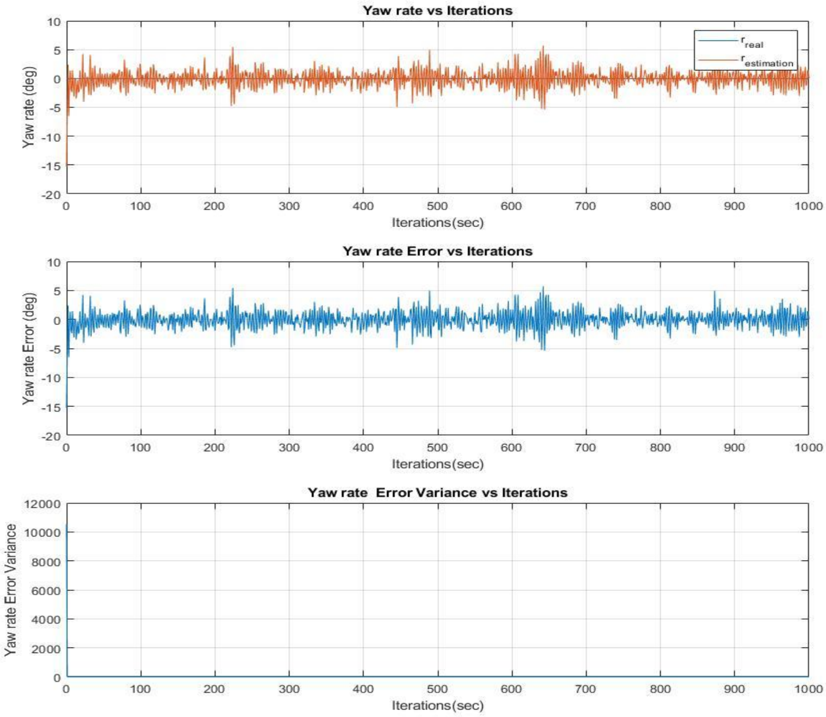

Figure A.3.2 : Yaw rate evolution, error and error variance in reconfigured Kalman filter (1 parameter (yaw rate) estimated).

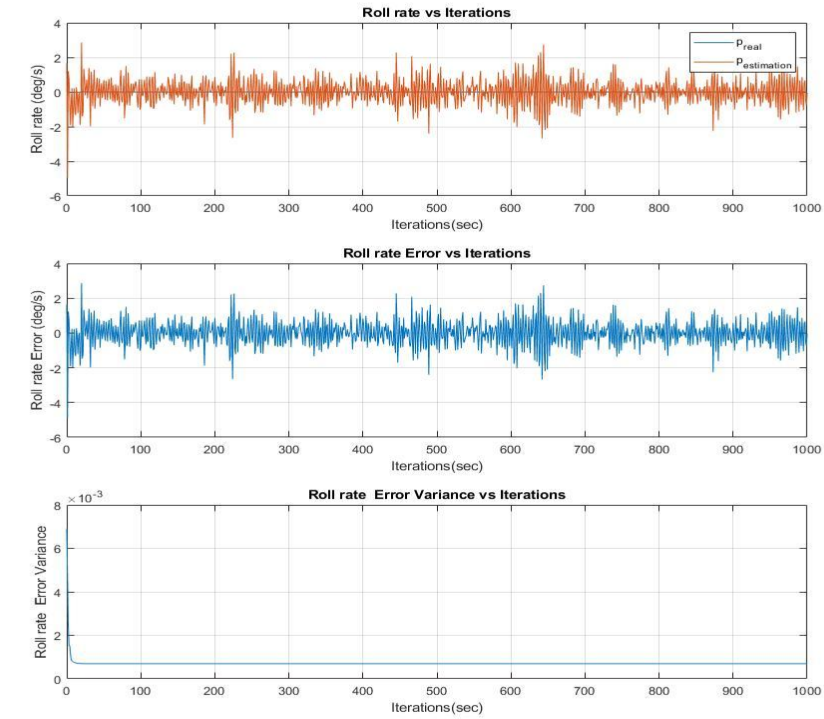

Figure A.3.3 : Roll rate evolution, error and error variance in reconfigured Kalman filter (1 parameter (yaw rate) estimated).

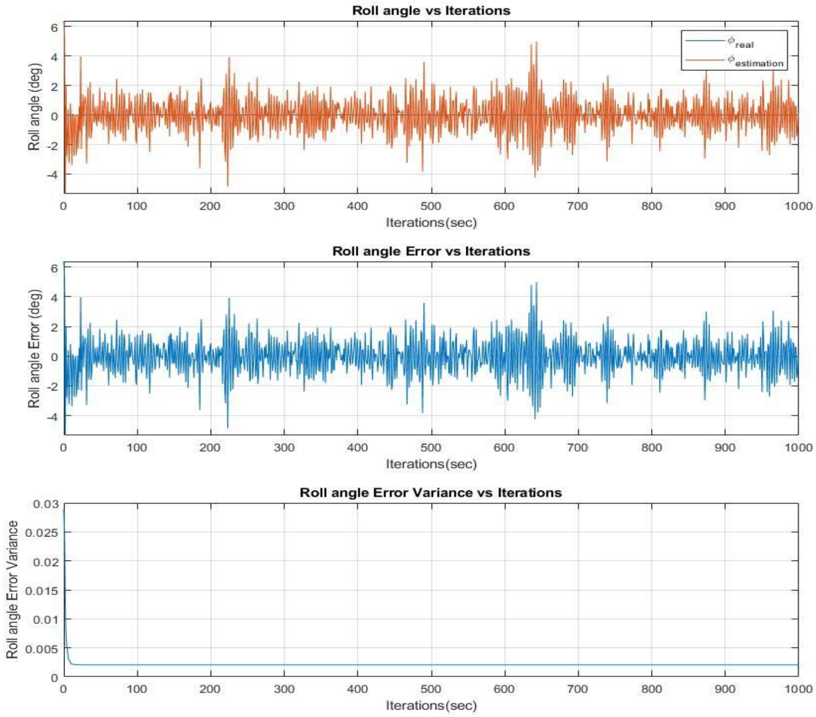

Figure A.3.4 : Roll angle evolution, error and error variance in reconfigured Kalman filter (1 parameter (yaw rate) estimated).

A.4. OKF for Roll Angle Sensor Fault

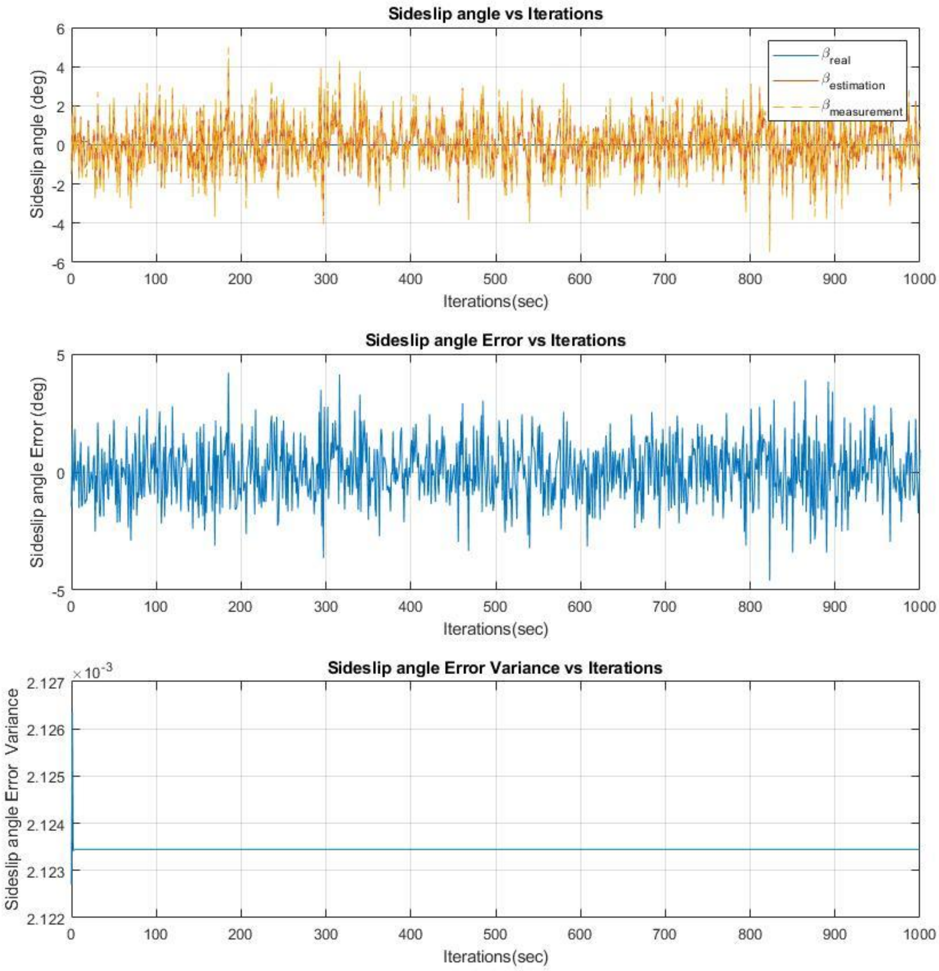

Figure A.4.1 : Sideslip angle estimation, error and error variance with olkf implemented in case of roll angle sensor fault.

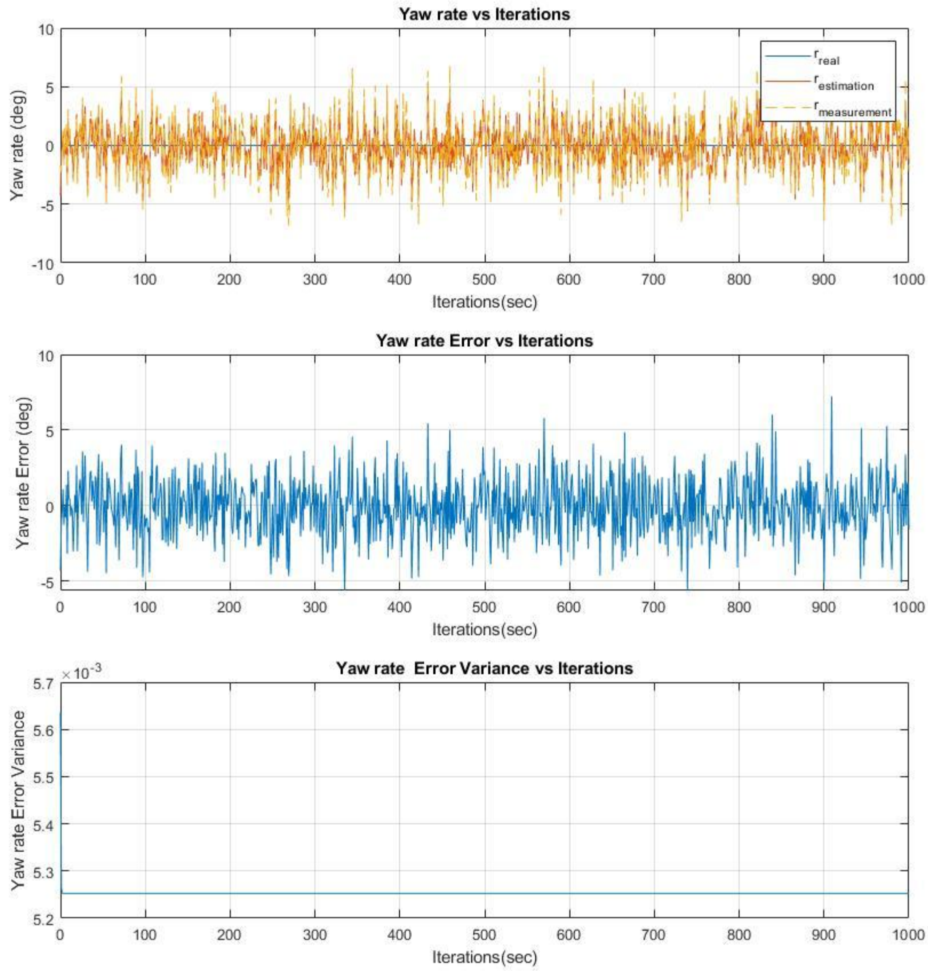

Figure A.4.2 : Yaw rate estimation, error and error variance with olkf implemented in case of roll angle sensor fault.

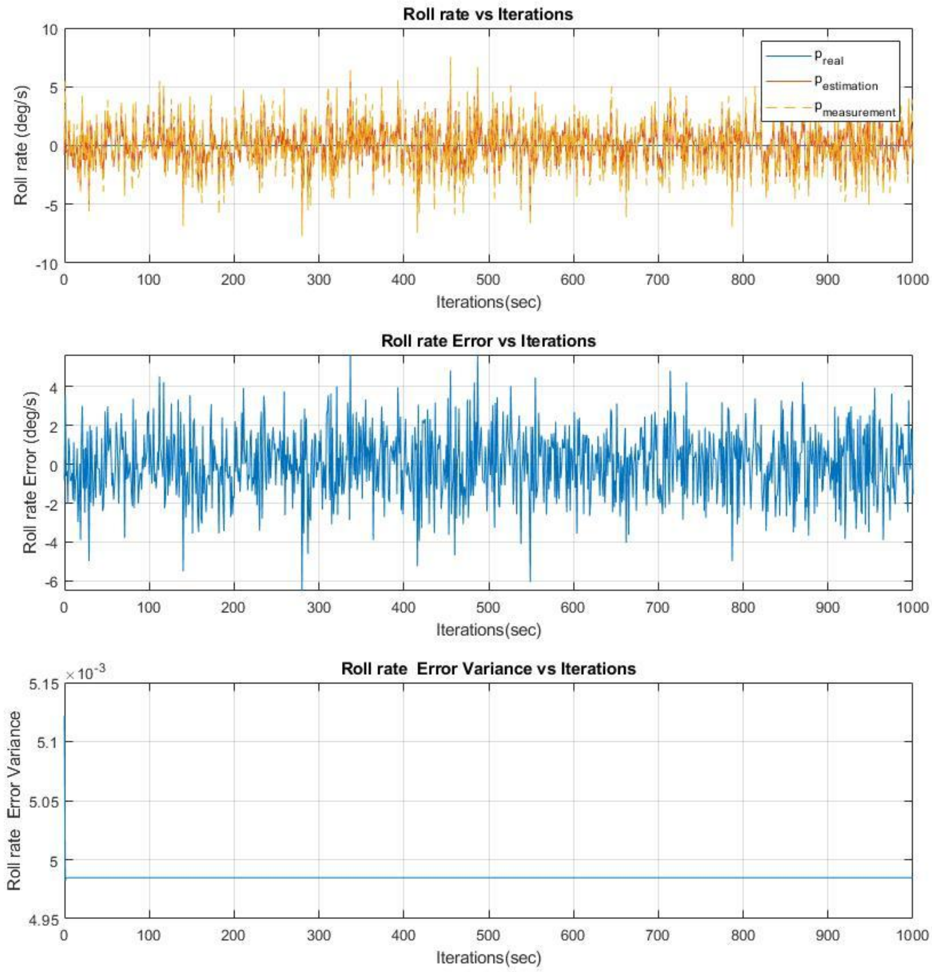

Figure A.4.3 : Roll rate estimation, error and error variance with plkf implemented in case of roll angle sensor fault.

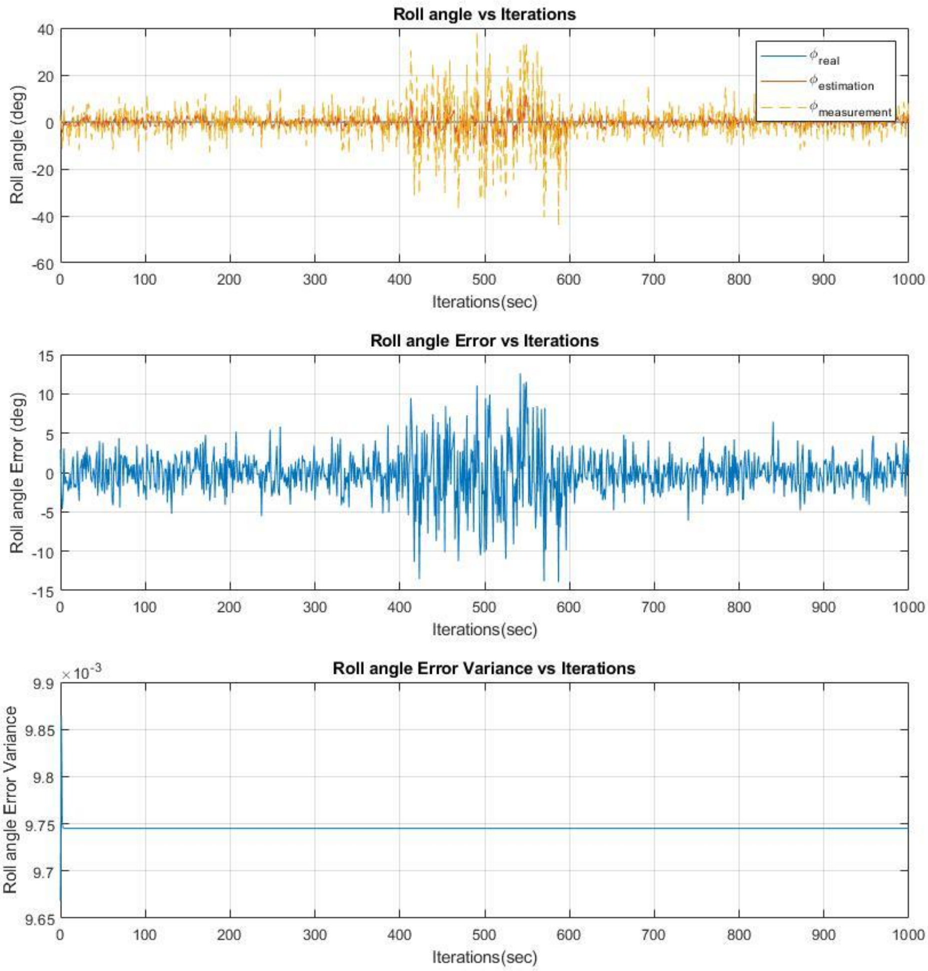

Figure A.4.4 : Roll angle estimation, error and error variance with olkf implemented in case of roll angle sensor fault.

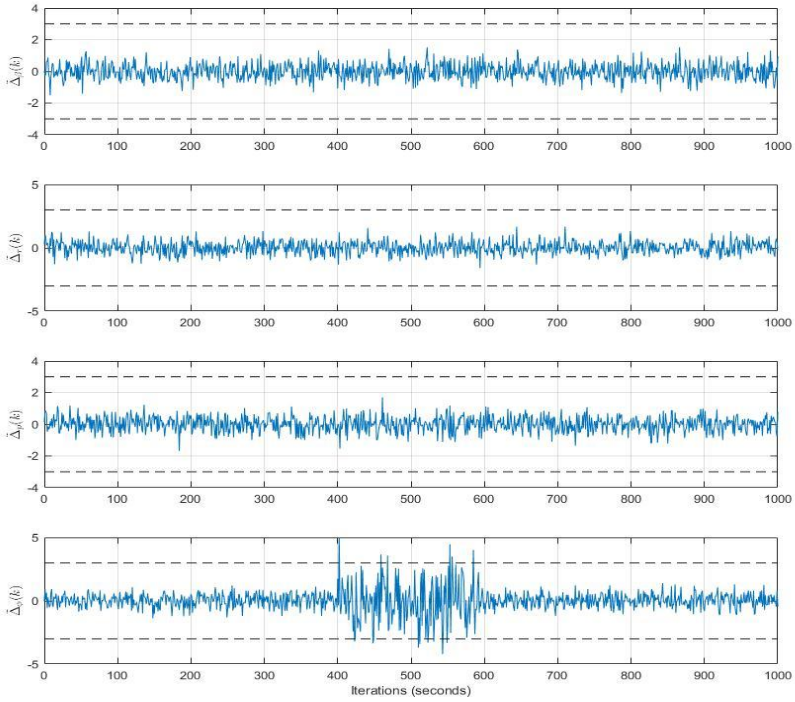

Figure A.4.5 : Normalized innovations of olkf for $\boldsymbol{\beta}, \boldsymbol{r}\ \boldsymbol{p}, \boldsymbol{\varphi}$ measurement channels in case of roll angle sensor fault.

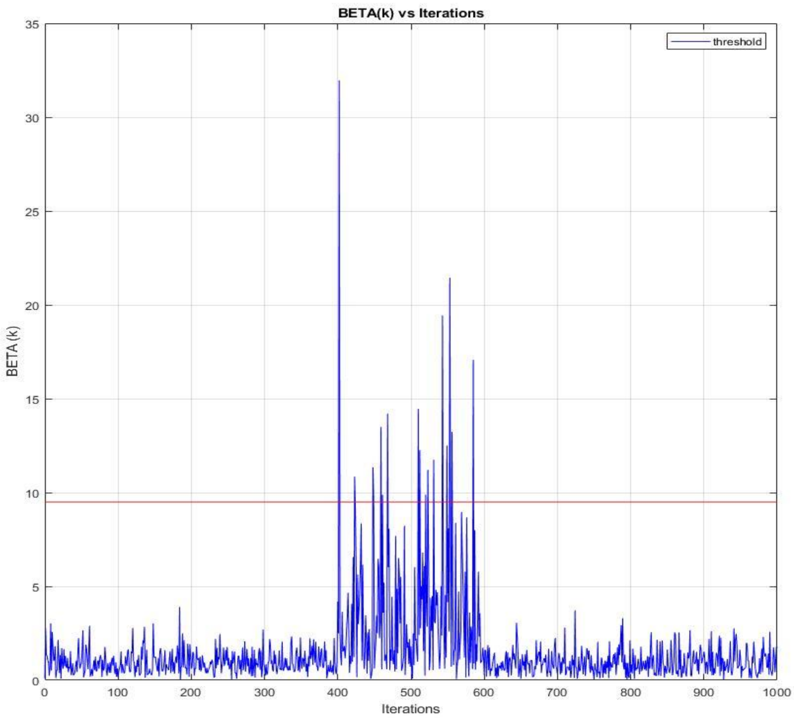

Figure A.4.6 : β(k) evolution for the case of measurement noise-increment fault at roll angle sensor.

A.5. RKF for Roll Angle Sensor Fault

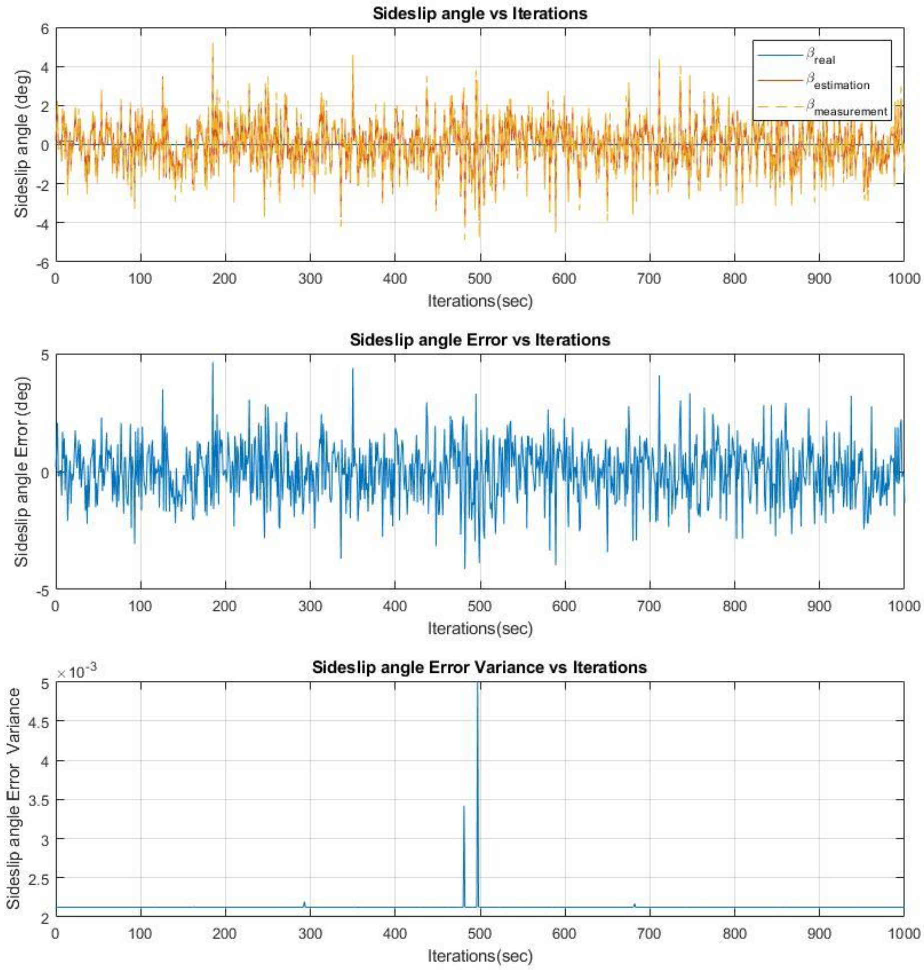

Figure A.5.1 : Sideslip angle estimation, error and error variance with rkf implemented in case of roll angle sensor fault.

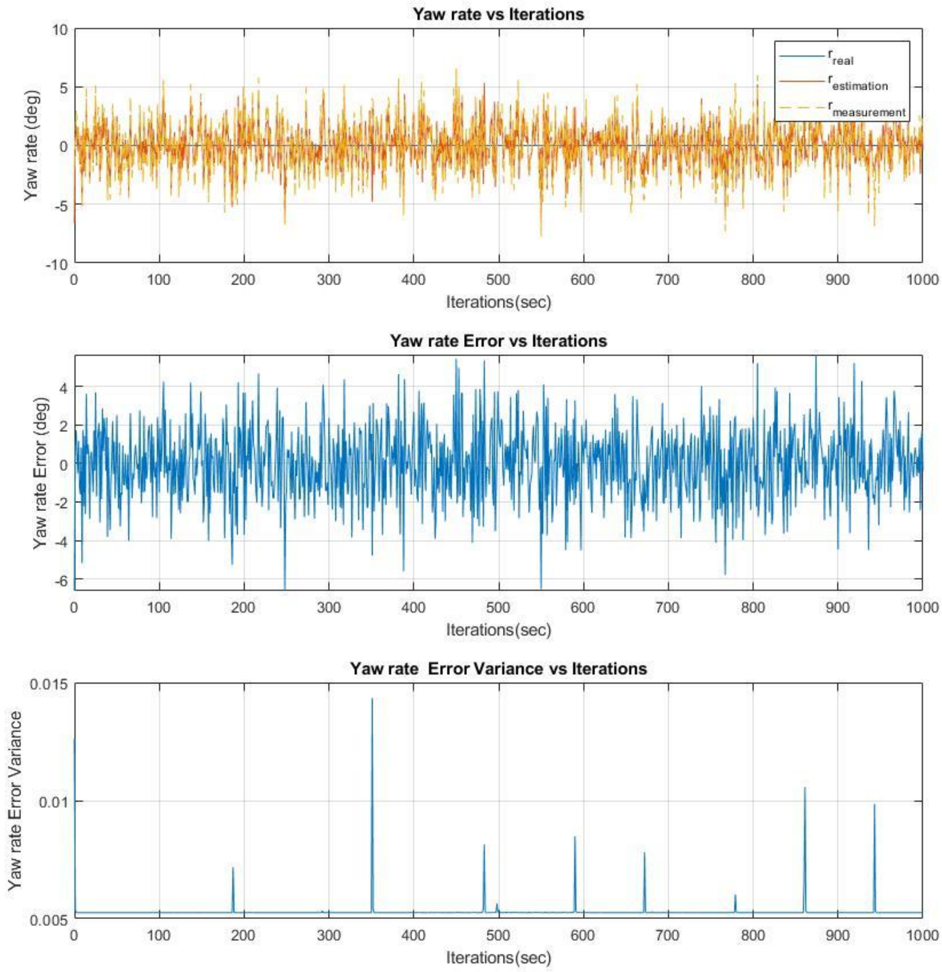

Figure A.5.2 : Yaw rate estimation, error and error variance with rkf implemented in case of roll angle sensor fault.

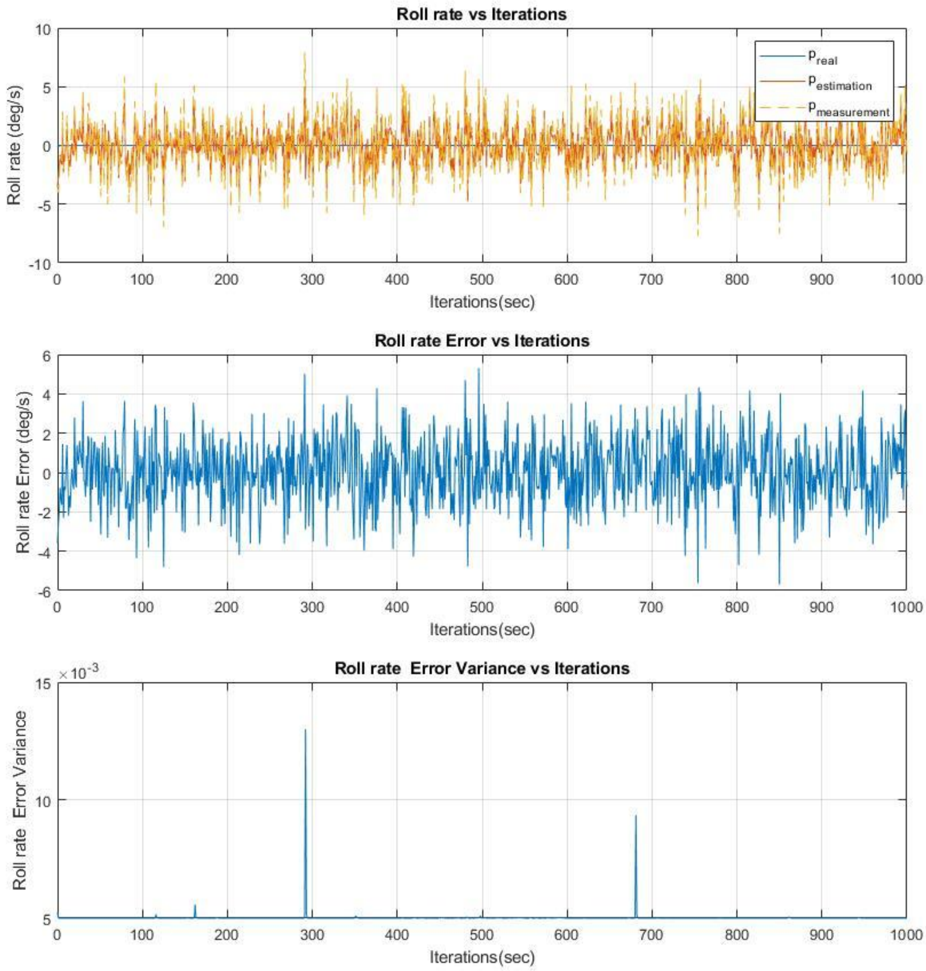

Figure A.5.3 : Roll rate estimation, error and error variance with rkf implemented in case of roll angle sensor fault.

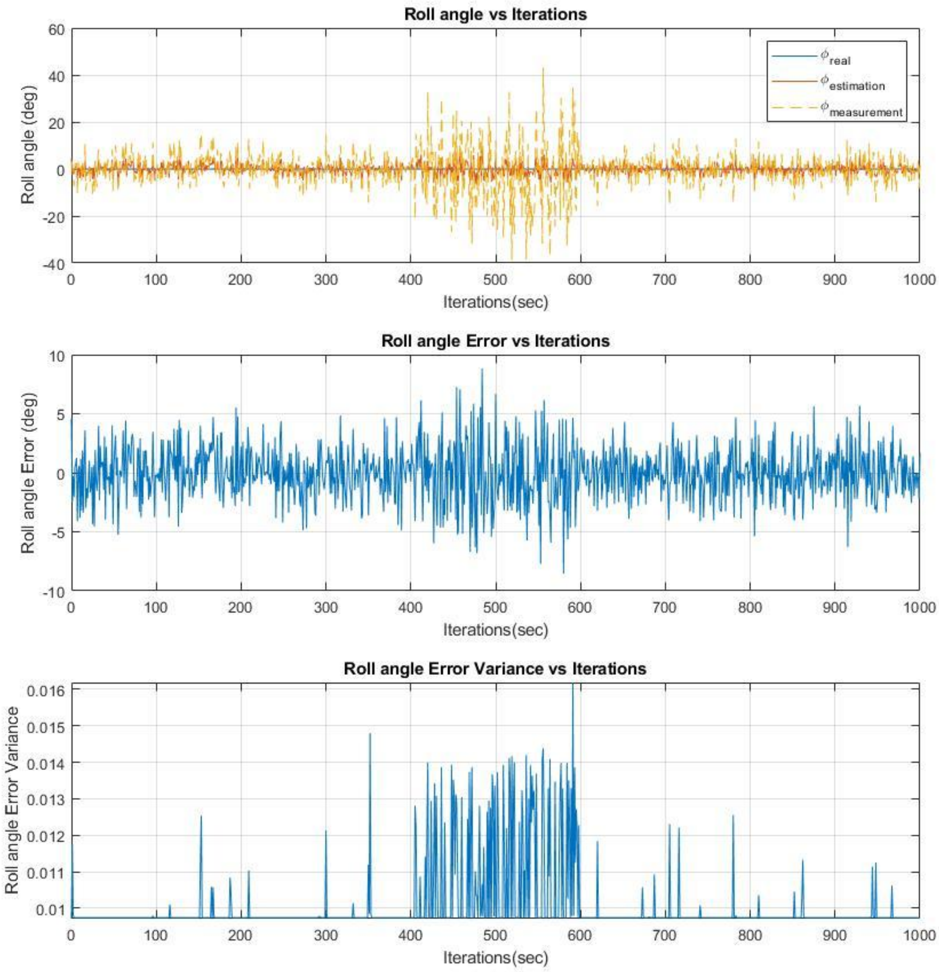

Figure A.5.4 : Roll angle estimation, error and error variance with rkf implemented in case of roll angle sensor fault.

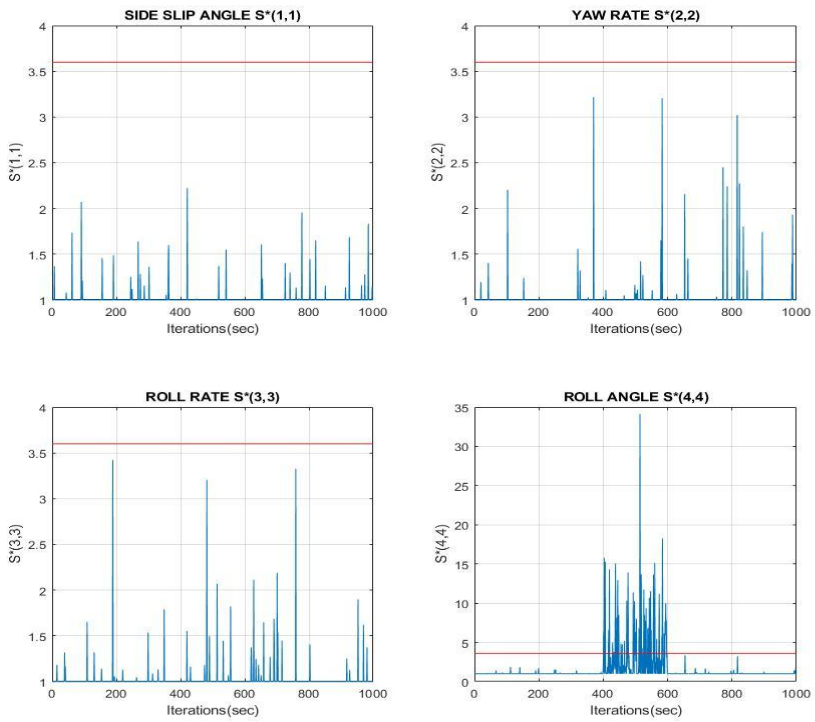

Figure A.5.5 : Sensor fault isolation with measurement noise-increment fault at roll angle ($\boldsymbol{\varphi}$) measurements.

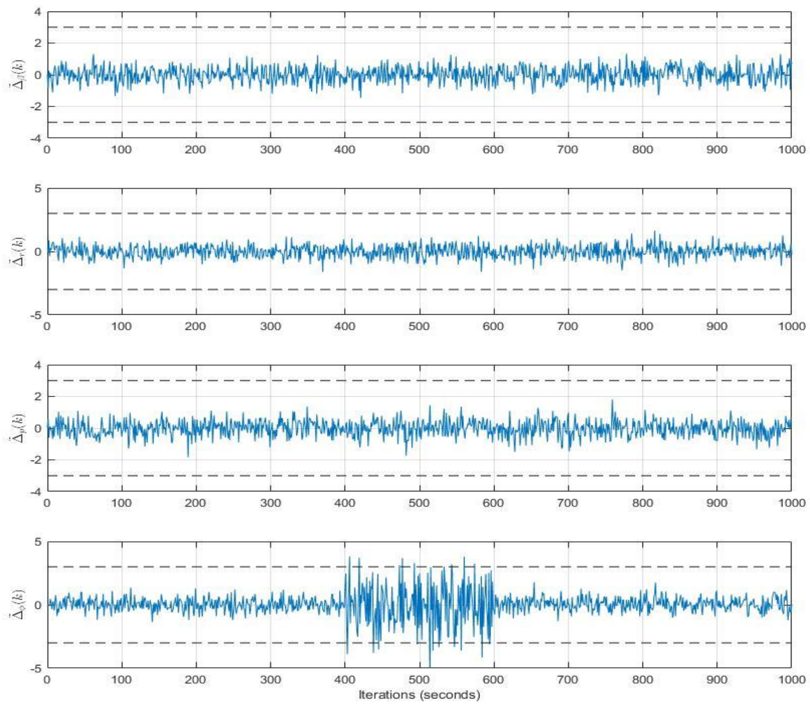

Figure A.5.6 : Normalized innovations of rkf for $\boldsymbol{\beta}, \boldsymbol{r}, \boldsymbol{p}, \boldsymbol{\varphi}$ measurement channels.

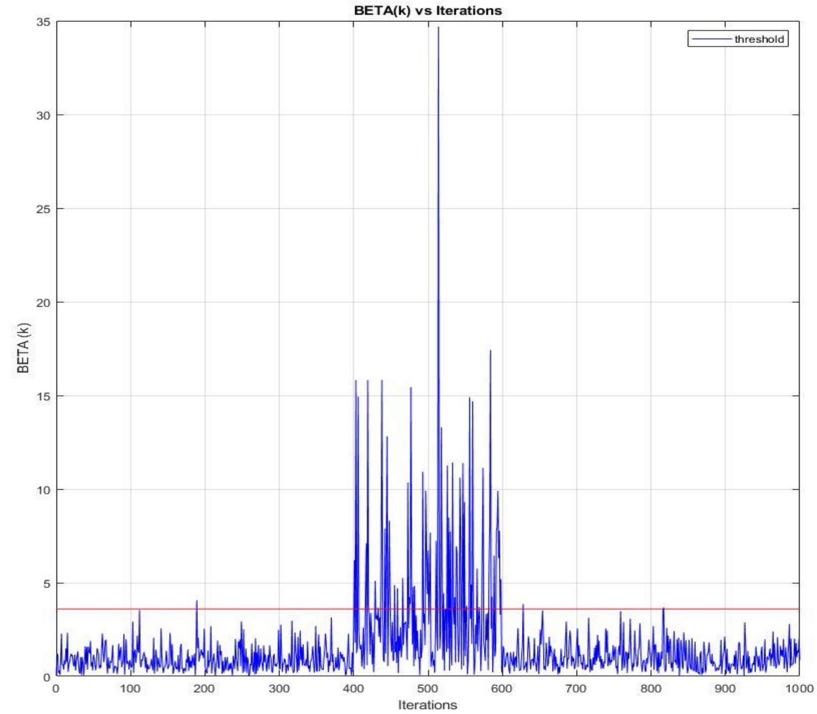

Figure A.5.7 : β(k) evolution for roll angle measurement noise-increment sensor fault.

A.6. Reconfigured KF for Roll Angle Sensor Fault

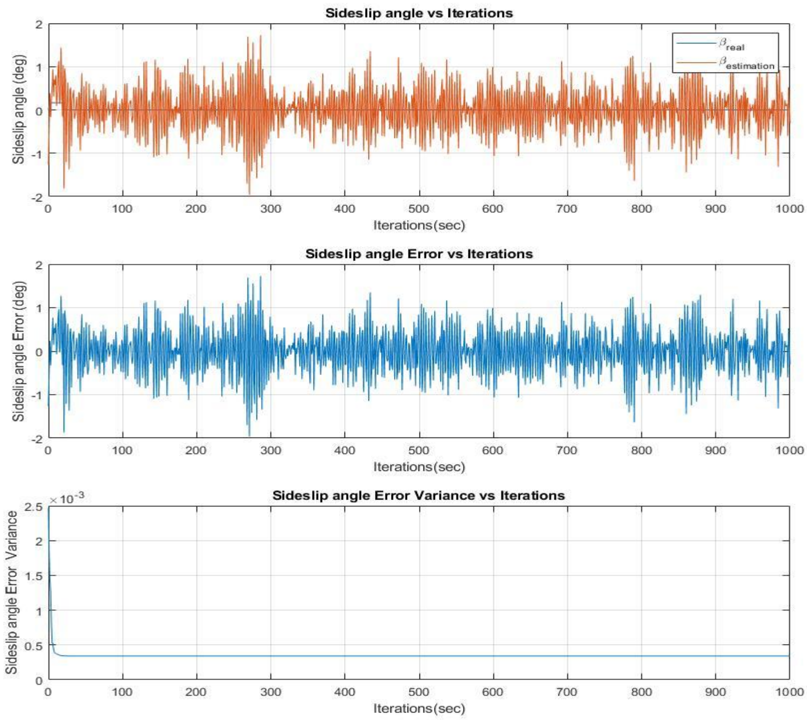

Figure A.6.1 : Sideslip angle evolution, error and error variance in reconfigured Kalman filter (1 parameter (roll angle) estimated).

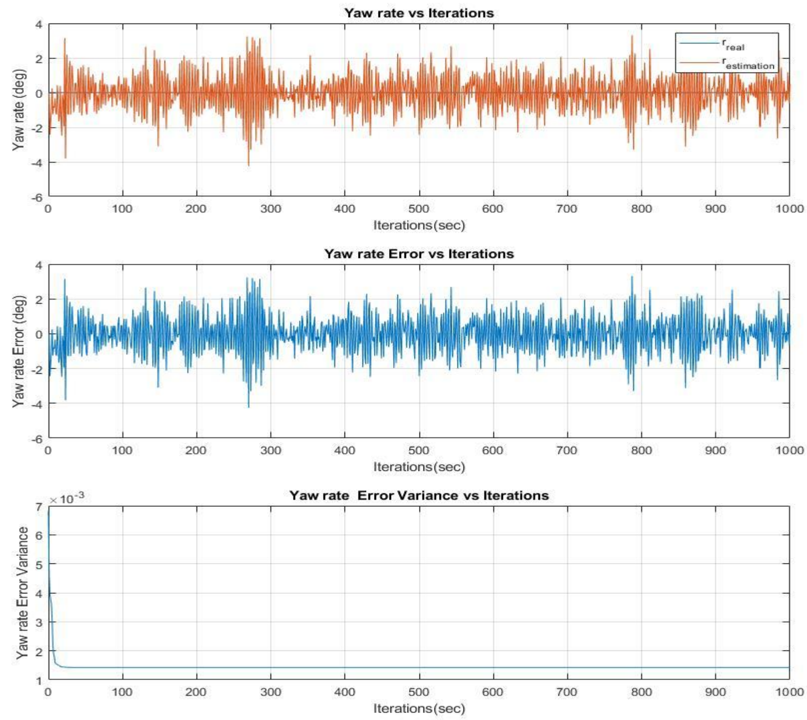

Figure A.6.2 : Yaw rate evolution, error and error variance in reconfigured Kalman filter (1 parameter (roll angle) estimated).

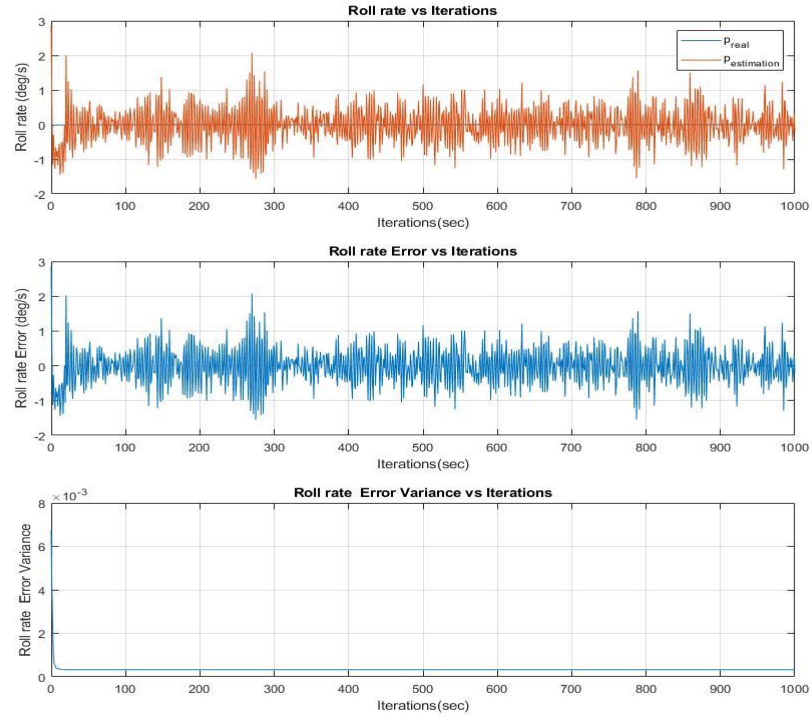

Figure A.6.3 : Roll rate evolution, error and error variance in reconfigured Kalman filter (1 parameter (roll angle) estimated).

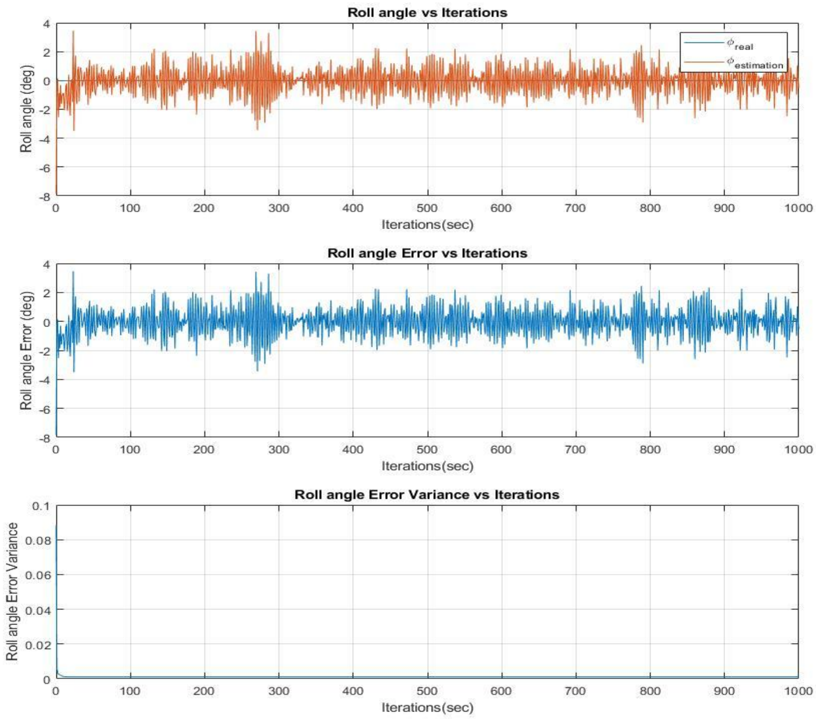

Figure A.6.4 : Roll angle evolution, error and error variance in reconfigured Kalman filter (1 parameter (roll angle) estimated).

APPENDIX B

B.1. Root Mean Square Error Comparison in Case of Yaw Rate SF

Table B.1 : Root mean square value comparison during yaw rate sensor fault.

Lateral States	No Fault Case RMSE Value	OLKF RMSE Value	RKF RMSE Value	Reconfigured KF RMSE Value
Sideslip angle (β)	0.8934	0.9805	0.6093	1.0079
Yaw rate (r)	1.6262	2.5636	2.073	2.4848
Roll rate (p)	1.0219	1.2757	1.105	1.1799
Roll angle (φ)	1.3540	1.7732	1.6770	2.0498

In case of a yaw rate sensor fault,

RKF gives the best estimation results that are close to actual value for sideslip angle, roll rate and roll angle.

For Sideslip angle sensor, the RKF has better result with 0.3712 degrees less error than closest OLKF value.

For Roll rate sensor, the RKF has better result with 0.0749 degrees less error than closest Reconf. KF value.

For Roll angle sensor, the RKF has better result with 0.0962 degrees less error than closest OLKF value.

B.2. Root Mean Square Error Comparison in case of Yaw rate SF

Table B.2 : Root mean square value comparison during roll angle sensor fault.

Lateral States	No Fault Case RMSE Value	OLKF RMSE Value	RKF RMSE Value	Reconfigured KF RMSE Value
Sideslip angle (β)	0.8934	1.2275	1.2215	1.2237
Yaw rate (r)	1.6262	1.9681	1.9305	1.9056
Roll rate (p)	1.0219	1.7996	1.7325	1.7263
Roll angle (φ)	1.3540	3.0455	2.3105	1.7593

In case of a roll angle sensor fault,

Robust KF gives the best estimation results that are close to actual value for sideslip angle, yaw rate and roll rate.

For Sideslip angle sensor, the RKF has better result with 0.0022 degrees less error than closest Reconf. KF estimation value.

Again for Yaw rate sensor, the Reconf. KF has better result with 0.0245 degrees less error than closest RKF value.

And last for Roll rate sensor, the Reconf. KF has better result with 0.00628 degrees less error than closest RKF value.

CIRRICULUM VITAE

Name Surname **: Akan GÜVEN**

EDUCATION **:**

- **B.Sc.** **:** 2015-2016, Yıldız Technical University, Mechanical Engineering Faculty, Mechanical Engineering Department
- **M.Sc.** **:**2020-2021, Istanbul Technical University, Aeronautics and Astronautics Engineering Faculty, Aeronautics and Astronautics Department

PROFESSIONAL EXPERIENCE AND REWARDS:

- 2015 Completed Bachelor’s at Yıldız Technical University
- 2016-2017 Verisoft Turkiye ltd.
- 2018-2019 Gamers arena ltd. Sales Eng.
- 2021 Completed Master of Science at Istanbul Technical University